Cape Peninsula
University of Technology

IMPROVEMENT OF POWER PLANT CONTROLLER DESIGN FOR EMERGENCY RESERVE SERVICES

by

Ntanganedzeni Tshinavhe

Thesis submitted in fulfilment of the requirements for the degree

Master of Engineering: Electrical Engineering

in the Faculty of Engineering & the Built Environment

at the Cape Peninsula University of Technology

Supervisor: Mr M Ratshitanga
Co-supervisor: Dr N Tshemese-Mvandaba

Bellville
Date submitted: September 2025

DECLARATION

I, Ntanganedzeni Tshinavhe declare that the contents of this dissertation/thesis represent my own unaided work, and that the dissertation/thesis has not previously been submitted for academic examination towards any qualification. Furthermore, it represents my own opinions and not necessarily those of the Cape Peninsula University of Technology.

16 January 2026

Signed **Date**

ABSTRACT

The increasing global demand for clean, sustainable energy has seen a growth in the integration of renewable energy sources (RES) such as photovoltaic (PV) systems and wind into the power grid. While RES offer economic and environmental benefits, their variability and intermittency introduce major challenges to frequency stability, particularly in low synchronous inertia systems. As these variations can potentially cause frequency deviation, traditional load frequency control (LFC) techniques would often struggle to maintain the system's stability during high levels of penetration of renewables. To address these problems, this research focuses on improving controller design for emergency reserve services through advanced optimisation-based LFC.

The study develops, models, and simulates a single-area and two-area power system with PV generation and a battery energy storage system (BESS) based on MATLAB/Simulink. A baseline performance test is conducted in a single-area system to understand the behaviour of the system due to different disturbances. This test is first conducted without a controller and then followed by a standard proportional-integral-derivative (PID) control tuning through the Ziegler-Nichols technique. The recently proposed algorithm, which is the Zebra Optimisation Algorithm (ZOA) is used to tune the PID parameters. This algorithm is validated under different operating conditions, such as load changes, varying PV generation, different levels of renewable penetration (0.3 pu and 0.7 pu), the effect of BESS, and generation loss. Performance indicators like overshoot, undershoot, settling time, steady-state error, and frequency deviation are used to quantify the results.

The simulation results show that the PID controller makes the system more stable compared to the baseline. However, its static gain reduces flexibility when conditions change. When the ZOA is applied, results showed improvement in reducing frequency deviation, reducing settling time and eliminating steady-state error and oscillations. A comparison study was conducted with the Particle Swarm Optimisation (PSO), in which the results showed that the ZOA is superior in reducing the overshoot and undershoot, while the PSO is superior in settling time. The ZOA was further implemented in a two-area system, and results show better performance in a higher-order system.

Keywords: Load frequency control, PID controller, renewable energy sources, battery energy storage system, Zebra Optimisation Algorithm, Particle Swarm Optimisation, Ziegler-Nichol's technique, renewable energy integration, metaheuristic algorithms

ACKNOWLEDGEMENTS

I wish to thank:

- The God of Mount Zion for His grace.
- My family for the support they provide
- My supervisor, Mr. Ratshitanga, for all the guidance, motivation, and patience during this journey.
- My co-supervisor, Dr. Tshemese-Mvandaba, for the encouragement and support she provided.
- My gratitude also goes to Mr. Mditshwa for his contribution to this study
- My colleagues at the Centre for Intelligent Systems and Emerging Technologies (CSIET) and the Centre for Substation Automation and Energy Management Systems (CSAEMS).

The financial assistance of the Mining Qualification Authority towards this research is acknowledged. Opinions expressed in this thesis and the conclusions arrived at, are those of the author, and are not necessarily to be attributed to the Mining Qualification Authority.

DEDICATION

This thesis is dedicated to my parents, Lugisani Zacharia Tshinavhe and Khathutshelo Violet Tshinavhe, and my siblings, Lugisani Tshinavhe and Khuliso Tshinavhe, for all their support and contribution.

Table of Contents

DECLARATION i
ABSTRACT ii
ACKNOWLEDGEMENTS iii
DEDICATION iv
LIST OF FIGURES ix
LIST OF TABLES xi
LIST OF ABBREVIATIONS xii
CHAPTER ONE 1
INTRODUCTION 1
1.1. Introduction 1
1.2. Problem statement 2
1.3. Research aim and objectives 3
1.4. Hypothesis 3
1.5. Delimitation of the research project 4
1.6. Motivation of the research project 4
1.7. Assumptions 5
1.8. Research design and methodology 5
1.8.1. Literature review 6
1.8.2. Data collection 6
1.8.3. Simulation 6
1.9. Thesis chapters 7
1.9.1. Chapter 1 7
1.9.2. Chapter 2 7
1.9.3. Chapter 3 7
1.9.4. Chapter 4 7
1.9.5. Chapter 5 7
1.9.6. Chapter 6 8
1.9.7. Chapter 7 8
1.10. Conclusion 8

CHAPTER TWO 9
LITERATURE REVIEW 9
2.1. Introduction 9
2.2. Literature search 10
2.3. Frequency control 11
2.3.1. Primary frequency control 13
2.3.2. Secondary frequency control 14
2.3.3. Tertiary and emergency frequency control 14
2.4. Load frequency control in power systems 15
2.5. Renewable energy integration and challenges 15
2.6. Energy storage system in power systems 17
2.7. Classification of load frequency control techniques 20
2.7.1. Traditional control techniques 20
2.7.2. Soft computing 23
2.8. Optimisation algorithms 24
2.8.1. Heuristic algorithms 25
2.8.2. Metaheuristic algorithms 26
2.8.3. Comparative study 29
2.8.4. Comparative analysis and discussion 33
2.9. Conclusion 35
CHAPTER THREE 36
MODELLING OF LFC SYSTEM OPTIMISATION ALGORITHM 36
3.1. Introduction 36
3.2. Single-area LFC power system model 36
3.2.1. The turbine speed governing system 36
3.2.2. Modelling the turbine 40
3.2.3. Modelling the generator-load model 41
3.2.4. Modelling a solar PV system transfer function 43
3.2.5. Steady state analysis of the system 47
3.2.6. Dynamic response of the system 50

3.3. Modelling a two-area power system 52
3.4. The Zebra Optimisation Algorithm 54
3.4.1. Adaptation of the Zebra Optimisation Algorithm 57
3.5. Conclusion 58
CHAPTER FOUR 59
SIMULATION AND ANALYSIS OF A SINGLE AREA SYSTEM 59
4.1. Introduction 59
4.2. Simulation scenarios 60
4.2.1. Case 1: Under normal operation with no load change 60
4.2.2. Case 2: Load changes 61
4.2.3. Case 3: With PV system and without BESS 62
4.2.4. Case 4: With PV system and BESS 64
4.2.5. Variable load and PV profile 65
4.2.6. Summary of uncontrolled results 66
4.3. PID-controlled cases 66
4.3.1. Load changes 67
4.3.2. Effects of the PV and BESS 69
4.3.3. Generation loss 70
4.4. Conclusion 71
CHAPTER FIVE 72
IMPLEMENTATION OF THE OPTIMISATION ALGORITHM 72
5.1. Introduction 72
5.2. Implementation in MATLAB/Simulink 72
5.3. Simulation scenarios 73
5.3.1. Parameter changes of the algorithm 73
5.3.2. Load variations 77
5.3.3. Impact of PV power and BESS 78
5.3.4. Generation loss 80
5.3.5. Variation in load disturbances 80
5.4. Comparison with other optimisation algorithms 81

5.5. Conclusion 82
CHAPTER SIX 83
SIMULATION AND ANALYSIS OF A TWO-AREA POWER SYSTEM 83
6.1. Introduction 83
6.2. Simulation scenarios 85
6.2.1. Load disturbance 85
6.2.2. Loss of generation 90
6.3. Conclusion 92
CHAPTER SEVEN 94
CONCLUSION 94
7.1. Introduction 94
7.2. Research aim and objectives 94
7.3. Thesis deliverables 95
7.3.1. Literature review 95
7.3.2. Modelling a single area, two-area system and the optimisation algorithm 95
7.3.3. Base simulation without a controller 95
7.3.4. Base simulation with a PID controller 95
7.3.5. Mathematical formulation of the ZOA 96
7.3.6. Single area system simulations and analysis using the ZOA 96
7.3.7. Multi-area system simulation and analysis using the ZOA 96
7.4. Overview of research findings and contribution to academic and industry 96
7.5. Publications 97
7.6. Recommendation for future research 97
7.7. Conclusion 98
REFERENCES 99
APPENDICES 113
APPENDIX A: Finding the PID parameters 113
APPENDIX B: ZOA MATLAB function 116
APPENDIX C: PSO MATLAB function 119

LIST OF FIGURES

Figure 2-1: Literature review outline 9
Figure 2-2: A graph of reviewed papers 11
Figure 2-3: Frequency response model and control loops (Bevrani, 2009) 12
Figure 2-4: LFC model with renewable energy integrated (Bevrani et al., 2010) 13
Figure 2-5: Evolution of renewable electricity generation (IEA, 2025) 15
Figure 2-6: Global trends for installed capacity (Lerede & Savoldi, 2023) 17
Figure 2-7: Grid services and ancillary support 18
Figure 2-8: Energy storage system technologies 19
Figure 2-9: PID controller block diagram 21
Figure 2-10: Different tuning methods 23
Figure 2-11: Optimisation algorithms 24
Figure 2-12: Optimisation algorithms taxonomy(Janga Reddy & Nagesh Kumar, 2020) 25
Figure 2-13: Metaheuristic optimisation algorithms 28
Figure 3-1: The turbine speed governing system (Elgerd, 1987) 38
Figure 3-2: Model of the speed governor (Adapted from (Elgerd, 1987; Saadat, 1999)) 39
Figure 3-3: A model of a two-stage steam turbine (Adapted from (Chakrabarti, 2010)) 40
Figure 3-4: A transfer function model of the turbine (Adapted from (Chakrabarti, 2010) 40
Figure 3-5: Generator-load model (Adapted from (Chakrabarti, 2010)) 42
Figure 3-6: Model of a single area LFC (Adapted from (Elgerd, 1987)) 43
Figure 3-7: Equivalent circuit of a PV solar cell (Eltanaly, 2018) 45
Figure 3-8: I-V, P-V characteristics of a PV module 45
Figure 3-9: Developed model of the single-area system 46
Figure 3-10: Reduced block diagram (Adapted from (Saadat, 1999)) 48
Figure 3-11: Dynamic response block diagram 51
Figure 3-12: Flow chart of the ZOA (Adapted from (Trojovska et al., 2022)) 55
Figure 4-1: Single-area load frequency control Simulink model (Akter et al., 2022) 60
Figure 4-2: Frequency response under normal operations 61
Figure 4-3: Frequency response due to load changes 61
Figure 4-4: Model of a single area system with a PV system 62
Figure 4-5: Frequency response due to changes in solar PV levels 63
Figure 4-6: Model of the single-area with PV and BESS 64
Figure 4-7: Frequency response when PV and BESS are integrated 64
Figure 4-8: Frequency response with a variable load profile 65
Figure 4-9: Frequency response with variable PV profile 66
Figure 4-10: Single area system model with PID controller 67
Figure 4-11: Frequency response due to a 15% load change 68
Figure 4-12: Frequency response due to 20% load change 68

Figure 4-13: Frequency response due to variable load 69
Figure 4-14: Frequency response due to 10% PV penetration 69
Figure 4-15: Frequency response due to variable PV generation 70
Figure 4-16: Frequency response due to loss of BESS 70
Figure 4-17: Frequency response due to generation loss (PID controlled) 71
Figure 5-1: Implementation of the objective function 72
Figure 5-2: Modified single-area system 73
Figure 5-3: Convergence curve at multiple boundaries 74
Figure 5-4: Frequency response due to boundary variations 74
Figure 5-5: Convergence curves due to search agents' variations 75
Figure 5-6: Frequency response due to search agents' variations 76
Figure 5-7: Convergence curve due to iterations variation 76
Figure 5-8: Frequency response due to different iterations 77
Figure 5-9: Frequency response due to load variation (ZOA-PID) 78
Figure 5-10: Frequency response due to variable PV profile (ZOA-PID) 79
Figure 5-11: Frequency response due to loss of BESS support (ZOA-PID) 80
Figure 5-12: Frequency response due to generation loss 80
Figure 5-13: Frequency response due to variable load 81
Figure 5-14: Comparison between ZOA and PSO 81
Figure 6-1: Model of the two-area power system 84
Figure 6-2: Frequency response in area 1 86
Figure 6-3: Frequency response in area 2 87
Figure 6-4: Frequency response in area 1 due to changes in areas 1 & 2 87
Figure 6-5: Frequency response in area 2 due to changes in areas 1 & 2 88
Figure 6-6: Load variation 89
Figure 6-7: Frequency response in area 1 89
Figure 6-8: Frequency response in area 2 90
Figure 6-9: Frequency response in area 1 due to generation loss 91
Figure 6-10: Frequency response in area 2 due to generation loss 91
Figure 6-11: Change in tie-line power due to generation loss 92
Figure 6-12: Frequency response due to increased iterations 92

LIST OF TABLES

Table 2-1: Control techniques 21
Table 2-2: Reviewed literature on optimization algorithms for LFC 30
Table 4-1: Parameters of the benchmark single-area system (Akter et al., 2022) 59
Table 4-2: Parameters of the PV generation unit and BESS 59
Table 4-3: Summary of results in uncontrolled cases 66
Table 4-4: PID parameters 67
Table 5-1: Results due to load change 78
Table 5-2: PID controller parameters for each case 81
Table 6-1: Parameters of the two-area system (Adapted from (Ogar, Hussain & Kelum A. A. Gamage, 2023)) 85
Table 6-2: The performance metrrics 86
Table 6-4: Simulation results due to changes in areas 1 and 2 88

LIST OF ABBREVIATIONS

ACO	Ant Colony Optimisation
AGC	Automatic Generation Control
ALO	Ant Lion Optimiser
BESS	Battery Energy Storage System
BFOA	Bacterial Foraging Optimisation Algorithm
CAES	Compressed Air Energy Storage
FO-PI	Fractional Order Proportional-Integral
GA	Genetic Algorithm
GWO	Grey Wolf Optimisation
PIDF	Proportional Integral Derivative Filter
PIDN-TIDF	PID with N-Filter and Tilted Integral Derivative Filter
PSO	Particle Swarm Optimisation
LFC	Load Frequency Control
RES	Renewable Energy Sources
TFOIDFF	Tilted Fractional Order Integral-Derivative with Feed Forward
TID	Tilted Integral-Derivative Controller
ZOA	Zebra Optimisation Algorithm
2DoF-PID	Two Degree of Freedom PID

CHAPTER ONE

INTRODUCTION

1.1. Introduction

Modern power grids face increasing complexity due to the growing integration of renewable energy sources (RESs) and the dynamic demand patterns (Dreidy et al., 2017). As the global energy policies prioritize sustainability and decarbonization, traditional power systems are transforming. This shift introduces new challenges, which include intermittency and uncertainties in power generation, especially looking at sources such as solar photovoltaic (PV) and wind **(Rahman et al., 2021; Seneviratne & Ozansoy, 2016)**. One important area affected by this change is how power plant controllers perform and are designed. These controllers handle real-time operations and ensure the electricity grid stays stable.

One of the important control mechanisms to maintain stability is Load Frequency Control (LFC). It is a continuous regulation that monitors and adjusts the output of generating units to balance supply and demand, keeping the system frequency within acceptable limits (Yousef, 2017; Umrao et al., 2012). Maintaining an effective LFC is important to prevent frequency deviations that could result in equipment failure, system blackout, or power quality issues.

Conventional LFC often rely on fixed-parameter controllers such as the Proportional Integral Derivative (PID) **(Hote & Jain, 2018)**, the Proportional Derivative (PD), and the Proportional Integrals (PI) **(Juang & Lu, 2004)** controllers. Although these controllers have been effective for traditional power grids, they are no longer sufficient for modern power systems, which are more variable and nonlinear due to the renewable energy integration. These controllers struggle to adapt to changes that are occurring in the system and have a slow response to disturbances. **(Basa Varajappa & Nagaraj, 2021; Omar et al., 2016)**. Because of these limitations, a need arises for controllers that can adapt and cope with real-time varying conditions.

One approach with promise to address these needs is the integration of high-level optimisation techniques in controller design. Some of the algorithms that have been demonstrated to possess excellent abilities in solving sophisticated, multi-objective optimisation problems, such as Particle Swarm Optimisation (PSO) (Sekyere et al., 2024), Genetic Algorithms (GA) (Nayak et al., 2019a), and Ant-Colony optimisation (ACO) (Dhanasekaran et al., 2020), amongst others. These metaheuristic approaches allow for dynamic tuning of the control parameters such that optimum performance is

obtained under different system conditions. More advanced adaptive control techniques and artificial intelligence (AI)-aided approaches, such as fuzzy logic (Li et al., 2005; Mohammed et al., 2017) and neural networks (Sadeq et al., 2022; Sabahi et al., 2009), also offer improved real-time decision-making.

Another important aspect of the controller improvement is its ability to offer emergency reserve services. Emergency reserve services refer to the capacity of the power system to provide rapid and dependable backup support during unexpected disturbances such as sudden generation outages or load surges. These services are a key safety net, which offers immediate and reliable backup power to correct sudden imbalances in the system, thereby preventing large frequency deviation (Dubitsky et al., 2015).

Emergency reserves can start operating within seconds to minutes. They play a role in keeping the power grid stable when major power sources stop suddenly or when sudden changes happen in the demand. To mitigate the impact of these events, advanced control systems are employed to manage these reserves. This research focuses on how controller designs, LFC performance, and reserve services for emergency operations are connected. By improving how controllers respond and optimising reserve strategies, this research aims to advance modern power system controls that are not only robust and reliable but also responsive to emerging energy trends.

1.2. Problem statement

The rising penetration of RES, especially PV systems, in contemporary power systems has presented substantial challenges in ensuring system stability and reliability. In contrast to traditional synchronous generators, PV-based RES possess inherent intermittency and non-dispatchability, generating time-varying levels of output that are governed by meteorological conditions such as solar irradiation and cloud cover. These variabilities are likely to result in frequency deviations, thereby undermining the stability of the electrical grid. Traditional power plant regulators, typically appropriate for predictable and controllable generation sources, are not equipped to handle the fast and random nature of PV generation.

To counter these imbalances and ensure frequency stability, power systems have increasingly integrated energy storage systems (ESS), including battery storage. Although ESS provides a practical solution for both absorbing and delivering power amidst generation-demand imbalances, its integration with the grid presents novel dynamic properties that traditional control approaches tend to be inadequate. This changing grid landscape demands more sophisticated, intelligent control strategies that adaptively address the compounded uncertainty of RES and ESS.

LFC optimisation under the presence of RES with PV and ESS is essential in guaranteeing system balance, in addition to enabling efficient emergency reserve services. Emerging control techniques such as AI-based algorithms, MPC, and adaptive tuning can enhance power plant controllers' flexibility, response speed, and precision. The optimisation techniques offer the means to vastly enhance the performance of the controllers in counteracting dynamic grid conditions, thereby keeping power systems secure and efficient amidst the variability and uncertainty introduced by high integration of renewable energy resources.

The primary problem examined in this study is: To develop an improved power plant controller for maximising the penetration of renewable energy sources, particularly PV systems and ESS, for stability in the grid and effective use of emergency reserves by employing enhanced LFC techniques.

1.3. Research aim and objectives

The research project aims to develop a robust LFC to improve the dynamic performance of power systems integrated with PV and an energy storage system.

The following steps will be utilised to achieve the aim of the research.

- Investigate the impact of integrating renewable energy sources on load frequency control.
- Review existing control strategies and optimisation techniques.
- Modify a standard power system model and integrate a PV and BESS and analyse its dynamic response under varying load conditions.
- Analyse the dynamic performance of the standard power system with a conventional controller.
- Develop an improved adaptive control system using the Zebra Optimisation Algorithm.
- Simulate and analyse the proposed control system in MATLAB/SIMULINK.
- Analyse the performance of the ZOA-based control system in both single-area and two-area power systems**.**

1.4. Hypothesis

Implementing a ZOA-based adaptive load frequency control system in a power system integrated with PV sources and BESS is expected to enhance the dynamic performance. This control system should significantly reduce frequency deviations and settling time compared to conventional control strategies when faced with varying load conditions.

The adaptive nature of the ZOA-based controller is likely to improve the system's robustness against disturbances, such as fluctuations in PV output or sudden load shedding, thus helping to maintain grid stability. The proposed control scheme is anticipated to demonstrate improved robustness and adaptability in both single-area and multi-area power systems, ensuring reliable performance across different operating conditions.

In comparison to traditional control methods, the ZOA-based strategy is expected to achieve faster convergence, reduced oscillations, and better damping of frequency fluctuations. This shift will, in the end lead to an improved overall stability and efficiency of the power grid.

1.5. Delimitation of the research project

This research focuses on developing and optimising a ZOA-based controller for load frequency control in power systems. The study will concentrate on single-area and two-area power systems, specifically incorporating PV systems and energy storage solutions like BESS. Other types of renewable energy sources, such as wind or hydro power, will be excluded from this research. The analysis will be simulation-based, utilising MATLAB/SIMULINK to evaluate the performance of the ZOA-based control system, and will primarily focus on the ZOA algorithm, with comparisons to other optimisation techniques like PSO or GA.

The research will investigate the performance of the ZOA-based control system under specific load conditions, including step changes and random load fluctuations, while excluding other types of load disturbances. Certain assumptions will be made about system parameters, such as the capacity of the PV system or ESS, to simplify the analysis. This study will not involve real-world implementation or testing and will instead focus on the technical aspects of controller design, algorithm development, and performance evaluation. Economic or policy implications of renewable energy integration will not be considered.

1.6. Motivation of the research project

Reliability and stability in power systems are important to ensure that quality and consistent supply is provided that meet the energy needs of today's world. Frequency control plays a role in maintaining grid stability by regulating the grid frequency within acceptable limits. Deviation in frequency may cause malfunction of equipment, blackouts, and even grid collapse, which disturbs the supply of energy. The growing penetration of RES into power networks has introduced fresh challenges for the LFC,

basically because of their inherent intermittency and variability. Conventional control strategies tend to be ineffective in countering such variations, which results in decreased stability and reliability of the grid.

The development of adaptive algorithms, as represented by the ZOA, is key to addressing these challenges. Such algorithms have the ability to learn from past experiences, adjust to changing conditions, and optimise control parameters in real time, thus enabling improved LFC.

This research project aims to develop an optimised load frequency control system using ZOA, tailored to the specific needs of power systems integrated with PV and energy storage systems. By improving the dynamic performance of LFC, this study seeks to enhance grid stability, reliability, and efficiency. The outcomes of this research will benefit the energy industry in several ways. This project will increase grid reliability and stability and reduce power outages and equipment loss frequency through improving controller design. It will further facilitate the control of increased penetration of solar and other RES into the grid, promoting greater renewable energy penetration. Furthermore, better control strategies will enable more efficient use of ESS, reducing energy waste and improving the overall system efficiency. Through encouraging adaptive control strategies to improve power system development, this study aims to achieve a more efficient, sustainable, and resilient power system infrastructure that will eventually aid in the transformation towards a low-carbon energy future.

1.7. Assumptions

In this research study, each control area is modelled into a single block equivalent model, which represents the turbine, governor and load block. The system parameters, including the damping factor, time constants, are assumed to remain constant throughout the simulation, and the load changes are modelled as sudden step-type disturbances. The PV generation is treated as deterministic, with output fluctuations modelled as external disturbances. Both the PV and BESS are represented by a first-order transfer function with constant parameters. All the simulations are done in MATLAB/Simulink under ideal numerical conditions, assuming that the sampling times and solver settings do not significantly affect the control performance.

1.8. Research design and methodology

This study employs a simulation-based research approach grounded in control systems theory and optimisation methods, leveraging the strengths of both fields to develop an effective LFC strategy for power systems integrated with RES and ESS. By utilising

simulation tools and techniques, this research aims to replicate real-world power system dynamics, allowing for the testing and validation of control strategies in a controlled environment. The simulation-based approach enables the exploration of a variety of scenarios, including sudden load fluctuations and high penetration levels of RES, providing valuable insight into complex power system dynamics and the design of resilient control solutions.

1.8.1. Literature review

A comprehensive literature review is conducted to examine the current state of power plant control, renewable energy integration, and energy storage systems, highlighting recent advancements and persisting challenges. This review specifically focuses on existing power plant controllers, analysing their capabilities and limitations in handling renewable energy sources, as well as advanced control strategies that have been proposed to enhance grid stability. The analysis examines a range of power system applications using optimisation algorithms, establishing whether they are effective and can be enhanced. By synthesising the findings from this literature review, this study aims to inform the development of an optimised control strategy that addresses the complexities of modern power systems. And will provide insights into effective approaches and identify potential areas for innovation and improvements that can contribute to the progress of more stable and sustainable power systems control design.

1.8.2. Data collection

All system parameters used in the simulations were obtained from standard LFC test models available in the literature. Load and PV generation were introduced using a step function. The PID parameters were initially tuned using Ziegler-Nichols rules and further optimised using the ZOA and PSO, and the results obtained are then compared.

1.8.3. Simulation

This research study uses MATLAB/Simulink for simulation, focusing on the key objectives to be achieved. Firstly, a standard single-area benchmark system from (Saadat, 1999) is used for the investigation of LFC. The Model is also developed in the MATLAB/Simulink environment based on the formulation presented in (Saadat, 1999; Akter et al., 2022) . This model includes the basic dynamic components of LFC, which include the governor, turbine and generator-load, which describe the frequency response of a single area under varying load. The investigation on the model is done to show the baseline frequency deviation characteristics of the system. The model is later modified to include the PV generation unit and BESS to examine their influence on the

system frequency response without a controller. Following this, a conventional PID controller, due to its simplicity and robustness, is introduced to regulate frequency and improve the dynamic performance of the system under varying conditions. To address the shortcomings of a conventional controller in managing nonlinear systems and the limitations of fixed parameters in a PID controller, the ZOA algorithm is used to tune the PID controller's parameters and is later compared to the PSO. Performance will be measured based on parameters like peak overshoot, frequency deviation, settling time, and response time

1.9. Thesis chapters

1.9.1. Chapter 1

This is the introductory chapter that includes the problem statement, aims and objectives, motivation of the research project, hypothesis, delimitation of the research, and research design and methodology.

1.9.2. Chapter 2

The chapter covers the literature review on LFC, the impact of high renewable energy penetration on the grid, and the different optimisation algorithms, and their application to LFC.

1.9.3. Chapter 3

In this chapter, the modelling of the single-area system, the solar PV system, and the BESS, along with steady-state analysis and the system's dynamic behaviour, are presented. This also includes the modelling of the two-area power system and the optimisation algorithm.

1.9.4. Chapter 4

This chapter first simulates the single-area LFC system without a controller to establish a baseline, then introduces a PID controller and subjects the system to disturbances to observe the response**.**

1.9.5. Chapter 5

This chapter presents a simulation of different scenarios using the introduced algorithm.

1.9.6. Chapter 6

This chapter presents several simulation cases to examine the algorithm's performance in a two-area system.

1.9.7. Chapter 7

This chapter concludes and also proposes future research related to this study.

1.10. Conclusion

The chapter introduced the research aim and objectives, outlining the focus on developing an optimised LFC strategy for power systems with integrated RES and ESS. The methodology and scope we also presented. The next chapter presents a detailed literature review exploring the research efforts on LFC and the application of optimisation algorithms in controller design.

CHAPTER TWO
LITERATURE REVIEW

2.1. Introduction

Understanding the fundamental concepts and existing and emerging technologies in LFC is important to addressing the challenges of maintaining frequency in modern power systems. A deeper understanding of frequency regulation, renewable energy integration, and energy storage is necessary to develop a control solution that can adapt to the dynamic behaviour of the modern system.

This chapter presents an overview of key concepts and recent developments in frequency control. Section 2.2 presents an overview of the development of the research, from the main articles that address the main and other related articles. Section 2.3 presents the frequency control levels, Section 2.4 focuses on LFC in power systems, Section 2.5 discusses renewable integration and challenges introduced, Section 2.6 discusses energy storage and application in power systems, Section 2.7 discusses the different LFC techniques, Section 2.8 presents the various optimisation algorithms, and Section 2.9 presents a comparative analysis of the different algorithms for LFC.

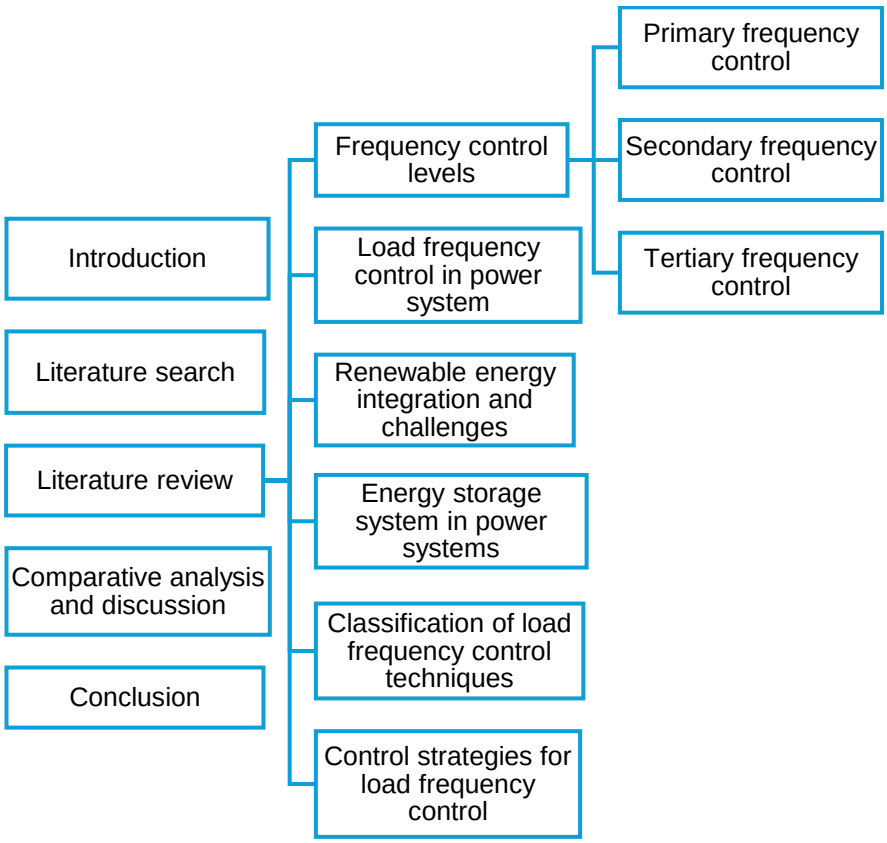

Figure 2-1: Literature review outline

2.2. Literature search

This literature review examines and analyse existing research and methodologies related to LFC, the integration of RESs and the role of ESSs. The objective of this research is to improve an optimised control algorithm, specifically using the ZOA for improving frequency regulation in single and multi-area power systems. To achieve this objective, it is necessary to gain deep knowledge in control theory, optimisation techniques, and dynamic power system simulations. The methods and knowledge to be developed in this research include:

- Mathematical modelling of a single area and multi-area LFC systems
- Dynamic modelling and control of PV and BESS integration
- PID controller tuning using classical and optimisation methods
- Implementation of bio-inspired and swarm optimisation algorithms
- MATLAB/Simulink-based simulation and validation of the LFC performance
- Performance analysis using criteria such as the settling time, frequency deviation, and control effort

The following list shows a summary of the main papers that have been reviewed in this research, and Figure 2-2 shows the number of papers reviewed in the chapter.

- Khan, I. A., Mokhlis, H., Mansor, N. N., Illias, H. A., Jamilatul Awalin, L., & Wang, L. (2023). New trends and future directions in load frequency control and flexible power system: A comprehensive review. In Alexandria Engineering Journal (Vol. 71, pp. 263–308). Elsevier B.V. https://doi.org/10.1016/j.aej.2023.03.040
- Singh, B., Slowik, A., & Bishnoi, S. K. (2023). Review on Soft Computing-Based Controllers for Frequency Regulation of Diverse Traditional, Hybrid, and Future Power Systems. In Energies (Vol. 16, Issue 4). MDPI. https://doi.org/10.3390/en16041917
- Trojovska, E., Dehghani, M., & Trojovsky, P. (2022). Zebra Optimisation Algorithm: A New Bio-Inspired Optimisation Algorithm for Solving Optimisation Algorithm. IEEE Access, 10, 49445–49473. https://doi.org/10.1109/ACCESS.2022.3172789
- Mohapatra, S., & Mohapatra, P. (2023). American zebra optimisation algorithm for global optimisation problems. Scientific Reports, 13(1). https://doi.org/10.1038/s41598-023-31876-2
- Qi, Z., Peng, S., Wu, P., & Tseng, M. L. (2024). Renewable Energy Distributed Energy System Optimal Configuration and Performance Analysis: Improved

Zebra Optimisation Algorithm. Sustainability (Switzerland), 16(12). https://doi.org/10.3390/su16125016

- Kouba, N. E. Y., Menaa, M., Hasni, M., & Boudour, M. (2017). A new optimal load frequency control based on hybrid genetic algorithm and particle swarm optimisation. International Journal on Electrical Engineering and Informatics, 9(3), 418–440. https://doi.org/10.15676/ijeei.2017.9.3.1

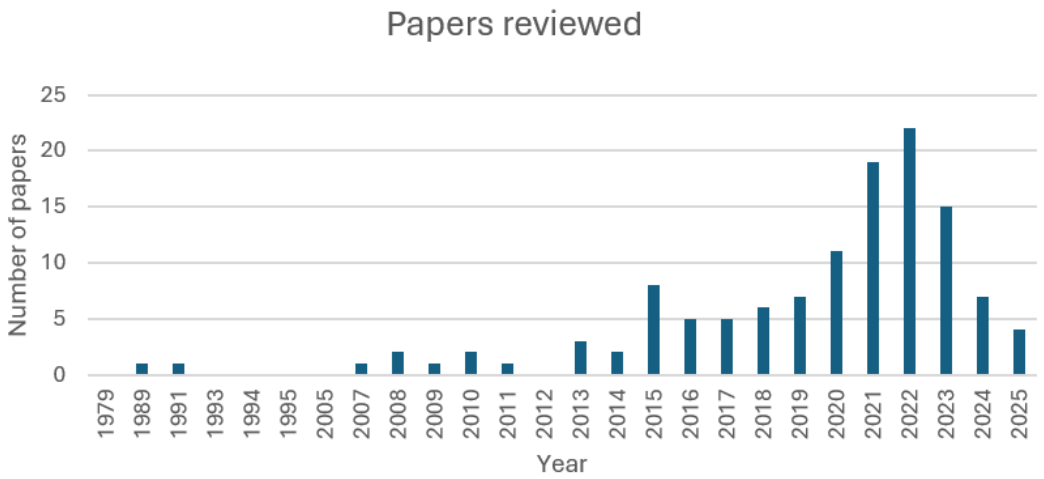

Figure 2-2: A graph of reviewed papers

The following are the keywords which were used during the search in databases such as the IEEE Xplore, ScienceDirect, and SpringerLink.

- Smart grid frequency control
- Load frequency control
- Frequency regulation in power systems
- Renewable energy integration
- Energy storage systems
- Photovoltaic grid integration
- Classical control in power systems
- PID tuning
- Metaheuristic algorithms in power systems
- Zebra optimisation algorithm
- Swam intelligence for LFC

2.3. Frequency control

Sustained off-nominal frequency deviations pose a risk to the security and stability of the power grid. Prolonged frequency disturbances can lead to the malfunctioning of protection devices and possible damage to the system equipment (Bevrani et al., 2021). The impact of a frequency deviation is determined by its magnitude and duration. The magnitude reflects the extent of the generation-load imbalance, and the duration refers

to how long the deviation persists. Both of these factors influence the type and urgency of the frequency control action required.

Frequency control is implemented through a hierarchical structure that includes primary, secondary, tertiary and, when necessary, emergency control levels. Each control level plays a role in mitigating frequency deviations and restoring grid balance. Figure 2-3 shows the frequency response model with the control loops.

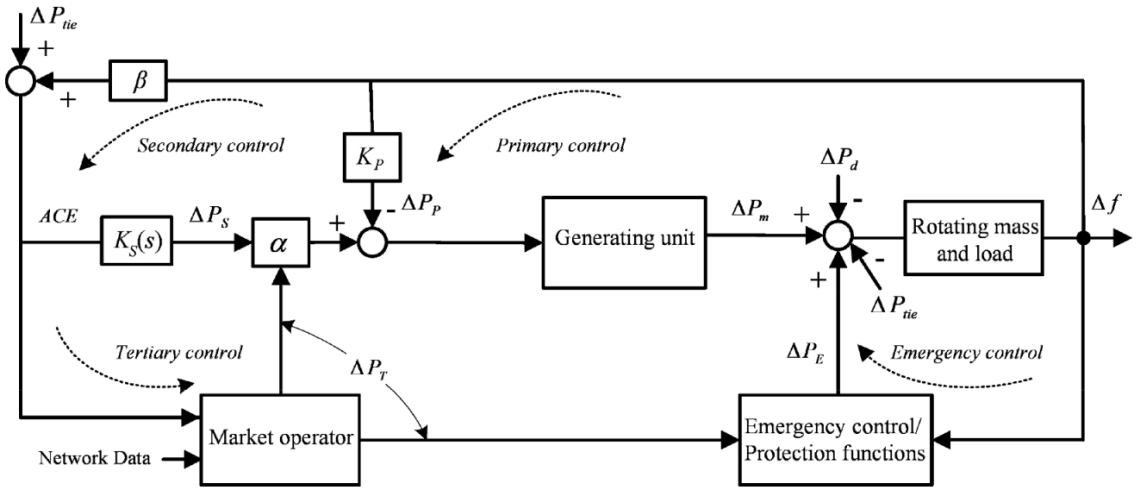

Figure 2-3: Frequency response model and control loops (Bevrani, 2009)

Where:

ΔP_{tie} is the tie line power change

β is the area bias factor

$K_s(s)$ is the transfer gain of the secondary control loop

ΔP_s is the control signal for secondary control

K_p is the transfer gain of the primary control loop

ΔP_p is the control signal for primary control

ΔP_T is the control signal for tertiary control

ΔP_m is the generator's mechanical power change

ΔP_d is the load or generation disturbance

ΔP_E is the control signal for emergency control

Δf is the transient change

While frequency regulation in conventional power systems is supported by the inherent inertia of synchronous machines and a well-defined control structure, the growing integration of inverter-based renewable energy sources has altered these dynamics. Solar power connects to the grid via inverters, which lack the rotational mass of synchronous generators and therefore cannot contribute to the system's inertia during disturbances. This results in traditional control mechanisms being insufficient in

renewable-connected systems. It is thus important to understand how PV integration affects the different frequency control levels. Figure 2-4 Illustrates this transition by presenting the LFC model with renewable energy integration.

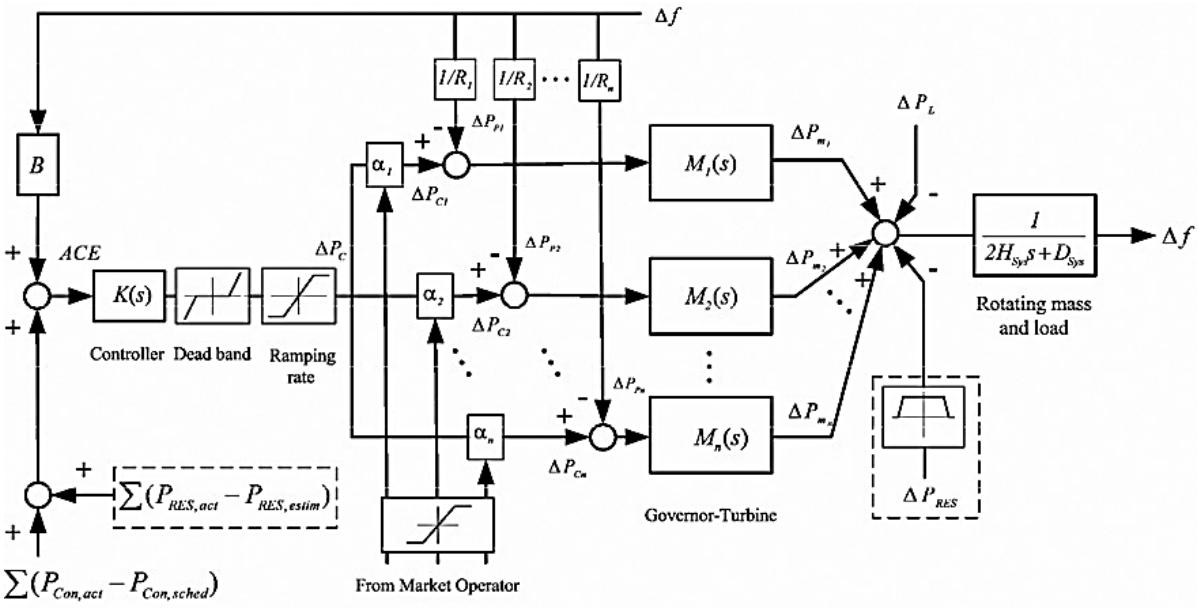

Figure 2-4: LFC model with renewable energy integrated (Bevrani et al., 2010)

2.3.1.Primary frequency control

Primary control is the first and fastest line of defence against minor frequency disturbances. It is decentralised and performed automatically by the governor-droop mechanism of synchronous generators (Datta et al., 2019) . Immediately following a disturbance, all participating generators adjust their output in response to local frequency changes. This response typically occurs within seconds and helps to arrest the frequency droop. However, due to the nature of droop control, the frequency settles to a new steady-state value that differs from the nominal frequency. In multi-area systems, the tie-line power exchange between the interconnected areas may also settle at levels different from the predefined values, which will require further actions to correct that error (Rajan et al., 2021; Fu et al., 2017).

When PV plants are integrated into the grid, they operate as grid-following inverters, which inject the maximum available power regardless of changes in frequency. Since they do not directly contribute to primary control, to address this limitation, advanced inverter controls such as droop-based virtual synchronous generator (VSG) control or synthetic inertia algorithms have been proposed (Meng et al., 2019). These allow PV inverters to adjust active power output in response to frequency deviations, thus emulating primary control behaviour.

2.3.2. Secondary frequency control

When frequency deviation persists beyond the primary loop's response time, the secondary control, often referred to as LFC, is engaged. The secondary control helps keep the frequency at its nominal level and adjusts the power flow between connected systems Click or tap here to enter text.(Rodrigues et al., 2020). This control is implemented through Automatic Generation Control (AGC), which adjusts generator outputs based on a centralised Area Control Error (ACE) signal (Ullah et al., 2021). The ACE considers both local changes in frequency and the overall power flow between areas. Secondary controls work over a period of seconds to minutes and use the available power reserves. It is more precise than the primary control for maintaining stability over time.

The variability of PV generation when integrated into the grid complicates secondary frequency control. As fluctuations in solar irradiance increase, a need for additional reserves and a faster response from the AGC arises (Ram Babu et al., 2023). PV plants can contribute if coupled with BESS, which provides the flexibility required for secondary regulation. The LFC model is therefore updated to include an additional disturbance term representing renewable fluctuations (ΔP_{RES}) as shown in Figure 2-4. The modified response, including RES integration, is expressed as:

$$\Delta f(s) = \frac{1}{2Hs + D}\left[\sum_{i=1}^{n} \Delta P_{Mi}(s) - \Delta P_{L}(s) - \Delta P_{RES}(s)\right] \quad \text{2-1}$$

2.3.3. Tertiary and emergency frequency control

For a severe disturbance, such as a major fault or significant loss of generation, primary and secondary controls may not be adequate to restore system balance. In such cases, tertiary control is activated. This control level involves more deliberate and coordinated actions, such as rescheduling generation, connecting or disconnecting standby units, and reconfiguring power reserves (Md. Alam et al., 2023). The tertiary control operates over minutes to hours and is important for restoring the frequency to its operational state and preparing for future contingencies.

If all previous levels fail to restore the system frequency or if the deviation is extreme and rapid, the emergency control mechanism must be employed. These include under-frequency load shedding (UFLS) schemes, which disconnect portions of the load to prevent a complete system collapse (Gordon et al., 2022). UFLS is typically triggered automatically when frequency falls below the threshold, which acts as the last line of

defence to maintain the system's integrity and prevent blackouts (Bevrani et al., 2010; Bustamante et al., 2023).

High PV penetration can increase the risk of rapid frequency decline, since inverter-based plants disconnect from the grid under abnormal conditions, unless specifically programmed for fault-tide-through. Modern grid regulations now require PV units to stay connected during emergencies. They must help restore the grid by providing reserved power or responding quickly to frequency changes (Al-Shetwi & Sujod, 2018).

2.4. Load frequency control in power systems

Power systems worldwide are designed to deliver a reliable and continuous electricity supply, balancing power generation and demand at every moment. One critical aspect in ensuring this balance is LFC, which maintains the system frequency within prescribed limits and stabilises power flows. LFC achieves this by managing the output of power plants and, in some cases, controlling energy storage systems to compensate for frequency deviations caused by fluctuations in load and generation (Gulzar et al., 2022a; Pan & Liaw, 1989; Rasolomampionona et al., 2024). Given the rapid integration of RES and the reduction in system inertia, the role of LFC has become more complex and important. Its performance is important for preventing failures and protecting the stability of the infrastructure. In modern systems, the challenge of LFC is amplified as variable RES, such as solar and wind power, introduce greater volatility and unpredictability in generation profiles, making precise frequency control more complex (Tungadio & Sun, 2019a; Tungadio & Sun, 2019b; Wang et al., 2024; Datta et al., 2016)

2.5. Renewable energy integration and challenges

The integration of RES has become central to modern power systems due to the benefits they offer. Figure 2-5 shows the increase in renewable energy generation in South Africa from 2000 to 2022.

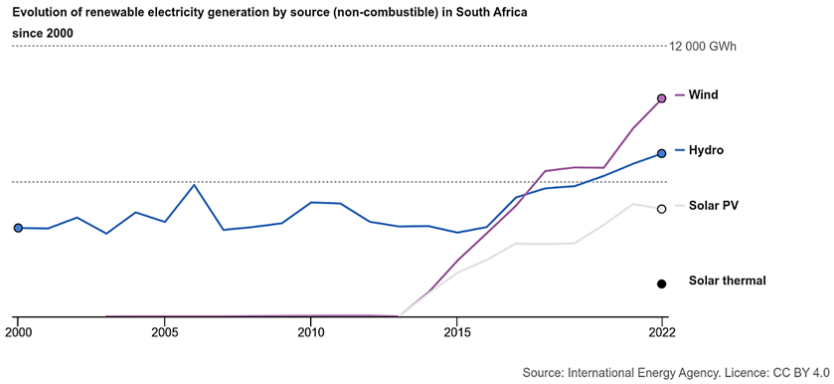

Figure 2-5: Evolution of renewable electricity generation (IEA, 2025)

With the benefits to the environment and meeting the energy demand, the transition to renewable energy, however, introduces various technical challenges. As renewable generation increases, these challenges become more noticeable, affecting the system's inertia, frequency stability, and the effectiveness of traditional LFC strategies (Mokhtar et al., 2022; Gulzar et al., 2022b). These energy sources can fluctuate and may not be available all the time. Their availability depends on factors such as weather and time of day. As a result, fluctuations in RES pose challenges for maintaining LFC. Frequency stability becomes more difficult to achieve as the fluctuating output of renewables leads to frequent imbalances between generation and demand. Changes in power generation make it harder to predict how much electricity will be generated. This complicates forecasting energy usage and managing the grid(Tungadio & Sun, 2019a).

One major challenge of having many RESs is the reduction in synchronous inertia. Unlike traditional synchronous generators, renewable energy systems connect to the grid via power converters that do not provide mechanical inertia. The absence of inertia reduces the grid's capability to withstand frequency deviations during sudden disturbances (Hajiakbari Fini & Hamedani Golshan, 2018). Thus, advanced strategies, including ESS, improved reserve capacities, and robust grid control technologies, are necessary to ensure the system's reliability. This results in a higher rate of change of frequency (RoCoF) during disturbances (Yousef, 2017).

The developments in control technology allow these systems to imitate inertia, though they are less effective when compared to traditional mechanical inertia, especially when dealing with significant disturbances. To mitigate these challenges, power systems rely on ESS, grid-forming inverters, and improved grid control methods to provide faster frequency response (Li et al., 2021; Yan et al., 2015).

The integration of solar PV systems has increased, driven by declining costs, supportive policies, and the global push towards renewable energy. In the past two decades, the improvement in manufacturing and production has reduced the costs of solar panels and related systems, making solar energy a more affordable option to consumers (see Figure 2-6). Government policies such as subsidies, tax incentives, and renewable portfolio standards have further accelerated adoption (Ma & Xu, 2023).

Solar PV is also a key factor in improving energy access, especially in remote and underserved regions. Off-grid solar PV systems, including microgrids, are providing electricity to millions of people who previously lacked access. Despite its rapid expansion, the growth of solar PV demands advanced solutions to address grid integration challenges and maintain power system stability (Chaianong & Pharino, 2015).

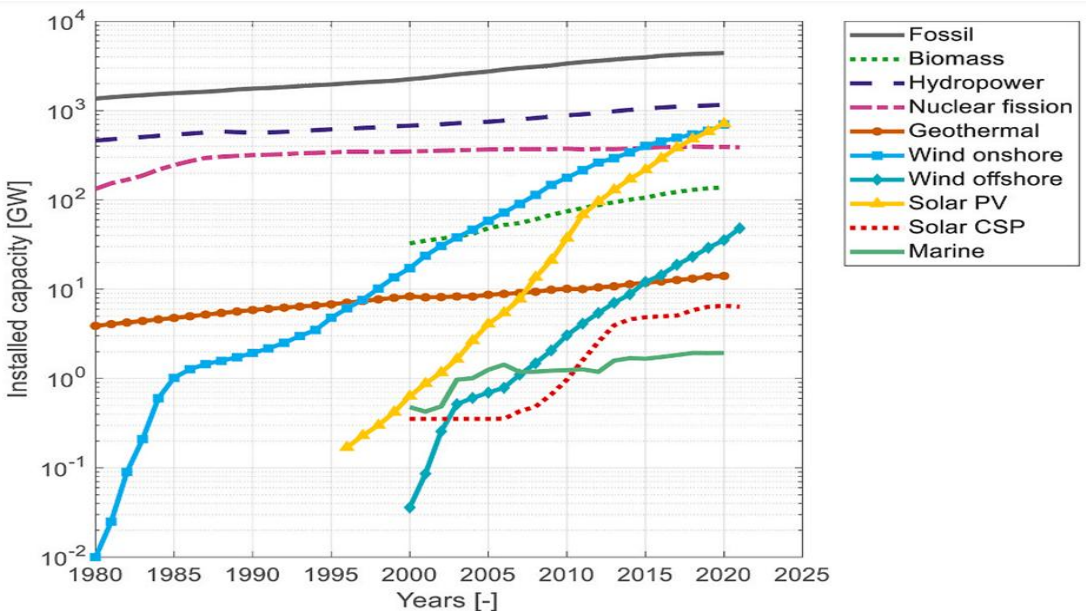

Figure 2-6: Global trends for installed capacity (Lerede & Savoldi, 2023)

This intermittency requires the deployment of complementary systems such as energy storage or backup generation to ensure a continuous power supply.

The integration of solar PV systems into power grids significantly impacts LFC. Unlike conventional synchronous generators, solar PV systems' lack of inherent inertia increases the grid's vulnerability to frequency deviations. This issue becomes more serious during abrupt changes in generation or load, as the grid's capacity to stabilise frequency relies on the available inertia (Akinyele & Rayudu, 2014).

2.6. Energy storage system in power systems

Integrating ESS with PV systems solves many challenges that are caused by the unpredictability of solar energy. The solar PV systems only generate power during the day. The output also varies based on the weather conditions and the solar irradiance. Without proper energy storage, the variation in the output causes problems for the power grid. It can lead to overgeneration when the sunlight is available and not enough during cloudy times or at night. Using ESS with the PV systems helps provide a steady and reliable energy supply. This improves stability within the grid (Akinyele & Rayudu, 2014).

One of the most important benefits of ESS in solar PV integration is its ability to smooth out power output. When solar PV generation exceeds demand, ESS can store the surplus energy for later use (Palizban & Kauhaniemi, 2016; Toledo et al., 2010). During cloudy periods or at night, the stored energy is dispatched, ensuring a steady supply to the grid. This capability reduces the reliance on conventional fossil-fuel-based peaking plants, making the overall energy system cleaner and more sustainable. In addition to

energy storage, ESS integrated with solar PV can provide a wide range of ancillary grid services. Figure 2-7 shows the grid services provided by the ESS.

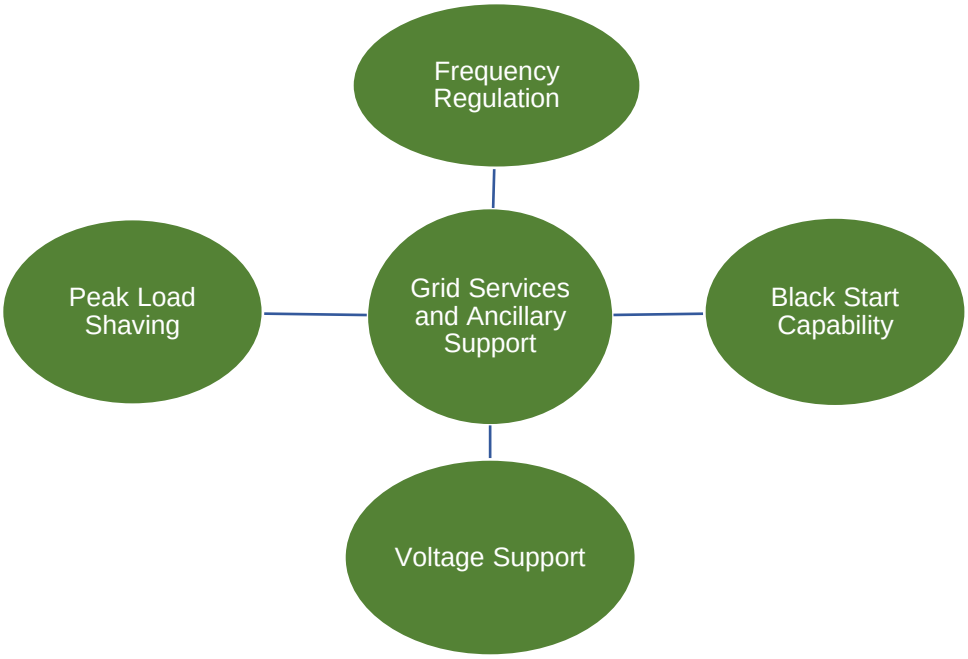

Figure 2-7: Grid services and ancillary support

- Frequency Regulation: ESS help maintain frequency stability by injecting or absorbing power. This is important in systems with high penetration of RESs, where power output varies, causing problems for the grid (Tan et al., 2021; Wang et al., 2022).
- Voltage Support: ESS can help maintain the voltage levels by supplying reactive power in renewable-rich systems (Xie et al., 2020; Li et al., 2018).
- Peak Load Shaving: ESS can store energy when the demand is low and release it back to the grid when demand is high. This helps ease the pressure on the grid and delays the need for expensive upgrades to the infrastructure (Chua et al., 2020; Lange et al., 2020).
- Black Start Capability: In the event of a grid outage, ESS with RESs can help restore power. They act as backup energy to restart the power grid (Abeynayake et al., 2022).

In areas with no reliable electricity supply, solar PV and ESS are improving energy access. Standalone PV systems and ESS are providing reliable, off-grid power, which reduces the dependency on diesel generators. In Microgrids, ESS helps communities and businesses to become more self-sufficient with energy. Which means they can maintain a stable power supply even when the main grid has issues. The integration can also be improved by implementing energy management systems (EMS), which use real data to optimise energy use and prioritise stability.

Integrating ESS with solar power presents its own challenges, like high cost, limited battery life, and energy loss. New storage technologies, such as lithium-ion and solid-state batteries, are helping to address these challenges (Ali et al., 2023; Saldarini et al., 2023).

There are different ESS technologies for various applications within the grid. They differ according to their energy density, power capacity, response time, cost, and lifespan (Maeyaert et al., 2020). They are categorised into either mechanical, electrochemical, chemical or electrical. The major types of energy storage technologies are included in Figure 2-8.

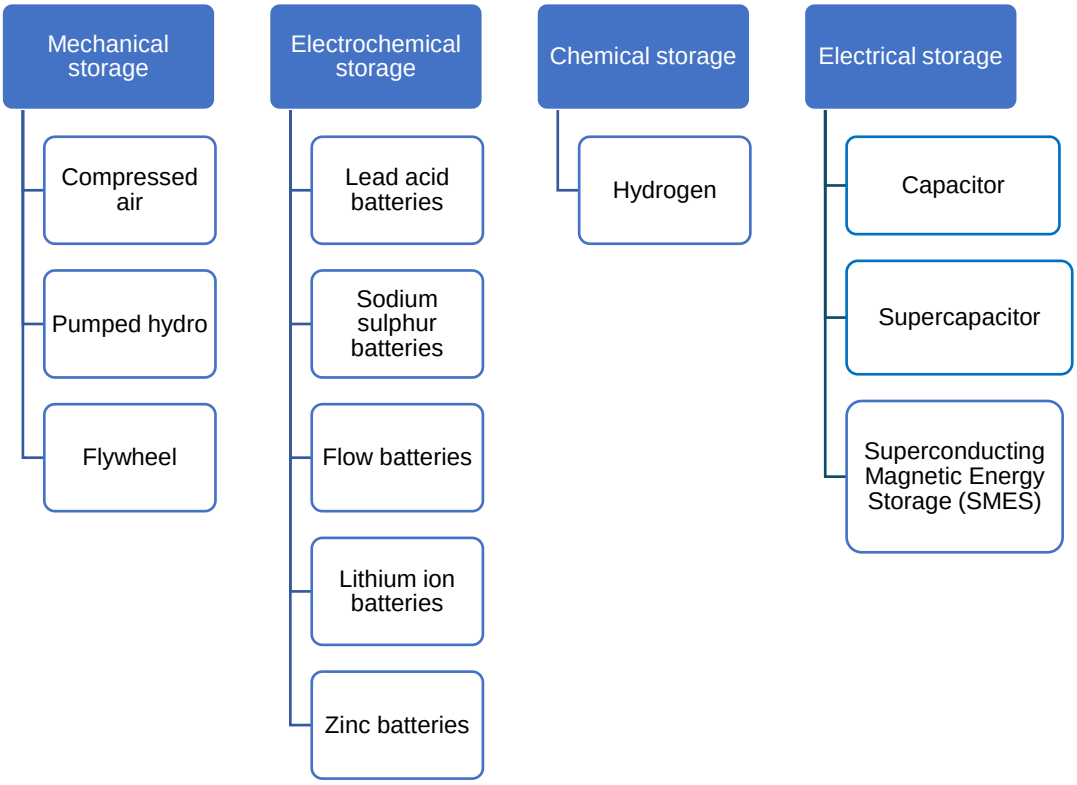

Figure 2-8: Energy storage system technologies

Mechanical energy storage systems, such as pumped hydro, flywheels, and compressed air energy storage (CAES), rely on physical mechanisms to store energy. Pumped hydro stores energy by pumping water and releasing it to generate electricity. It offers high efficiency and a longer lifespan, making it an ideal solution within power system applications (Coban et al., 2022; Zeng et al., 2013). Flywheels store energy through rotational motion, allowing for quick charging and discharging capabilities with high efficiency. However, these systems are often constrained by geographical requirements such as reservoirs for pumped hydro and large space needs, which make them less viable for all locations (Amiryar & Pullen, 2017; Choudhury, 2021; Takahashi & Tamura, 2008).

Electrochemical energy storage stores energy in the form of chemical energy, which includes lithium-ion, lead-acid, and flow batteries. Lithium-ion batteries are popular for portable devices and electric vehicles because they store a lot of energy and work efficiently. Flow batteries, on the other hand, can be easily scaled up for use in power grids (Arsalis et al., 2022). These technologies have some challenges. They don't last long, cost a lot, and rely on materials that are hard to find, like lithium and cobalt. Despite these issues, they remain key players in renewable energy integration and portable power systems (Šimić et al., 2021; Brivio et al., 2016; Cucchiella et al., 2016).

Chemical energy storage focuses on storing energy in fuels such as hydrogen, synthetic fuels, and ammonia (Alzahrani et al., 2022; Arsad et al., 2022; Vichos et al., 2022). These systems have the advantage of high energy density and are well-suited for long-term and large-scale energy storage. For instance, hydrogen can be produced through electrolysis and later used in fuel cells to generate electricity. Their efficiency is relatively low (30–50%), and the production, storage, and transport infrastructure is costly. Safety concerns, such as flammability, also pose challenges for widespread adoption.

ESS, encompassing technologies like supercapacitors and SMES, stores energy in electric or magnetic fields. These systems excel in rapid charge and discharge cycles with exceptional efficiency (90–99%). Supercapacitors, for example, are used in applications requiring high power delivery over short durations. However, their low energy density and high material costs make them less suitable for large-scale or long-term storage, limiting their applications to niche markets like power stabilisation (Fagiolari et al., 2022; Kim et al., 2019; Inthamoussou et al., 2013; Krpan & Kuzle, 2021). These diverse technologies provide flexibility to address various challenges in modern power systems, from short-term frequency regulation to long-duration energy shifting.

The ESS can participate in all control levels by injecting or absorbing power in response to sudden frequency deviation, which acts as a form of virtual inertia. These ESS technologies, unlike synchronous machines, can provide immediate active power compensation without mechanical delay. They can also be charged or discharged based on the ACE, which helps bring the system frequency back to nominal. This will further be shown in the simulation cases.

2.7. Classification of load frequency control techniques

2.7.1. Traditional control techniques

One of the most commonly used approaches in LFC is the PID controller, which adjusts the power generation output based on frequency deviations. The PID controller is one of

the most widely used feedback control mechanisms in industrial and power systems due to its simplicity and effectiveness in ensuring system stability and performance. The PID controller combines three control actions—proportional, integral, and derivative—to manage the error between a system's desired setpoint and its output (Hote & Jain, 2018). The proportional (P) term provides a corrective action proportional to the error, offering an immediate response to deviations. Proportional control alone cannot eliminate steady-state error, which the integral (I) term addresses. The integral term accumulates the error over time and adjusts the control action to ensure the system eventually reaches its desired setpoint without any persistent offset. Finally, the derivative (D) term predicts future errors by measuring the rate of change of the error, adding damping to the system, and improving stability by mitigating overshoot and oscillations. Figure 2-9 shows a block diagram of a PID.

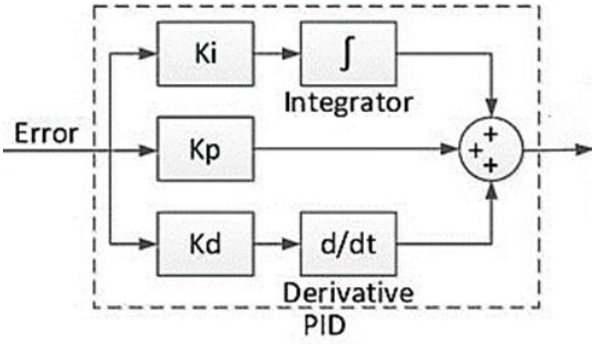

Figure 2-9: PID controller block diagram

In LFC systems, PID controllers are essential for regulating frequency and ensuring a balance between power generation and demand. PID controllers minimise frequency deviations caused by load variations by dynamically adjusting parameters like generator output or valve positions. The PID controller's versatility extends to various applications, from simple temperature regulation to complex multi-area power systems performance. Researchers have also made use of the properties of the P and I to implement controllers such as the PD-(1+PI) (Benbouhenni et al., 2022), PDF+(1+PI), which is a combination of the Proportional Derivative Filter and PI (Nayak et al., 2019b; Biswal et al., 2023). These controllers offer quicker error response and improve the stability of the system, however, challenges such as the inability to adapt to changing system dynamics, difficulties handling nonlinearities and uncertainties, sensitivity to disturbances, and complexity require further tuning (Ahmed et al., 2022). Table 2-1 shows some of the control techniques derived from the classical controllers P, I, and D.

Table 2-1: Control techniques

Control technique	Reference
PIDF	(Shouran et al., 2021)

FO-PI	(Yousef et al., 2020)
FO-PID	(Qasim et al., 2024)
2DoF-PID	(Sahu et al., 2013)
PIDN-TIDF	(Zare et al., 2023)
TID	(Topno & Chanana, 2018)
TIDN	(Lalngaihawma et al., 2024)
TIDF	(Kumar Sahu et al., 2016)
I-TDF	(Singh et al., 2021)
3DoF-ID	(Rahman et al., 2015)
3DoF-PID	(Naga Sai Kalyan & Suresh, 2022)
2DoF-TIDF	(Sahu, Simhadri, Mohanty, Hota, Abdelaziz, Albalawi, Sherif S. M. Ghoneim, et al., 2023)
2DoF-TID	(Sahu, Simhadri, Mohanty, Hota, Abdelaziz, Albalawi, Sherif S.M. Ghoneim, et al., 2023)
TFOIDFF	(Mohamed et al., 2022)

Even though these techniques offer better performance than the PI or PID, the added parameters to be tuned add complexity to the system and mean heavier computation. They can still be tuned for faster dynamic response, which often comes at the expense of robustness. With LFC, aggressive tuning that prioritises quick settling time and minimal overshoot may make the system more sensitive to large disturbances or variations in the system parameters (Khalil et al., 2023).

Since these controllers depend on tuning for better performance, proper tuning is important to ensure a balance between fast response, minimal overshoot, and stability. Poorly tuned controllers can result in slow responses or unstable behaviour. Figure 2-10 shows the tuning methods that can be used to tune the parameters of the controller. This consists of manual tuning methods and computational methods.

The manual tuning methods, such as the Ziegler-Nichols and trial and error, rely on hands-on adjustments and empirical rules, while computational methods use mathematical optimisations and algorithms to determine the controller parameters. Manual tuning methods require minimal computational resources and can be applied without a precise mathematical model of the system, but they are heavily dependent on the operator's skill. They may not produce true optimal performance, especially when complex or nonlinear systems are considered. In contrast, computational methods such as the swarm-intelligence-inspired use numerical search techniques to optimise the performance criterion. They can handle multi-parameter tuning, nonlinear systems, and complex systems (Nagaraj et al., 2008).

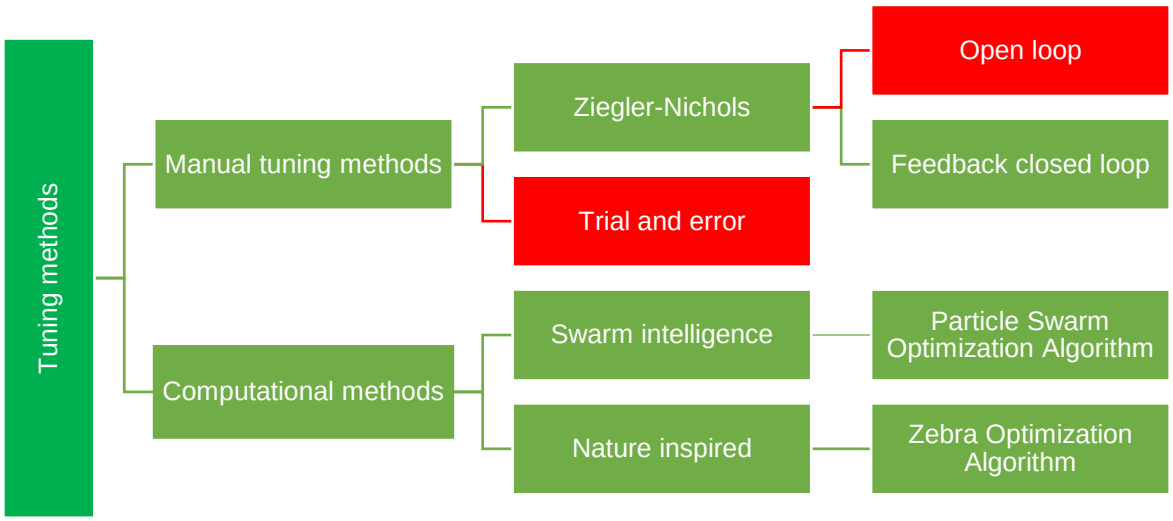

Figure 2-10: Different tuning methods

2.7.2. Soft computing

LFC systems face increased challenges due to the variability and uncertainty of the energy sources. Soft computing techniques have emerged as powerful tools to tackle these challenges, providing robust and adaptive solutions for managing frequency and power balance in such dynamic environments. Unlike traditional computing methods, soft computing mimics human reasoning and decision-making under uncertainty. Techniques such as Artificial Neural Networks (ANN) (Khadarvali et al., 2022), fuzzy logic (Suganthi et al., 2015), metaheuristic optimisation, non-predictive algorithms, and probability-based approaches have been employed to improve the performance of LFC systems(Behera et al., 2015). Figure 2-11 shows the soft computing techniques, which are tailored to address the stochastic nature of power systems integrated with RES.

ANNs are particularly well-suited for LFC due to their ability to learn and generalise from historical data. They model nonlinear and time-varying system behaviour, making them highly adaptable to the dynamic nature of RES. ANN-based LFC systems can predict control actions in real time, ensuring rapid and effective frequency regulations. Fuzzy logic, on the other hand, provides a rule-based framework that interprets imprecise inputs and delivers smooth, reliable control actions (Maji & Ganguli, 2025). By employing linguistic rules, fuzzy logic controllers (FLC) manage power dispatch from devices like BESS, mitigating frequency deviations caused by renewable variability (Mohammed et al., n.d.; Bhat Nempu et al., 2019; Sanki et al., 2021). Metaheuristic optimisation algorithms, such as PSO and GA, further improve LFC by optimising control parameters and strategies (Chang et al., 2007; Huang & Lv, 2023). These algorithms handle complex, multi-dimensional problems, ensuring optimal global solutions for frequency recovery and power sharing.

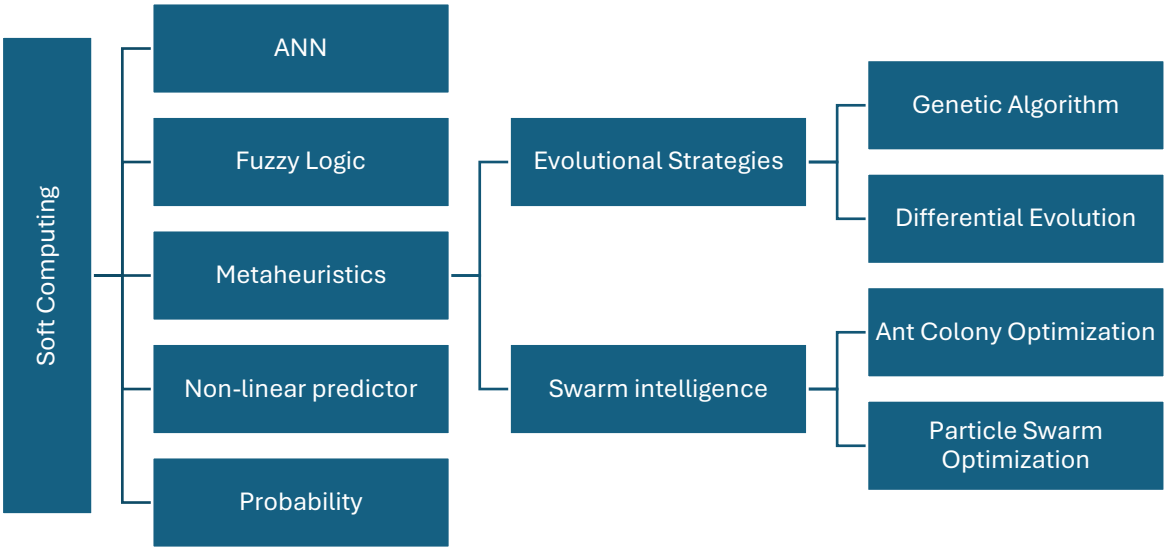

Figure 2-11: Optimisation algorithms

These non-predictive algorithms, which rely on real-time data instead of forecasts, offer another effective approach. These algorithms are particularly advantageous in scenarios where forecast errors are significant, providing immediate corrective actions to stabilise the grid.

Probability-based approaches model the stochastic behaviour of RES and load variations, which enables the LFC systems to make informed decisions under uncertainty and allocate resources effectively (Tayri & Ma, 2025). Hybrid systems that combine these techniques often deliver superior performance. For example, integrating ANN with FLC allows for adaptive and explainable control solutions, while metaheuristic optimisation can fine-tune fuzzy membership functions and ANN parameters. Such hybrid frameworks ensure better handling of renewable energy variability and improve the overall stability of the power grid. By leveraging these soft computing techniques, LFC systems can meet the challenges of modern, RES-integrated power systems with improved adaptability, efficiency, and resilience (M. S. Alam et al., 2023).

2.8. Optimisation algorithms

Optimisation algorithms play a role in improving the performance and efficiency of energy systems, particularly in renewable energy integration, LFC, and ESS management. These algorithms aim to find optimal solutions to complex, multi-variable problems by minimising costs, maximising efficiency, or achieving the best system performance under

given constraints. Optimisation methods are broadly categorised into heuristic and metaheuristic algorithms, each offering unique strengths and applications in energy systems. Figure 2-12 shows the taxonomy of the optimisation algorithms.

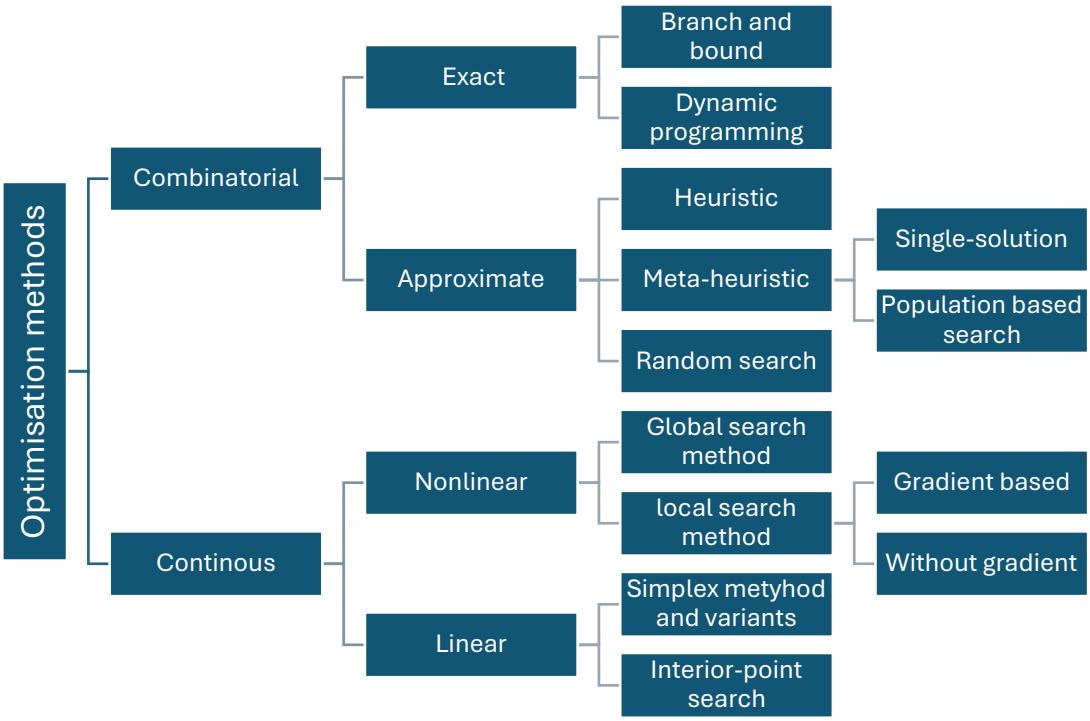

Figure 2-12: Optimisation algorithms taxonomy(Janga Reddy & Nagesh Kumar, 2020)

2.8.1.Heuristic algorithms

Heuristic algorithms are problem-solving techniques that employ rule-based approaches to find feasible solutions quickly. They use strategies such as the rule of thumb, educated guesses, intuitive judgment, or common sense to arrive at satisfactory solutions faster (Desale et al., 2015). Within optimisation, heuristics are meant to provide quicker or near-optimal solutions when classical algorithms are too time-consuming or cannot find the exact solutions. Though they do not ensure the best solution, they do give solutions near the best one, and sometimes even the optimal solution.

The decision to use heuristics involves a trade-off between completeness, optimality, accuracy, precision, and run time (Kokash, 2014). Heuristics often sacrifice finding the best or all possible solutions in favour of speed and aim to find satisfactory solutions that are acceptable to the problem. They deliver quick responses, but without a guarantee of accuracy, and at times, their margins of error may be great. Some heuristics are much faster than traditional approaches, and others only offer marginal speedups. It may be hard to judge their solution quality, especially when the optimal solution is not known, which makes quality estimation an issue that requires intense mathematical analysis.

Famous heuristics include the greedy heuristic and Hill climbing. The greedy heuristic builds solutions step-by-step by starting with an empty set and sequentially adding elements until a complete, feasible solution is formed (Chvatal, 1979). They are valued for their simplicity, ease of implementation and low computational complexity. The quality of the solutions they produce largely depends on the selection criteria used for adding elements, and they do not always guarantee optimal results. Hill climbing algorithm works well for complex problems but can get trapped in the local optima (Al-Betar, 2017).

2.8.2.Metaheuristic algorithms

Metaheuristic algorithms extend the capabilities of heuristic methods by incorporating mechanisms to explore and exploit the solution space more broadly. These algorithms are designed to avoid local optima and provide high-quality solutions to complex, multi-dimensional optimisation problems (Desale et al., 2015; Kapoor et al., n.d.). Metaheuristic approaches are particularly well-suited for energy systems optimisation, where multiple objectives, such as cost minimisation, emission reduction, and stability improvement, must be balanced (Ali et al., 2018). They are characterised by their ability to perform global search across a wide solution space, enabling them to identify near-optimal or globally optimal solutions. One of their key strengths is adaptability, as they are problem-independent and can be applied to a diverse array of optimisation problems with minimal adjustments (Adetunji et al., 2021). These algorithms strike a balance between exploration and exploitation; they use strategies to explore new, potentially better solutions while simultaneously refining and exploiting the most promising ones. This balance allows metaheuristics to efficiently explore complex optimisation landscapes.

Optimisation algorithms have emerged as a powerful tool for improving the performance of LFC by fine-tuning controller parameters, improving response time, and ensuring optimal system operation under dynamic conditions. Various optimisation techniques, such as the Ant Colony Optimisation (ACO)(Pal & Singh, 2024), Grey Wolf Optimiser (GWO) (c et al., 2019) and Artificial Bee Colony (ABC) (Fathy et al., 2022) have been applied to LFC problems. These algorithms offer advantages such as faster convergence, adaptability to nonlinear systems, and robustness against uncertainties (Gulzar et al., 2025). Figure 2-13 shows other metaheuristic algorithms.

The main difference between all the classes lies in the biological or physical phenomenon they draw inspiration from. Swarm intelligence algorithms are a class of optimisation techniques that draw inspiration from collective behaviours found in nature, such as the movement of bird flocks, the foraging patterns of ant colonies, or the schooling behaviour of fish (Tang et al., 2021). Simple agents in natural systems interact

with each other and their environment, resulting in highly efficient problem-solving abilities through their combined actions. Swarm intelligence-based computing techniques stem from the idea of decentralised, self-organised decision-making.

In LFC, these algorithms are employed to optimise controller parameters, so that the frequency deviation in power systems is minimised and maintain stability is maintained despite the variations in the system caused by the load changes and renewable energy integration (Tang et al., 2021). Unlike manual tuning methods, swarm intelligence algorithms explore the search space globally, relying on a population of candidate solutions (which are the agents or particles) that improve their performance through cooperation and sharing information. The process starts with a group of agents, each representing a potential solution. A fitness function evaluates how well each solution meets the objectives, using metrics like ITAE or ISE. The agents then update their positions using rules from the chosen algorithm. As the agents iterate and share information, they balance exploration and exploitation. This cooperative search continues until a stopping point is reached, like a maximum number of iterations or a convergence threshold (Janga Reddy & Nagesh Kumar, 2020).

These algorithms are increasingly being used in LFC due to the growing complexity of modern power systems. RES like wind and solar introduce variability, which causes frequency regulation to be more challenging. The system's nonlinearities and uncertainties add to the complexity. In multi-area networks, each area may operate differently, requiring coordinated and adaptive control, and faster and more reliable responses to frequency deviations (Gouran-Orimi & Ghasemi-Marzbali, 2023). These algorithms are well-suited for LFC applications because they can handle complex and high-dimensional problems, can adapt to changing conditions in real-time, making them effective for a dynamic grid environment where robustness is important.

Evolutionary algorithms, on the other hand, are a type of optimisation technique that uses the idea of natural evolution to find the best solution (Janga Reddy & Nagesh Kumar, 2020). They work by creating a group of possible solutions and then using processes such as selection, recombination, and mutation to improve them over time. This helps the group of solutions get better and better at solving the problem. A key challenge in using evolutionary algorithms is finding the right balance between keeping the group solution diverse and pushing them to be the best they can be (Zhan et al., 2022). If pressured, the solution might not be the best overall, but if not pressured, it might take too long to find good solutions.

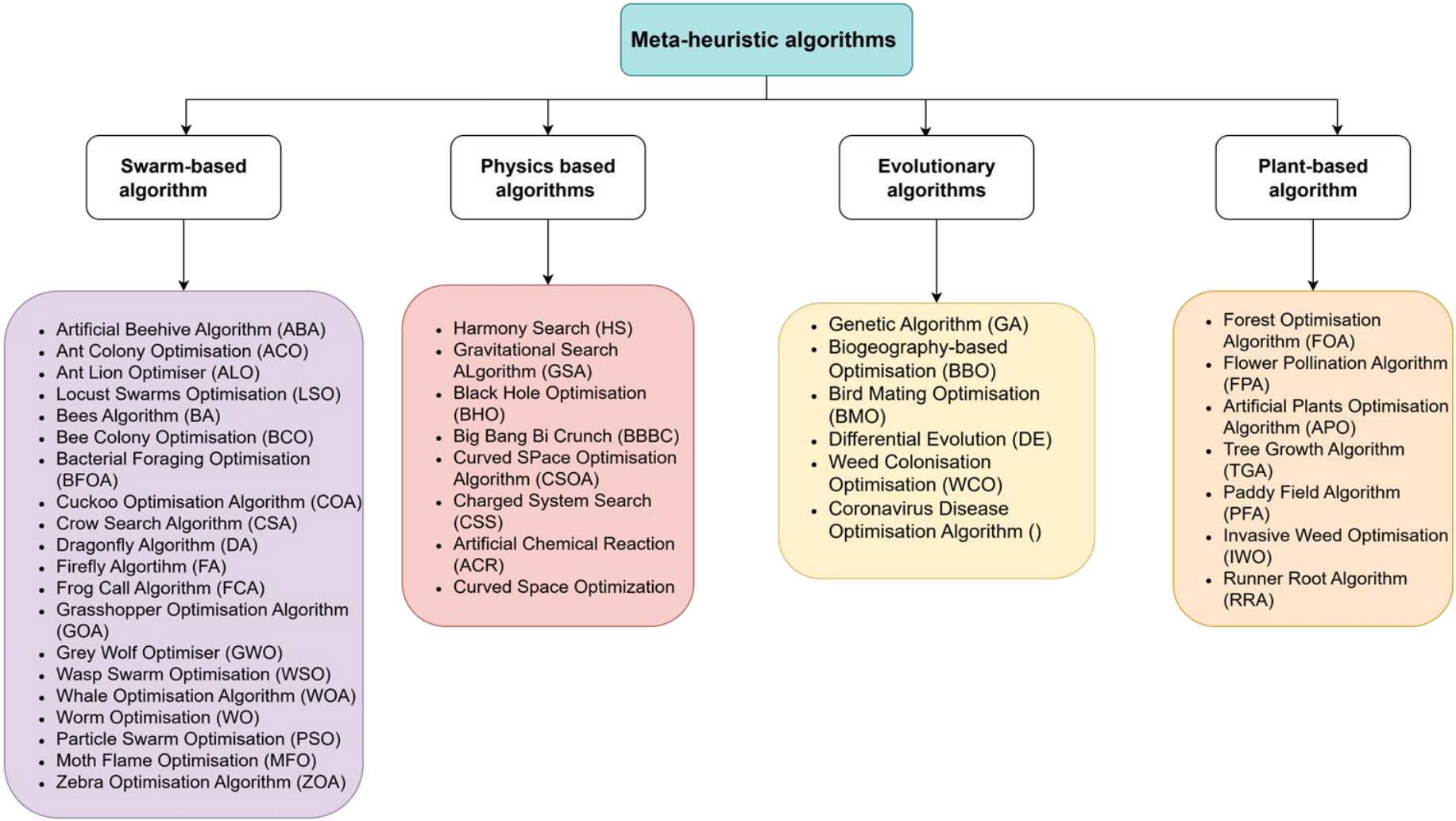

Figure 2-13: Metaheuristic optimisation algorithms

To solve this problem, researchers use a different method, like probabilistic selection, to keep the balance right (Richter & Tauritz, 2018). They can also combine the evolutionary algorithms with other techniques to make them work even better and achieve better results.

Evolutionary algorithms are useful for solving complex problems that are complex and have different possible solutions. Some common types of these algorithms include the Genetic Algorithm (GA) (Katoch et al., 2021; Alhijawi & Awajan, 2024), and Differential Evolution (DE) (Deng et al., 2021; Lambora et al., 2019).

Researchers have also developed hybrid systems that combine different algorithms to get even better results. These systems have been used in different engineering applications. Some of these algorithms include the GWO-CA for LFC controller design (Khadanga et al., 2022), GWO-WOA and BAT_PSO (Laiju et al., 2021), PSO_GA (Xu et al., 2024), GWO-PSO (Shaheen et al., 2021), and the WOA-SA algorithm (Nayak et al., 2023) amongst others. These algorithms are developed to combine the strengths of the different algorithms, improve performance, and achieve greater robustness in complex problems.

2.8.3. Comparative study

This comparative study aims to evaluate and analyse different optimisation algorithms applied to LFC, focusing on their efficiency in minimising frequency deviations, improving system damping, and ensuring stable operation. This study provides insights into the strengths and limitations of various optimisation approaches by examining basic performance indicators such as settling time, overshoot, computational efficiency, and robustness. The findings will contribute to developing more efficient LFC strategies, particularly in modern power systems integrating renewable energy and distributed generation.

Table 2-2 presents the reviewed literature on optimization algorithms applied to LFC in both single-area and multi-area systems.

Table 2-2: Reviewed literature on optimization algorithms for LFC

Author	Aim	Methodology	Achievement	Drawbacks
(Dhanasekaran et al., 2020)	The paper aims to improve the LFC of a single-area nuclear power generating system using the Ant Colony Optimisation.	Optimising a PID controller	An ACO-optimised ITAE-PID controller provides better performance than traditional tuning methods. fast settling time, reduced overshoot, and improved system stability	(ACO) requires significant computational resources due to its iterative nature.
(Dhillon et al., 2016)	To improve LFC in a multi-area power system by optimising PI controllers using a hybrid heuristic approach that combines the Bacterial Foraging Optimisation Algorithm (BFOA) and PSO	Optimise a PI controller	Developed a hybrid BFOA–PSO algorithm to optimise PI controller gains, improving response time and system stability. Successfully reduced frequency deviations and minimised the Area Frequency Control Error (AFCE) in a three-area interconnected power system	The study is based on MATLAB simulations, and practical implementation on a real power grid remains untested.
(E. S. Ali & Abd-Elazim, 2011)	to enhance LFC in an interconnected two-area power system using the BFOA to optimise PI controllers. The objective is to suppress oscillations, improve system stability, and minimise frequency deviations and tie-line power fluctuations by optimising PI controller parameters.	To tune a PI controller	Demonstrated superior damping characteristics compared to conventional and GA-based controllers, ensuring better frequency regulation.	BFOA involves multiple iterations, leading to higher computational demands than conventional tuning methods
(Luo, 2023a)	to improve frequency control in an islanded microgrid by designing an optimised PID controller using an Improved BFO algorithm. The goal is to enhance system stability, reduce frequency deviations, and provide a robust and adaptive control strategy for microgrids operating independently of the main power grid.	Optimise a PI controller	Successfully reduced frequency deviations and improved the stability of the islanded microgrid. Demonstrated superior performance compared to ACO and GA-based PID controllers, with lower oscillations, overshoot, and settling time.	The Improved BFO algorithm requires higher computational power
(Puneet Garg & Singh Brar, n.d.)	to enhance frequency stability, reduce settling time and overshoot, and optimise controller parameters to ensure better	Optimised a PID controller	Provided optimal values of proportional gain (Kp) for better system stability	requires more iterations and computational resources

Author	Aim	Methodology	Achievement	Drawbacks
	power system performance under dynamic load conditions.			
(Doan et al., 2022)	to improve LFC in a three-area interconnected power system that includes renewable energy sources (wind and solar) by using a PSO-based PID-like fuzzy logic controller.	Optimise a fuzzy-PID controller	Reduced overshoot and settling time compared to traditional methods, ensuring a faster and more stable frequency response.	the study is based on simulations only, without experimental verification in actual power grids.
(Ogar, Hussain & Kelum A.A. Gamage, 2023)	Developed a PSO-optimised PID controller that effectively stabilises load frequency and tie-line power flow in the transmission network.	Optimise a PID controller	Achieved a low ITAE of 0.0005757, indicating superior control performance, and successfully reduced settling time, overshoot, and oscillations, outperforming conventional PID, GA-PID, ANN-PID, and fuzzy logic controllers.	The study is limited to MATLAB simulations, and real-world implementation on a large-scale power grid is not tested
(Kumar et al., 2021)	To minimise frequency deviations and improve system stability using a Grey Wolf Optimisation (GWO)-	Optimise a PID controller	Achieved superior stability compared to the CS-optimised PI controller, with lower overshoot and shorter settling time.	GWO requires more iterations
(Amiri & Hatami, 2023)	To improve the frequency control in a two-area hybrid microgrid by implementing a Model Predictive Controller (MPC) optimised using a Hybrid Grey Wolf Optimiser–Pattern Search (HGWO–PS) algorithm	Optimise an MPC	Successfully reduced peak overshoot, peak undershoot, and settling time, outperforming Grey Wolf Optimiser (GWO)-based MPC and Social Spider Optimiser (SSO)-based PID controllers	The HGWO–PS optimisation process requires significant computational resources
(Mokhtar et al., 2022)	To improve the frequency in a power system with high renewable energy penetration, implement an adaptive control strategy.	Fine-tune a PI controller	Successfully damped frequency deviations and minimised oscillations compared to conventional controllers.	The controller's performance is influenced by the selection of initial tuning parameters, which may require fine-tuning for different power system configurations.
(Bayati et al., 2015)	Designing and optimising a Fractional Order Proportional-Integral-Derivative	Optimise a FOPID controller	The study utilised optimisation algorithms to fine-tune the controller	The implementation of FOPID controllers in

Author	Aim	Methodology	Achievement	Drawbacks
	(FOPID) is to enhance system stability and dynamic performance by applying optimisation techniques for controller tuning.		parameters, leading to improved transient response and reduced frequency deviation	real-world systems requires precise parameter selection, which can be challenging.
(Kouba et al., 2017)	Developing a hybrid GA-PSO technique for optimal tuning of PID controller parameters to minimise frequency deviations and reduce settling time.	Optimise a PID controller	Reduced peak overshoot and settling time, outperforming traditional tuning methods like Ziegler-Nichols, GA, PSO, BFO, and Artificial Bee Colony (ABC) algorithms	The hybrid GA-PSO approach requires significant processing power, making it computationally expensive.
(Neeli et al., 2022)	The study compares WOA-optimised controllers with other heuristic techniques like Harmony Search (HS), Flower Pollination Algorithm (FPA), and PSO.	Fine-tune the PID	Compared performance with other optimisation methods (HS, FPA, and PSO) and demonstrated that WOA achieves the best results.	The PID parameters remain static once optimised
(Kumar & Sharma, 2020)	Investigate the impact of Thyristor-Controlled Phase Shifters (TCPS) and Capacitive Energy Storage (CES) units on system performance.	Fine-tune a PI controller	Implemented a CES–TCPS combination in the tie-line to enhance transient performance and dampen frequency oscillations more effectively than conventional control methods.	
(Ojha & Obaiah, 2025)	Presents a FOPIDN(1+PIDN) controller in response to the uncertainties brought by RES	Fine-tuned a FOPIDN(1+PIDN) using a GWO	Mitigates the negative impact of renewable energy variability.	The use of GWO and cascade control increases the computational complexity

2.8.4. Comparative analysis and discussion

(Dhanasekaran et al., 2020) presented an LFC in a single-area nuclear power system by optimising a PID controller using ACO. The research evaluates different cost functions, IAE, ITAE, and ISE, to determine the most effective tuning method for minimising frequency deviations. The results show that the ITAE-based ACO-PID controller provides superior performance compared to conventional tuning methods. The study further examines the impact of energy storage units, SMES, Redox Flow Battery (RFB), and Hydrogen Aqua Electrolyser (HAE), on system stability under sudden load disturbances. Among these, SMES is found to enhance system response the most, reducing settling time and improving frequency regulation. Despite its advantages, the methodology has several limitations. ACO is computationally intensive, making it less efficient for large-scale power systems. The study is limited to a single-area system, and its applicability to multi-area interconnected grids is uncertain. The research does not explore real-world variability, such as unpredictable load fluctuations or the integration of RES, which could introduce additional complexities.

Another study was done by (Yang et al., n.d.), which presented a hybrid BFOA–PSO optimisation technique for tuning PI controllers in multi-area LFC. The proposed method improves the system's stability, reduces frequency deviations, and improves tie-line power flow under sudden load changes and renewable energy integration. Comparative simulations show that BFOA–PSO outperforms individual BFOA and PSO approaches, achieving faster settling times and lower error values. The robustness of the controller is tested with ±30% variations in system parameters, demonstrating resilience to disturbances. However, the computational complexity, lack of real-world testing, and fixed controller gains remain key limitations, requiring further research for practical deployment in larger power networks.

A similar study was conducted by (E.S. Ali & Abd-Elazim, 2011), the study presented a BFOA-based optimisation technique for tuning PI controllers in a two-area interconnected power system to improve LFC. The proposed method successfully reduces frequency deviations, minimises tie-line power fluctuations, and improves damping characteristics. Comparative analysis with conventional PI controllers and GA-based controllers conducted demonstrates that the BFOA provides superior stability, lower settling time, and better oscillation damping. The system's robustness is confirmed through parameter variation tests, showing its effectiveness under changing conditions. However, high computational complexity and limited scalability remain challenges that future research should address. (Luo, 2023b) proposed an improved BFO algorithm for tuning a PID controller to enhance frequency control in an islanded microgrid. The

optimised controller minimises frequency deviations, improves system stability, and adapts to load disturbances more effectively than conventional methods. The results were compared to those obtained from ACO and GA-based PID controllers, which show that the improved BFO-PID controller provides superior damping performance, faster settling time, and reduced oscillations. The robustness of the controller is validated through parameter variation tests and benchmark function analysis.

(Puneet Garg & Singh Brar, n.d.)presented an optimised LFC strategy for a three-area interconnected power system using BFOA to tune the PID controllers. The optimised controller significantly reduces the frequency deviations, settling time, and peak overshoot**,** ensuring better system stability than conventional PID controllers. MATLAB Simulink simulations validated how effective BFOA is in comparison, showing its superior performance in achieving optimal gain values. The computational complexity shows a trend within the application of the BFOA in the LFC.

(Doan et al., 2022) presented a PSO-optimised PID-like fuzzy logic controller for frequency control in a three-area interconnected power system with RES**.** The controller successfully minimises frequency deviations, improves tie-line power stability, and outperforms conventional controllers such as GA, BFOA, FPID, and fuzzy logic-based PI controllers**.** MATLAB/Simulink simulations validate its effectiveness under different load variations and nonlinear conditions, showing reduced overshoot, faster settling time, and improved robustness. (Ogar, Hussain & Kelum A.A. Gamage, 2023) also presented a PSO-optimised PID controller aimed at improving frequency stability and minimising load deviations**.** By dynamically tuning PID gains, the proposed controller achieves faster response times, reduced overshoot, and superior error minimisation compared to traditional controllers like GA-PID, ANN-PID, and fuzzy logic controllers. The MATLAB/Simulink-based analysis also validated the controller's robustness under varying load conditions, achieving a low ITAE value of 0.0005757. However, high computational demands, sensitivity to parameter selection, and testing remain key challenges with optimisation problems.

(Singh & Gope, 2021) proposed a GWO-optimised PID controller for frequency control in a two-area multi-microgrid system with renewable energy integration. The proposed controller significantly reduces frequency deviations and improves system stability compared to a CS-optimised PI controller. Simulation results demonstrate that GWO provides better tuning than CS, and PID controllers offer superior performance over PI controllers, due to their faster settling time and lower overshoot. The study confirms the effectiveness of GWO in optimising LFC strategies but has increased computational complexity.

2.9. Conclusion

The literature review highlights the significant advancements and challenges associated with improving power plant controller design, particularly through the optimisation of LFC in the presence of RES and ESS. Various studies emphasise the need for robust and adaptive control strategies to address the frequency instability caused by the intermittent nature of PV generation. Traditional LFC methods, while effective in conventional systems, require improvement through modern optimisation techniques, such as artificial intelligence, model predictive control, and adaptive tuning, to better manage the dynamic nature of modern power grids. The integration of RES and ESS into power systems has shown promise in improving sustainability and efficiency, but it also presents new challenges in maintaining grid stability, requiring more exploration of advanced control methodologies. While many existing studies have contributed to this field, gaps remain in achieving an optimal balance between conventional power plants, RES, and ESS for frequency regulation. This study explores the Zebra Optimisation Algorithm (ZOA) as an alternative solution for tuning a PID controller.

CHAPTER THREE
MODELLING OF LFC SYSTEM OPTIMISATION ALGORITHM

3.1. Introduction

This chapter presents the basic concepts of a single-area LFC system. This helps in understanding how the system is modelled and its natural behaviour. The single-area system is the basic LFC configuration, but it shows the important principles and challenges found in multi-area systems by examining the main components, such as the governor, turbine, generator, and how they interact. The simplified model provides an understanding of the frequency control levels and the overall performance of the system. The analysis will also include the effects of integrating a PV system and BESS in the overall system. The two-area power system is also modelled as a continuation from the single-area power system. Lastly, the optimisation algorithm used in this study is also discussed.

3.2. Single-area LFC power system model

A single-area LFC system is the foundation for understanding frequency regulation in power systems. This system ensures that the supply-demand balance is maintained by regulating the frequency and power output of a single generation area. It serves as a building block for more complex, multi-area LFC systems by addressing key aspects such as system dynamics, control mechanisms, and performance under varying load conditions and integration of renewable energy generation.

This section provides an in-depth study of the core components that make up a single-area LFC system. Specifically, it examines the turbine speed governing system, which dynamically adjusts the steam flow to regulate the turbine speed, the turbine model, which describes the conversion of energy input into mechanical power, and the generator-load model, which captures the relationship between mechanical power, electrical power, and system frequency. Together, these models form the backbone of the single-area LFC system, allowing for a comprehensive analysis of its behaviour and performance. By developing mathematical models for these subsystems and understanding their interactions, this section lays the groundwork for analysing frequency control strategies and designing effective control mechanisms.

3.2.1. The turbine speed governing system

The turbine speed governing system plays a role in maintaining the frequency stability by adjusting the steam flow to the turbine based on changes in load demand and frequency deviations (Moura et al., 2012). Figure 3-1 shows the turbine speed governing

system designed to regulate the turbine's rotational speed and, thus, the system frequency by controlling the steam flow to the turbine. This system includes several interconnected components that work together to monitor, adjust, and stabilise the turbine speed in response to frequency deviations.

•Speed Changer

The speed changer acts as the manual input for setting the desired reference speed of the turbine. It includes two control options: Lower and Raise. These controls allow operators to adjust the reference speed or load setpoint, thereby determining the base operating condition for the system. Changes made at the speed changer propagate downstream to influence the turbine's operation.

•Point B: flyball speed governor

At point B, the speed governor monitors the rotational speed of the turbine shaft. It detects any deviation from the reference speed set by the speed changer. The governor outputs a control signal proportional to the detected deviation, which is then sent to the hydraulic amplifier at point D. The governor includes droop characteristics, allowing proportional sharing of load changes in multi-generator systems while maintaining stability.

•Hydraulic Amplifier

At point D, the hydraulic amplifier acts as the speed control mechanism. It amplifies the relatively small output signal from the speed governor and converts it into a powerful mechanical force (Bevrani, 2014) . This force is transmitted to the main piston and valve control at point E. The hydraulic amplifier ensures that even small deviations in speed result in precise and effective adjustments to the steam flow.

•Main Piston and Valve Control

The main piston is directly linked to the speed control mechanism (hydraulic amplifier) and the valve control, which regulates the flow of steam into the turbine. Based on the amplified signal, the piston moves to either open or close the control valve. If the turbine speed is below the reference, the valve opens to allow more steam into the turbine, increasing the turbine's rotational speed. If the turbine speed is above the reference, the valve closes to reduce steam flow, lowering the speed. This dynamic adjustment of steam input ensures that the turbine operates within its desired speed range.

•Turbine Dynamics and Load

Once the valve regulates the steam flow, the turbine converts the steam's thermal energy into mechanical rotational energy. This rotational energy is then transmitted to the generator, which converts it into electrical energy to meet the load demand. Changes in the load create a feedback loop, where deviations in frequency are detected by the speed governor, initiating corrective actions throughout the entire system.

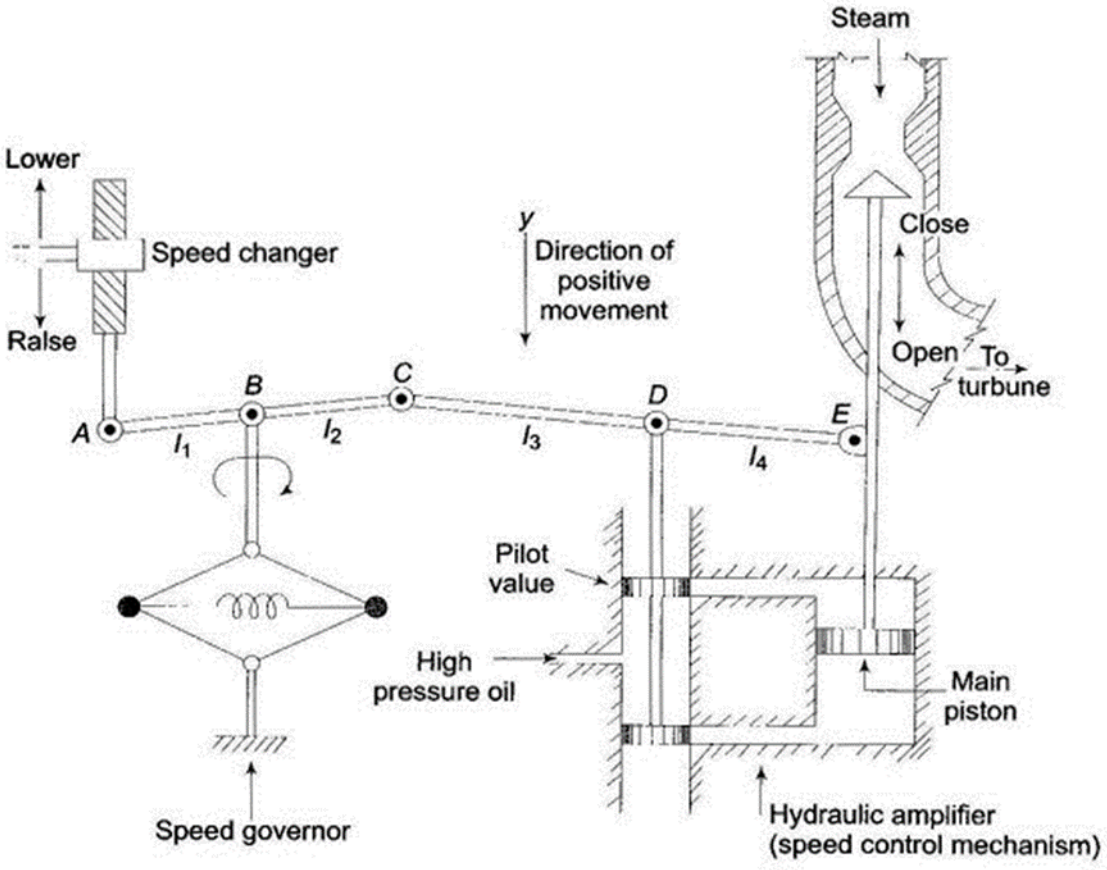

Figure 3-1: The turbine speed governing system (Elgerd, 1987)

To model the speed governor, the following movements of the rigid links are considered: Movement of A: $\Delta X_A = X_C \cdot \Delta P_C$, which represents the displacement of the speed changer that sets the reference speed for the governor; Movement of B $\Delta X_B = k_F \cdot \Delta F$, which describes the relative displacement at the governor's joint due to changes in turbine speed or frequency deviations, and Movement of C, which reflects the adjustment of the control signal transmitted to the hydraulic amplifier. These movements collectively capture the dynamic relationship between the speed deviation and the corrective actions initiated by the governor, forming the foundation for its mathematical representation (Elgerd, 1987) .

Due to the movement of A by ΔX_A, that is ΔX_c (point B is fixed), The equation becomes :

$$\Delta X_A \ell_2 + \Delta X_C \ell_2 = 0 \qquad 3\text{-}1$$

The flyball moves outwards due to the increase in frequency. Point B now moves downwards by the proportion of $k_F \cdot \Delta F$, i.e. ΔX_C , therefore:

$$\Delta X_C = k_F \cdot \Delta F \qquad 3\text{-}2$$

Now, to get the movement at point C, the equation 3-1 + equation 3-2 to obtain :

$$\Delta X_C = -k_1 \cdot \Delta P_C + k_2 \cdot \Delta F \qquad 3\text{-}3$$

Now movement of point D is due to ΔX_C and ΔX_E and is represented as:

$$\Delta X_D = k_3 \cdot \Delta X_C + k_4 \cdot \Delta X_E \qquad 3\text{-}4$$

On the movement of E, the volume of oil entered into the cylinder is proportional to the line integral of ΔX_D:

$$\Delta X_E = k_5 \int_0^t (-\Delta X_D) dt \qquad 3\text{-}5$$

From equation 3-5, the downward movement is considered positive, and the upward movement is a negative value. The next step is to take the Laplace transform of (3), (4), (5) and substitute into ΔX_E to obtain :

$$\Delta X_E(s) = -\frac{-k_3 k_5}{s} \frac{\left(-k_1 \cdot \Delta P_C(s) + k_2 \cdot \Delta F(s)\right)}{\left(1 + \frac{k_4 k_5}{s}\right)} \qquad 3\text{-}6$$

Which can further be simplified to :

$$\Delta X_E(s) = \frac{K_g}{1 + sT_g} \left[\Delta P_C(s) - \frac{1}{R} \Delta F(s)\right] \qquad 3\text{-}7$$

Where:

$R = \frac{k_2}{k_1}$ is the speed regulation of the governor

$K_g = \frac{k_2 k_3}{k_4 k_5}$ is the gain of the speed governor

$T_g = \frac{1}{k_4 k_5}$ is the time speed constant of the speed governor

ΔP_C is the incremental control input

And thus, the transfer model of the speed governor is :

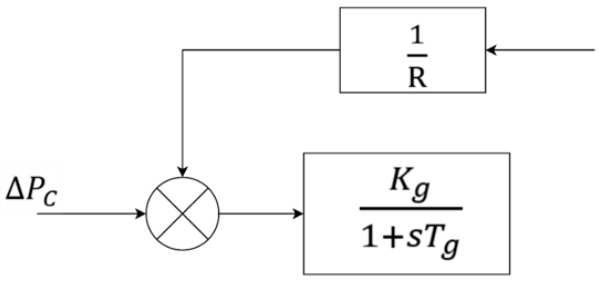

Figure 3-2: Model of the speed governor (Adapted from (Elgerd, 1987; Saadat, 1999))

3.2.2. Modelling the turbine

To model the turbine, a two-stage steam turbine configuration is considered, containing a steam valve, a high-pressure (HP) stage, a low-pressure (LP) stage, and a reheater, as shown in Figure 3-3 The steam valve regulates the flow of steam into the turbine, adjusting the energy input based on the control signal received from the speed governing system. In the HP stage, the steam undergoes its initial expansion, converting thermal energy into mechanical energy, which drives the turbine shaft. The partially expanded steam then passes through the reheater, where it is reheated to increase its enthalpy before entering the LP stage for further expansion. This two-stage process improves the overall efficiency of the turbine by minimising moisture formation in the LP stage and extracting maximum energy from the steam. Each of these components can be represented mathematically by transfer functions, with the steam valve dynamics governing the input and the combined HP and LP stages, along with the reheater determining the output power.

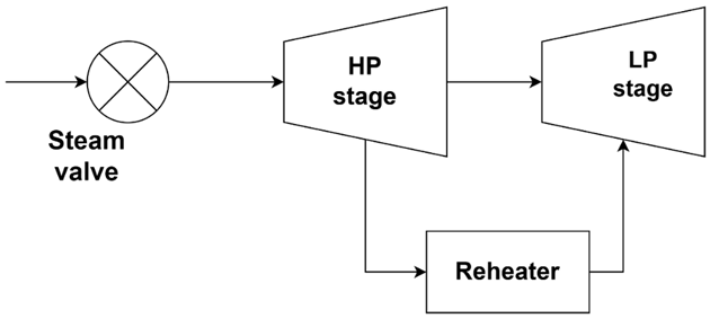

Figure 3-3: A model of a two-stage steam turbine (Adapted from (Chakrabarti, 2010))

The model provides an accurate representation of the turbine's response to changes in steam input and load demand. The relationship between the changes in the power output of the steam turbine and the changes in its steam valve opening, $\Delta \boldsymbol{X_E}$ describes how variations in valve position directly influence the turbine's mechanical power output. The turbine transfer function is typically characterised by two distinct time constants that represent the dynamics of the high-pressure and low-pressure stages. For simplicity and ease of analysis in this research, it will be assumed that the turbine can be approximated by a single equivalent time constant, successfully capturing its overall dynamic behaviour in a more simplified manner.

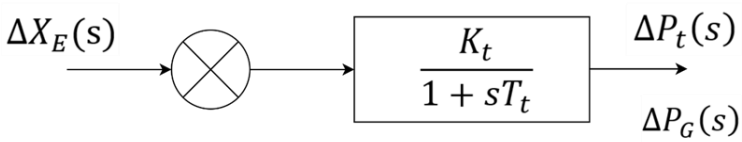

Figure 3-4: A transfer function model of the turbine (Adapted from (Chakrabarti, 2010)

3.2.3. Modelling the generator-load model

The generator-load model represents the interaction between the generator, which converts mechanical power from the turbine into electrical power, and the load, which consumes the generated electricity. This model is important for understanding how changes in power demand or supply affect the system frequency. It captures the dynamic behaviour of the generator rotor, which responds to imbalances between mechanical power input and electrical power output, as well as the characteristics of the load, including its frequency dependence. The model describes how the generator and load together influence the stability and regulation of system frequency, forming a key factor of load frequency control analysis. By integrating the generator's rotational dynamics and the load's response to frequency changes, the model enables the analysis of transient and steady-state behaviour under varying operating conditions. The generator-load model is thus essential for predicting frequency deviations and designing control strategies to restore balance in the power system. Suppose there is a real load change of $\Delta \boldsymbol{P_D}$ in the power system, which requires an adjustment in generation to maintain the balance between supply and demand. In response to this change, the turbine controllers regulate steam flow into the turbine, thereby increasing mechanical power input. This results in an increase in the generator's electrical power output by an amount $\Delta \boldsymbol{P_G}$. The net surplus power, $\Delta \boldsymbol{P_G} - \Delta \boldsymbol{P_D}$ is distributed within the system through two different mechanisms. The generator rotor stores kinetic energy, given by :

$$W_{k \cdot E} = H \times P_r \qquad 3\text{-}8$$

Where: $\boldsymbol{P_r}$ is the kW rating of the turbo generator $\boldsymbol{H}$ is the inertia constant.

The kinetic energy of the generator rotor is directly proportional to the synchronous speed of the system. So, this means that the kinetic energy at a frequency of $\boldsymbol{f_0} + \Delta \boldsymbol{f}$ is expressed as (Elgerd, 2005; Gómez Expósito et al., 2018)

$$W_{kE} \propto (f_0 + \Delta f)^2 \qquad 3\text{-}9$$

Now, the rate of change in kinetic energy will be expressed as:

$$\frac{dW_{kE}}{dt} = \frac{\partial {W_{kE}}^o}{\partial f_0} \frac{d}{dt} \Delta f \qquad 3\text{-}10$$

Second, the remaining surplus power is absorbed by the load, increasing power consumption. Since most loads exhibit a frequency-dependent characteristic, they experience an increase in power consumption proportional to:

$$B = \frac{\partial P_D}{\partial f} \qquad 3\text{-}11$$

The rate of change of load with respect to the frequency will thus be :

$$B \cdot \Delta f = \frac{\partial P_D}{\partial f} \Delta f \quad \text{3-12}$$

Therefore, the net-surplus power equation is thus:

$$\Delta P_G(s) - \Delta P_D(s) = \frac{2H}{f_0} s\, \Delta F(s) + B\Delta F(s) \quad \text{3-13}$$

Therefore, the frequency deviation can thus be expressed as :

$$\Delta F(s) = \frac{K_p}{1 + sT_p} [\Delta P_G(s) - \Delta P_D(s)] \quad \text{3-14}$$

Where:

$$\boldsymbol{K_{ps}} = \frac{\mathbf{1}}{\boldsymbol{B_1}} \quad \text{3-15}$$

$$\boldsymbol{Tps} = \frac{\boldsymbol{2\pi}}{\boldsymbol{B_1 f_1^0}} \quad \text{3-16}$$

The block diagram representing the frequency deviation dynamics of the system is illustrated in Figure 3-5 . This diagram visually shows the relationship between the mechanical power input from the turbine, the electrical power output delivered to the load, and the resulting frequency deviation.

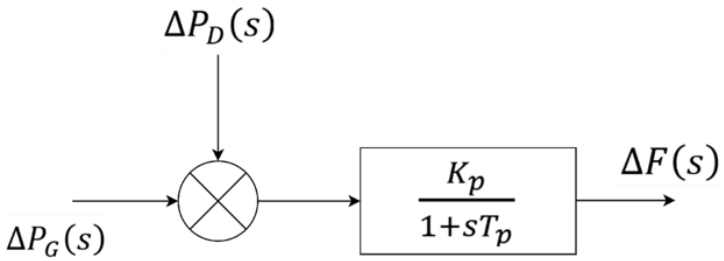

Figure 3-5: Generator-load model (Adapted from (Chakrabarti, 2010))

The complete model of the LFC system for a single-area power system is presented in , integrating the turbine, governor, and generator-load dynamics. This final model summarises the interactions between these components, showing how frequency deviations are detected and corrected through the governing mechanism. The system operates as a closed-loop control structure, where the governor regulates the steam flow to the turbine in response to changes in frequency, ensuring that the generator maintains a stable power output to match the varying load demand.

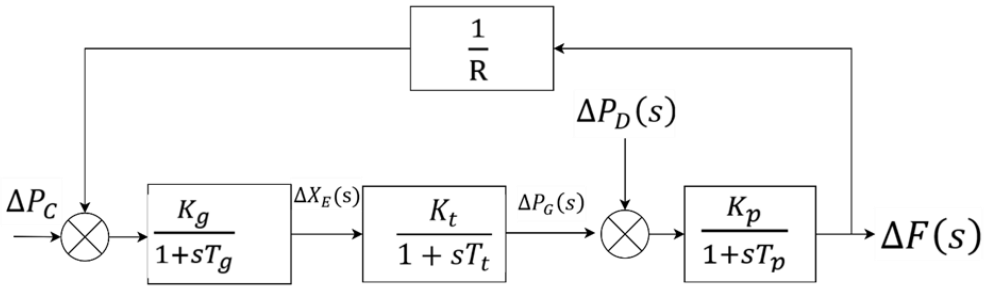

Figure 3-6: Model of a single area LFC (Adapted from (Elgerd, 1987))

3.2.4. Modelling a solar PV system transfer function

PV modelling is important for understanding the electrical behaviour of a solar cell and predicting its performance under different environmental conditions. A solar PV model represents the relationships among the output current, voltage, and power of a solar cell based on its physical and electrical characteristics. The most widely used approach for modelling PV cells is the single-diode equivalent circuit.

The single-diode equivalent circuit of a PV cell is used because it balances accuracy and efficiency, making it a powerful tool for analysing PV performance. The circuit consists of four primary elements: a photocurrent source, a diode, s series resistor, and a shunt resistance. Each of these components plays a role in determining the PV cell's overall characteristics. The photocurrent source represents the current generated by sunlight; it is directly proportional to incident solar irradiance and is influenced by temperature variations and the spectral content of light. The diode model captures the p-n junction behaviour of the solar cell and accounts for charge-carrier recombination losses. Its behaviour is governed by the Shockley diode equation, which defines how current flows through the diode under different voltage conditions. The series resistance accounts for resistive losses within the PV cell, including those due to semiconductor material, metal contacts, and interconnections. A HIGH Rs reduced the fill factor (FF) and lowers the overall efficiency by limiting the maximum power output. Ideally, this resistance should be minimised to improve performance (Eltanaly, 2018). The shunt resistance represents the leakage currents caused by manufacturing defects or material imperfections. A lower $\boldsymbol{Rsh}$ increases power losses by lowering current to bypass the load, thereby reducing efficiency. For optimal PV performance, $\boldsymbol{Rsh}$ should be as high as possible.

The governing equation of the model is derived from Kirchhoff's Current Law (KCL), which states that the output current of the PV cell is the difference between the photocurrent and the sum of the diode and shunt currents. This is the nonlinear current-voltage characteristics and is represented as:

$$I = I_{ph} - I_D - I_{sh} \quad (3\text{-}17)$$

Where:

$$I_{ph} = I_{sc}\left(\frac{S}{1000}\right) + k_i\left(T - T_{ref}\right) \quad (3\text{-}18)$$

$$I_D = I_0\left[exp\left\{\frac{q(V + R\_s\, I)}{nkT}\right\} - 1\right] \quad (3\text{-}19)$$

$$I_{sh} = \frac{V + R_s I}{R_{sh}} \quad (3\text{-}20)$$

Where:

$\boldsymbol{I_{ph}}$ is the photocurrent (A),

$\boldsymbol{I_d}$ is the diode current (A),

$\boldsymbol{I_p}$ is the current of the parallel resistance (A),

$\boldsymbol{I_{PV}}$ is the PV current (A),

$\boldsymbol{I_{SC}}$ is the short-circuit current (A),

$\boldsymbol{I_o}$ is the saturation current (A),

$\boldsymbol{I_{do}}$ is the diode reverse current (A),

$\boldsymbol{S}$ is the solar irradiance (W/m2),

$\boldsymbol{J_o}$ is the temperature coefficient,

$\boldsymbol{T}$ is the PV cell temperature (K),

$\boldsymbol{T_{ref}}$ is the reference temperature (298 K),

$\boldsymbol{q}$ is the charge of the electron (C),

$\boldsymbol{k}$ is a Boltzmann's constant,

$\boldsymbol{n}$ is the diode ideality factor,

$\boldsymbol{V_{PV}}$ is the terminal voltage of the PV modules (V),

$\boldsymbol{E_g}$ is the bandgap energy of the cell semiconductor (e.v),

$\boldsymbol{R_p}$ is the parallel resistance (Ω), and

$\boldsymbol{s}$ is the series resistance (Ω).

The I-V and P-V characteristic curves of a PV module, shown in Figure 3-7 Illustrate the module's electrical behaviour under varying voltage and current conditions.The I-V curve represents the nonlinear relationship between the output current and voltage of the PV module. At zero voltage (V = 0), the current reaches its maximum value, known as the short-circuit current. As the voltage increases, the current remains nearly constant until it reaches a critical point, after which it drops sharply to zero at the open-circuit voltage.

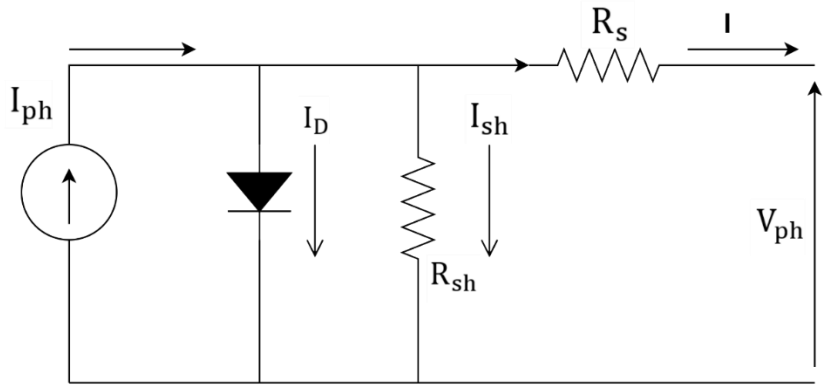

Figure 3-7: Equivalent circuit of a PV solar cell (Eltanaly, 2018)

The P-V curve is derived from the I-V curve and shows the power output of the module as a function of voltage. It has a distinct peak known as the Maximum Power Point (MPP), where the module operates at its highest efficiency. The MPP corresponds to an optimal combination of voltage and current where the product $P = V \times I$ is maximised. The shape of both curves is influenced by environmental factors such as irradiance and temperature, where higher irradiance increases. This is illustrated in Figure 3-8.

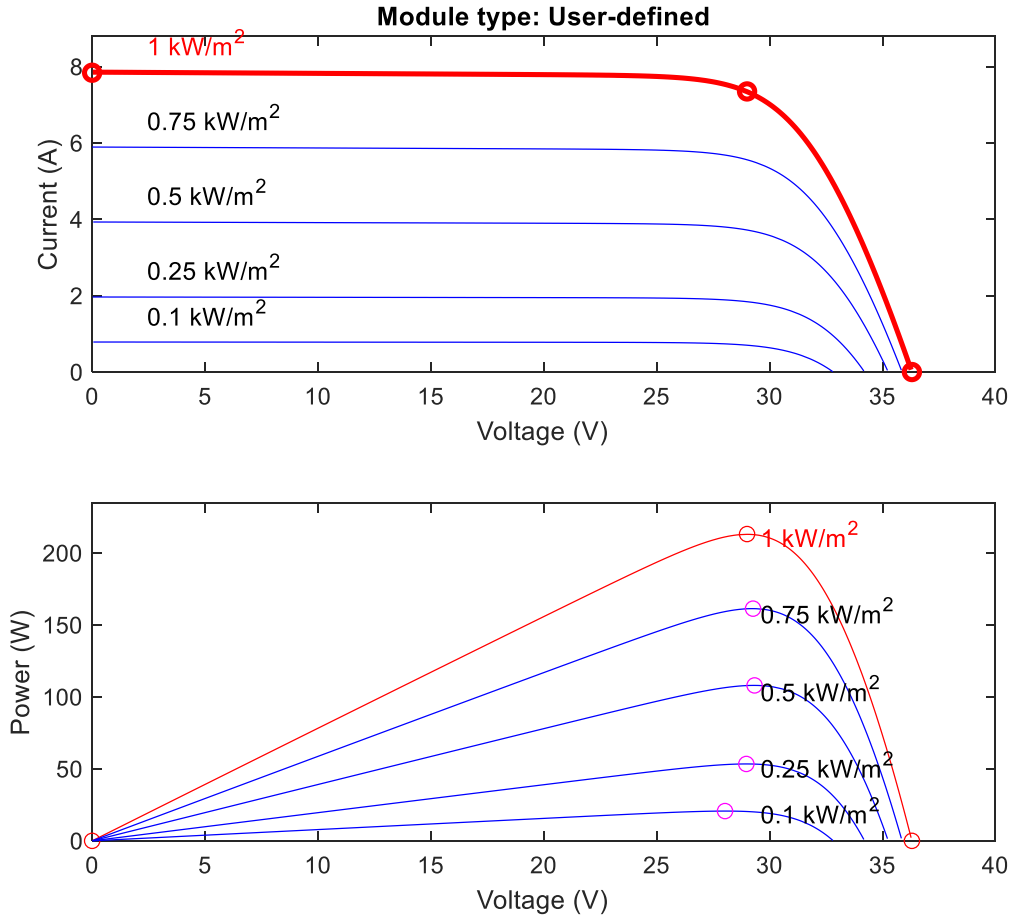

Figure 3-8: I-V, P-V characteristics of a PV module

In this research, a first-order transfer function will be employed to model the dynamic response of the PV system. Although PV modules exhibit nonlinear behaviour due to their dependence on environmental factors like irradiance and temperature, a linear approximation is often necessary for control system applications, such as MPPT and grid integration. A first-order transfer function is selected because it effectively captures the relationship between input (irradiance, duty cycle, or voltage reference) and output (current, voltage, or power) while simplifying system analysis.

The general form of a first-order transfer function is:

$$\Delta P_{PV} = \frac{K_{PV}}{sT_{PV} + 1} \qquad 3\text{-}21$$

K represents the steady-state gain, reflecting the PV module's proportional response to input changes. τ is the time constant, defining the response speed and representing the impact of capacitance and inductance in the PV system. s is the Laplace variable. This approximation enables stability analysis, controller design, and optimisation of PV system performance using classical control techniques. It's particularly useful in MPPT algorithms, where PV voltage and current dynamics must be considered for efficient power tracking. By utilising a first-order transfer function, this research can develop a control strategy that ensures the PV system operates near the MPP while maintaining stability and fast transient response.

The complete system with the added PV system and BESS is shown in Figure 3-9.

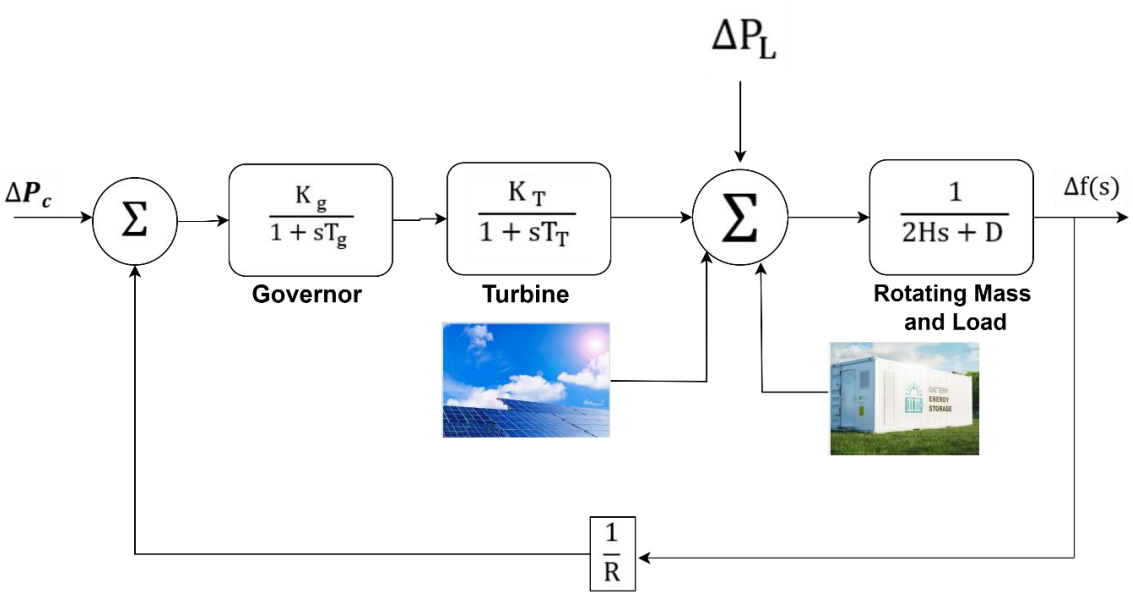

Figure 3-9: Developed model of the single-area system

3.2.5. Steady state analysis of the system

Steady state analysis focuses on the final stage of the system after the disruptions have stopped and the system has settled. The main goal is to ensure that the system frequency returns to the predefined value with no errors, while keeping the system stable. This involves checking that the power generation has been adjusted to balance new load levels, that the frequency deviations have been eliminated, and that each control area carries its own demand in a multi-area system. This can be achieved by using integral action in controllers, which guarantees zero steady-state error. The analysis verifies that the system reaches equilibrium with accurate and stable performance. This section presents the steady state analysis of a single area with solar PV and BESS integrated.

3.2.5.1. Steady state analysis without the solar PV system

The standard single area system has two important increments of input, i.e. the change in speed changer setting $\Delta \boldsymbol{P_C}$, and the change in load demand $\Delta \boldsymbol{P_D}$. For a free governor operation, the speed changer settings remain fixed ($\Delta \boldsymbol{P_C} = \mathbf{0}$), and the system experiences a sudden change in load demand.

$$\frac{\Delta F(s)}{\left(-\frac{\Delta P_D(s)}{s}\right)} = \frac{\frac{K_p}{1+sT_p}}{1+\frac{K_s}{1+sT_g} * \frac{K_t}{1+sT_t} * \frac{1}{R} * \frac{K_p}{1+sT_p}} \quad \text{3-22}$$

Which can be simplified to the following equation :

$$\Delta F(s) = \frac{K_p}{(1+sT_p) + \frac{K_t K_g K_p / R}{(1+sT_t)(1+sTg)}} * \left(-\frac{\Delta P_D(s)}{s}\right) \quad \text{3-23}$$

The steady state frequency response can be obtained by finding the limits of the equation 3-23.

$$\Delta f_{ss} = \lim_{s \to 0} s \Delta F(s) \quad \text{3-24}$$

$$\Delta f_{ss} = \lim_{s \to 0} s \left(\frac{K_p}{\left(1+sT_p\right) + \frac{\frac{K_t K_g K_p}{R}}{(1+sT_t)(1+sTg)}} * \left(-\frac{\Delta P_D(s)}{s}\right) \right) \quad \text{3-25}$$

The steady state frequency is thus:

$$\Delta f_{ss} = -\frac{K_p}{1+\frac{K_g K_t K_p}{R}} * \Delta P_D \qquad 3\text{-}26$$

The gains $\boldsymbol{K_t}$ **and** $\boldsymbol{K_p}$ **are fixed while** $\boldsymbol{K_g}$ is adjustable by adjusting the length of the linkage, and also considering the assumption $\boldsymbol{K_g * K_t \approx 1}$. Also, $\boldsymbol{K_p = \frac{1}{B}}$, as such, the steady state changes in frequency are:

$$\Delta f_{ss} = -\frac{1}{B+\frac{1}{R}} * \Delta P_D \qquad 3\text{-}27$$

The single-area system block diagram is reduced as shown in Figure 3-10.

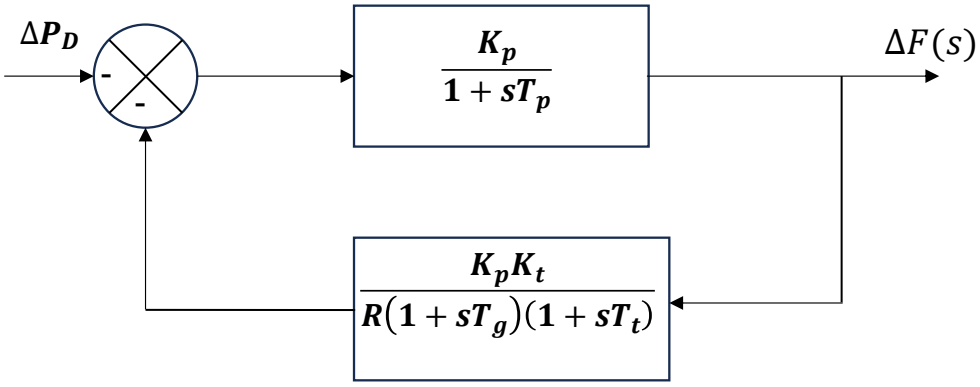

Figure 3-10: Reduced block diagram (Adapted from (Saadat, 1999))

When considering a case where the load demand remains fixed ($\Delta P_D = 0$), and the speed changer setting is changed ($\Delta P_c = \frac{\Delta P_c}{s}$), then Δf_{ss} is:

$$\frac{\Delta F(s)}{\Delta P_c(s)} = \frac{\frac{K_g}{1+sT_g} * \frac{K_t}{1+sK_t} * \frac{K_p}{1+sT_p}}{1+\frac{K_g}{1+sK_g} * \frac{K_t}{1+sT_t} * \frac{K_p}{1+sT_p} * \frac{1}{R}} \qquad 3\text{-}28$$

$$\Delta F(s) = \frac{K_g K_t K_p}{(1+sT_g)(1+sT_t)(1+sT_p)+\frac{K_g K_t K_p}{R}} * \Delta P_c(s)/s \qquad 3\text{-}29$$

The steady state value will be the limit of 3-29:

$$\Delta f_{ss} = \lim_{s\to 0} s\Delta F(s) \qquad 3\text{-}30$$

Therefore, the steady state change in frequency is :

$$\Delta f_{ss} = \frac{K_g K_t K_p}{1+\frac{K_g K_t K_p}{R}} * \Delta P_c \qquad 3\text{-}31$$

Using the same approximation as in the equation 3-27, the equation 3-31 is expressed as:

$$\Delta f_{ss} = \frac{1}{B + \frac{1}{R}} * \Delta P_c \qquad 3\text{-}32$$

Combining the two cases (i.e. change in load demand and change in speed changer setting), the resultant change in frequency is expressed as:

$$\Delta f_{ss} = \left(\frac{1}{B + \frac{1}{R}} \right) (\Delta P_c - \Delta P_D) \qquad 3\text{-}33$$

Larger system disturbances, such as changes in load demand, result in greater frequency deviations as the system adapts to new load conditions, causing frequency fluctuations. The system's stability is influenced by the damping factor, where a higher damping value reduces frequency deviation by slowing the frequency change rate and minimizing fluctuations. Speed regulation also plays a role in frequency stability, as a lower governor droop enables the system to respond quickly to load changes, reducing frequency deviations.

Since the system operates in free governor mode, frequency deviation is not corrected to zero. Instead, it settles at a new equilibrium value, determined by the balance between the load change and speed regulation characteristics (Subramanian, 2010). So, the system frequency stabilises at a new steady-state value reflecting the changed load conditions, rather than returning to its original frequency.

3.2.5.2. Steady state analysis with the solar PV system

The steady-state analysis of LFC with PV looks at how changes in the demand and solar power output affect the system's frequency. This analysis is important because it helps in understanding how solar power affects the system's ability to maintain a stable frequency. By studying how the system responds to changes, potential problems can be identified and solutions developed to minimise the impact of solar power fluctuations on system frequency.

In addition to that, the analysis must consider how different levels of solar power affect the system's dynamics. As more solar power is added to the system, its frequency response may change, potentially leading to reduced stability. Therefore, it's essential to investigate how different levels of solar power affect the LFC system's performance and develop control strategies that can handle the unique characteristics of solar power. In this model, the mechanical power input $\Delta \boldsymbol{P_m}$ is affected by both the conventional generator and PV generation, which is represented by:

$$\Delta P_m = \Delta P_g + \Delta P_{PV} \quad (3\text{-}34)$$

Where:

$\Delta \boldsymbol{P_g}$ is the power from the generator

$\Delta \boldsymbol{P_{PV}}$ is the power from the PV system

Governed by the swing equation, the system frequency deviation is :

$$\frac{d\Delta f}{dt} = \frac{1}{M}(\Delta P_g + \Delta P_{PV} - \Delta P_D - D\Delta f) \quad (3\text{-}35)$$

For steady state analysis, the assumption made is that a sudden change in load demand and a change in PV power output occur. The system equation is:

$$s\Delta f(s) = \frac{1}{M}(\Delta P_g(s) + \Delta P_{PV}(s) - \Delta P_D(s) - D\Delta f(s)) \quad (3\text{-}36)$$

at steady state, $\boldsymbol{s = 0}$, obtaining:

$$0 = \frac{1}{M}(\Delta P_g + \Delta P_{PV} - \Delta P_D - D\Delta f_{ss}) \quad (3\text{-}37)$$

Rearranging for steady state frequency deviation:

$$\Delta f_{ss} = \frac{\Delta P_{PV} - \Delta P_D}{D + 1/R} \quad (3\text{-}38)$$

When solar power increases, it helps meet some of the load demand, which reduces frequency fluctuations. This is because solar power can provide some of the power needed, reducing the load on the grid and minimising frequency changes. On the other hand, when solar power decreases, it can cause the frequency fluctuations to worsen, requiring help from traditional power sources or energy storage systems. If there's no control system in place, frequency fluctuations will continue to occur, depending on the balance between demand and solar power fluctuations. But adding a BESS can help reduce frequency fluctuations by providing extra support to stabilise the grid. The BESS can absorb or release power as needed to balance the grid and minimise frequency fluctuations. Using a BESS can also help reduce the impact of solar power fluctuations on the grid. By storing extra energy generated by solar power during sunny periods, the BESS can release this energy during cloudy periods, helping to stabilise the grid and minimise frequency fluctuations. This can improve the grid's efficiency and reliability, while also reducing the load on traditional power sources.

3.2.6. Dynamic response of the system

In the absence of a control mechanism, the single-area power system operates in an uncontrolled state, where any disturbance in load demand directly affects system

frequency. When there is a sudden increase in load, the electrical power demand exceeds the mechanical power supplied by the turbine, causing a temporary power imbalance. This results in a decrease in generator speed, leading to a drop in system frequency. Equally, if the load decreases, excess mechanical power causes the generator to accelerate, increasing the frequency beyond its nominal value. Since there is no automatic corrective action, the system relies solely on natural damping and inertia to mitigate frequency deviations, which may lead to slow and insufficient recovery. Prolonged frequency deviations can compromise system stability, potentially leading to cascading failures or even system collapse. Therefore, dynamic analysis of this uncontrolled case highlights the necessity of implementing LFC to restore frequency stability and maintain power system reliability.

In modelling the dynamic response of the single-area power system, a systematic approach to derive the frequency deviation equation is followed. To simplify the analysis, certain approximations are made based on the relative time constants of system components. The time constants of the governor and turbine are relatively small compared to those of the generator-load system, meaning their response is much faster and can be assumed to be instantaneous for frequency deviation analysis. As a result, we neglect their time constants, allowing for a simplified representation of the overall system dynamics. The product of the governor's gain $\boldsymbol{K_G}$ and the turbine gain $\boldsymbol{K_t}$ can be approximated to 1, meaning that the mechanical power output follows changes in the control signal almost directly. This approximation helps reduce the complexity of the system's transfer function while still accurately capturing the essential dynamics of frequency deviations due to power imbalances. The simplified model is represented in Figure 3-11.

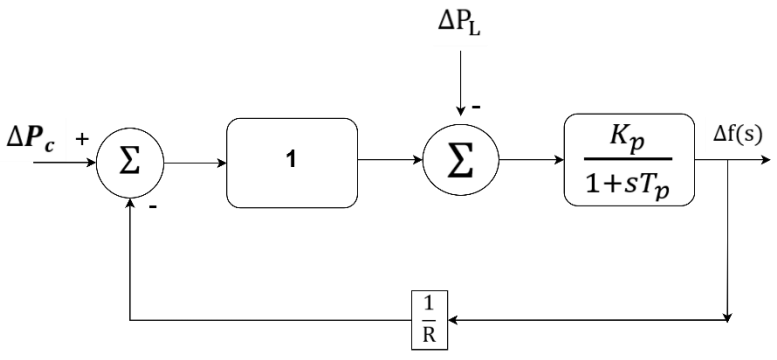

Figure 3-11: Dynamic response block diagram

The frequency deviation thus becomes :

$$\Delta F(s) = \frac{\frac{K_p}{1+sT_p}}{1+\frac{K_p}{R(1+sT_p)}} * -\Delta P_D(s) \quad \text{3-39}$$

For a step load change:

$$\Delta P_D(s) = \frac{\Delta P_D(s)}{s} \quad \text{3-40}$$

Therefore**:**

$$\Delta F(s) = \frac{K_p}{T_p s\left(s+\frac{1}{T_p}+\frac{K_p}{RT_P}\right)} * -\Delta P_D(s) \quad \text{3-41}$$

Inverse Laplace of the equation **3-41**:

$$\Delta f(t) = -\frac{RK_p}{R+K_p}\left[1-exp\left(-\frac{1}{T_p}\left(\frac{R}{R+K_p}\right)\right)\right]\Delta P_D \quad \text{3-42}$$

This equation represents the dynamic behaviour in an uncontrolled case, for a step load change.

3.3. Modelling a two-area power system

A multi-area power system consists of areas interconnected by tie-lines. The frequency trend in each area indicates the overall power mismatch in the entire system, rather than just the local area. Secondary frequency control requires managing both the local frequency and tie-line power exchange with other areas. To achieve this, the LFC system is modified to include a tie-line power signal, allowing coordinated control across the interconnected system. The following equations show how the frequency deviation in each area and the tie-line power exchange can be obtained in a two-area system.

Under normal operating conditions, area 1 may export or import power from area 2, provided that the system frequency remains constant. In this state, the tie-line power flow is represented by the equation 3-43 (Saadat, 1999; Nagrath et al., 1982):

$$P_{tie1,2} = \frac{V_1 V_2}{X_{12}} \sin(\delta_1 - \delta_2) \quad \text{3-43}$$

Any changes in the load or generation will result in frequency deviation. This deviation is followed by a change in rotor angles, which will affect the power exchange between the two areas. The incremental tie-line power flow between the areas is given by:

$$\Delta P_{tie1,2} = T_{12}(\Delta\delta_1 - \Delta\delta_2) \quad \text{3-44}$$

Where T_{12} is the synchronising torque coefficient which defines the sensitivity of the tie-line power to changes in the rotor angle and is given by :

$$T_{12} = \frac{|V_1||V_2|}{X_{12}} cos(\delta_1 - \delta_2) \quad \text{3-45}$$

$|V_1|, |V_2|$ are the voltage magnitudes of the two areas, X_{12} is the reactance of the tie-line, and $\delta_1 - \delta_2$ the initial load angle difference between the two areas. By relating the relationship between the angle deviation and frequency deviation, the equation 6-2 can be written as:

$$\Delta P_{tie12} = 2\pi T_{12}\left(\int \Delta f_1 dt - \int \Delta f_2 dt\right) \quad 3\text{-}46$$

$\Delta f_1, \Delta f_2$ are the frequency deviations in areas 1 and 2, and the Laplace transform is:

$$\Delta P_{tie12}(s) = \frac{2\pi}{s} T_{12}\big(\Delta f_1(s) - \Delta f_2(s)\big) \quad 3\text{-}47$$

The dynamic power balance for area 1, considering for mechanical (ΔP_{m1}) input power , and load demand (ΔP_{D1}), and tie-line power is expressed as :

$$\Delta P_{m1} - \Delta P_{D1} = \frac{2\pi}{f_1}\frac{d}{dt}(\Delta f_1) + B_1 \Delta f_1 + \Delta T_{tie1} \quad 3\text{-}48$$

Taking the Laplace transform, the frequency deviation in area 1 can be written as :

$$\Delta F_1(s) = \big[\Delta P_{m1}(s) - \Delta P_{D1}(s) - \Delta P_{tie,12}\big] * \frac{K_{ps}}{sT_{ps} + 1} \quad 3\text{-}49$$

The incremental tie-line power flow from area 2 to area 1 is given by :

$$\Delta P_{tie,21}(s) = \frac{2\pi}{s} T_{21}\big(\Delta F_2(s) - \Delta F_1(s)\big) \quad 3\text{-}50$$

When a PV system and BESS is integrated area 1, the frequency deviation is expressed as:

$$\Delta F_1(s) = \big[\Delta P_{m1}(s) - \Delta P_{D1}(s) - \Delta P_{BESS}(s) - \Delta P_{PV}(s) - \Delta P_{tie,12}\big] * \frac{K_{ps}}{sT_{ps} + 1} \quad 3\text{-}51$$

The frequency deviation in frequency 2, without a PV system and BESS is :

$$\Delta F_2(s) = \big[\Delta P_{m2}(s) - \Delta P_{D2}(s) + \Delta P_{tie,12}\big] * \frac{K_{ps}}{sT_{ps} + 1} \quad 3\text{-}52$$

In the ACE, each control area serves as an input signal. The ACE reflects the deviation in power balance and frequency stability, guiding the controller's corrective actions to maintain equilibrium by ensuring that the power system remains within its operational limits by regulating tie-line power exchange and frequency variations. The ACE equations for the system are given as :

For areas 1 and 2:

$$ACE_1 = \Delta P_{tie,12} + \beta_1 \Delta f_1 \quad \text{3-53}$$

$$ACE_2 = \Delta P_{tie,21} + \beta_2 \Delta f_2 \quad \text{3-54}$$

Where:

$\Delta P_{tie,12}$ is the tie-line power deviation from area 1 to area 2.

$\Delta P_{tie,21}$ is the tie-line power deviation from area 2 to area 1.

β_1, β_2 is the frequency bias factor for areas 1 and 2, defining the ACE's sensitivity to frequency deviations.

3.4. The Zebra Optimisation Algorithm

The ZOA is a new optimisation method that mimics zebras' behaviour in the wild. It's based on two main things zebras do: how they eat (exploration) and how they defend themselves (exploitation) (Trojovska et al., 2022). These natural behaviours give ideas for solving complex problems. The ZOA algorithm is based on how zebras search for food in large areas. In the wild, zebras travel through different landscapes to find the best grazing spots, which is like the exploration phase in optimisation (Lalngaihawma, Datta, Das, et al., 2024). During exploration, the algorithm considers all possible solutions to ensure it doesn't miss any good ones. This helps the algorithm gather many different solutions, just like zebras spread out to find the best resources.

Zebras protect themselves from predators in a way that is similar to how an optimization algorithm works. When the algorithm finds a good solution, it focuses on that area and searches more deeply there. This behaviour mirrors how zebras quickly band together to evade threats and ensure their safety. In optimisation, this approach focuses on improving the best solutions even further (Mohapatra & Mohapatra, 2023). The ZOA balances exploration and exploitation, just like zebras' balance between finding food and staying safe. If the algorithm explores too much, it might not find the best solution. If it exploits too much, it might get stuck in a suboptimal solution. By copying the zebra's adaptable behaviours, the ZOA finds a good balance and is both strong and efficient.

The ZOA's nature-inspired approach offers a new way to solve optimisation problems and shows how natural behaviours can inspire new computational techniques. The algorithm's settings can be adjusted to mimic different zebra behaviours, which makes it flexible and adaptable for many different applications.Whether used in engineering design, machine learning, or other complex problem areas, the ZOA shows how nature's insights can create powerful optimisation tools.

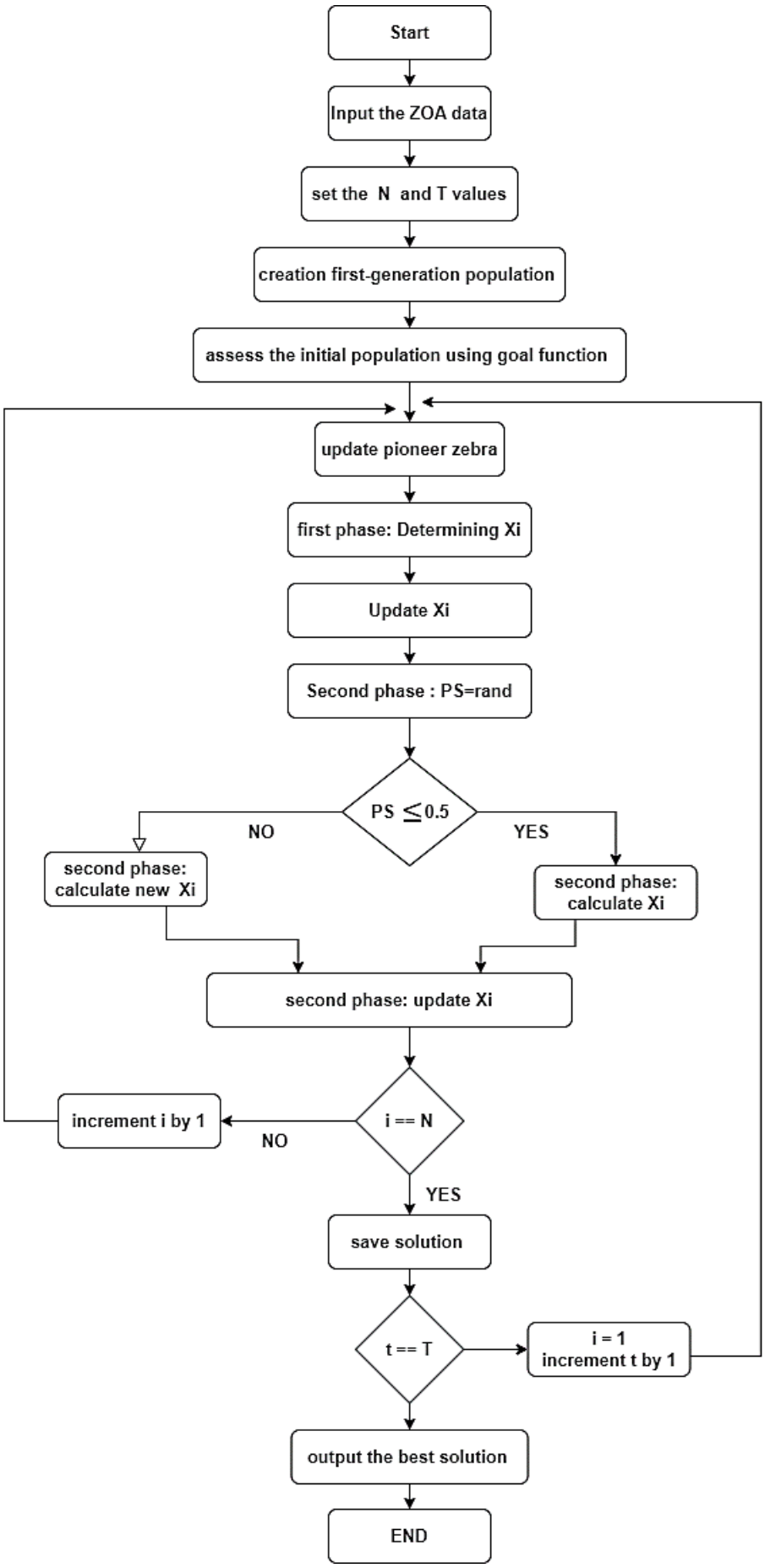

Figure 3-12: Flow chart of the ZOA (Adapted from (Trojovska et al., 2022))

The flowchart in Figure 3-12 shows how the ZOA works. It explains how the algorithm uses zebra behaviours to solve complex optimisation problems.

The following shows the step-by-step explanation:

i. Input and initialisation: The algorithm starts by getting the problem's details. Then, it sets two important parameters: the number of iterations (T) and the size of the zebra population (N). With these parameters set, the algorithm randomly places the zebras (each representing a possible solution) and evaluates them using the objective function. This step ensures that the search starts with a variety of possible solutions.

ii. Iterative process: The algorithm then enters its main loop, repeating from t = 1 to T. This loop helps the algorithm improve the possible solutions through a combination of exploration and exploitation.

iii. Pioneer zebra update: At the start of each iteration, the algorithm updates the "pioneer zebra" (This zebra is usually the best possible solution or a guiding solution that influences the rest of the population). By updating the pioneer zebra, the algorithm strengthens promising areas in the solution space.

iv. Foraging behaviour (Exploration): Within each iteration, the algorithm processes each zebra individually. Phase 1 – Foraging behaviour: The algorithm calculates a new status for each zebra using a formula that simulates the foraging behaviour of zebras. This step is like how zebras move to find food, representing an exploration of the solution space. The new status is then used to update the zebra's position using the equations:

$$x_{i,j}^{new,P1} = x_{i,j} + r \cdot (PZ_j - I \cdot x_{i,j}) \quad 3\text{-}55$$

$$X_i = \begin{cases} X_i^{new,P1}, F_i^{new,P1} < F_i; \\ X_i, \quad else, \end{cases} \quad 3\text{-}56$$

Where:

- $X_i^{new,P1}$ represents the updated status of the i^{th} zebra after the first phase.
- The j^{th} dimensional value of this status is denoted by $x_{i,j}^{new,P1}$.
- The objective function value corresponding to this status is $F_i^{new,P1}$.
- The pioneer zebra, denoted as PZ, is the best-performing member of the population, with its j^{th} dimensional value represented as PZ_j.

v. Defence mechanisms (balancing exploration and exploitation): After the foraging phase, the algorithm shifts to mimic zebras' defensive strategies against predators. The algorithm checks a probability parameter (Ps). If Ps is less than 0.5, it is reassigned to a random value. The defence mechanism is represented by the equation:

$$x_{i,j}^{new,P2} = \begin{cases} S_1: x_{i,j} + R \cdot (2r - 1) \\ \quad \cdot (1 - \frac{t}{T}) \cdot x_{i,j}, \quad P_s \leq 0.5; \\ S_2: x_{i,j} + r \cdot (AZ_j - I \cdot x_{i,j}), \quad else, \end{cases} \quad 3\text{-}57$$

$$X_i = \begin{cases} X_i^{new,P2}, F_i^{new,P2} < F_i; \\ X_i, \quad else, \end{cases} \quad 3\text{-}58$$

- Where, $X_i^{new,P2}$denotes the updated status of the i^{th} zebra during the second phase.
- Its j^{th} dimensional value is denoted by $x_{i,j}^{new,P2}$, and the corresponding objective function value is $F_i^{new,P2}$.
- The iteration counter is t, with T as the maximum iterations.
- R is a constant.
- The attacked zebra's status is denoted by AZ, with its j^{th} dimensional value is given as AZ_j.
- The probability of selecting one of two strategies is represented by P_s.

vi. Strategy 1: Against lion (exploitation phase) - If the condition is met, the algorithm applies an exploitation strategy using a specific mode (S1) of the updating formula. This strategy is like zebras focusing on a secure area after sensing a threat, intensively searching for an optimal solution in a promising region.

vii. Strategy 2: Against other predators (exploration phase) - Otherwise, the algorithm applies an alternative strategy (mode S2) that encourages further exploration of the solution space. This mechanism prevents premature convergence by diversifying the search when necessary. After the appropriate strategy is applied, the zebra's new status is finalised

viii. Selection and output: Once all zebras have been processed for the current iteration, the algorithm saves the best possible solution found so far. This ensures that the highest-quality solution is retained even as the population evolves. The iterative process continues until the specified number of iterations (T) is reached, at which point the algorithm outputs the best solution.

3.4.1. Adaptation of the Zebra Optimisation Algorithm

To apply the ZOA in the context of LFC, it is important to integrate with an appropriate objective function that will reflect the dynamic performance requirements of the power system. In this case, the main goal is to optimise the PID controller parameters such that the system responds quickly is accurately to disturbances while at the same time maintaining the frequency stability. A commonly used cost function in the study is the ITAE (Çelik et al., 2023) , given as:

$$ITAE = \int_0^T t \cdot |\Delta f(t)| \, dt \quad 3\text{-}59$$

This function ensures that the frequency deviation is not only minimised but also corrected quickly. This is in conjunction with the other performance indices, i.e. over-

/undershoot, settling time, and the steady state error. To ensure that the algorithm performs effectively in finding the gain parameters, the tuning of its internal parameters is necessary. The main parameters that influence the ZOA's behaviour are:

- Population size
- Maximum number of iterations
- Exploration/exploitation balance coefficient
- Convergence criteria
- Search area

The tuning ensures that the algorithm navigates the solution space, avoids local optima, and identifies global optimal control parameters.

3.5. Conclusion

This chapter presented the modelling of a single-area power system for analysis, the two-area system and the optimisation algorithm. The components included the governor, turbine, generator and load, which were mathematically represented and will be implemented in MATLAB/Simulink. The next chapter implements the model to create a baseline framework for the controller evaluation.

CHAPTER FOUR
SIMULATION AND ANALYSIS OF A SINGLE AREA SYSTEM

4.1. Introduction

The power network model is important for analysing grid behaviour under various operating conditions, identifying potential issues, and developing strategies to improve the grid's stability and efficiency. The integration of renewables introduces new dynamics into power networks, posing challenges for grid management due to their decentralised, intermittent, and variable nature. A well-developed power network model enables the simulation and study of these dynamics, providing insights into effective renewable energy integration without compromising grid reliability. This section's dynamic analysis will be performed without considering the effects of the solar PV system. The scenarios of load changes will be analysed at this stage to evaluate the system's inherent behaviours and stability characteristics. After this, integrating PV and BESS into the analysis will enable a thorough discussion of their impact on system dynamics. The approach provides a step-by-step understanding of how PV and BESS affect the system structure under changing load conditions, thereby improving frequency stability and overall performance. The addition of the BESS and PV presented a larger frequency deviation, which affects the stability of the system. As such, a conventional PID controller was developed to mitigate the instability. A benchmark model with its parameters was adopted from (Akter et al., 2022), and used to study the system behaviour and later modified by adding a PV and BESS. Table 4-1 presents the benchmark model data and

Table 4-2 shows the added PV generation unit and BESS parameters, considering a nominal frequency of 50 Hz.

Table 4-1: Parameters of the benchmark single-area system (Akter et al., 2022)

Parameter	Symbol	Typical value
Governor gain constant	K_g	1
Governor time constant	T_g	0.2 s
Turbine gain constant	K_t	1
Turbine time constant	T_t	0.5 s
System inertia constant	H	5
Load-damping coefficient	D	0.8
Speed regulation constant	$1/R$	20 Hz/MW

Table 4-2: Parameters of the PV generation unit and BESS

Parameter	Symbol	Typical value

PV system gain constant	K_{PV}	1
PV system time constant	T_{PV}	0.3 s
BESS gain constant	K_{BESS}	1
BESS time constant	T_{BESS}	0.1 s

4.2. Simulation scenarios

In this section, a benchmark model is simulated in MATLAB/Simulink, and later, the renewables (PV and BESS) are included to further study how the system behaves. The following case studies evaluate the behaviour of the single-area power system. By analysing the load variations, renewable energy integration, and the role BESS plays in the system, these findings further guide improvements in controller design to maintain frequency stability. Figure 4-1 illustrate the adopted benchmark single-area LFC model used in the analysis.

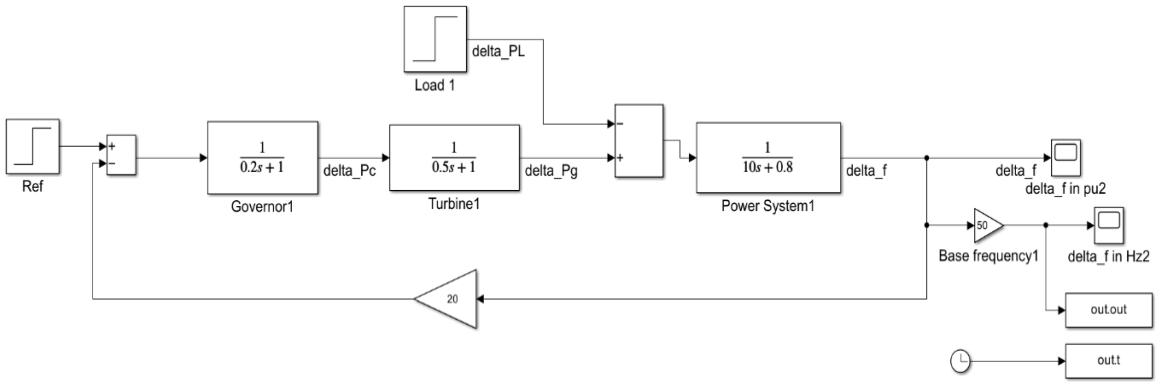

Figure 4-1: Single-area load frequency control Simulink model (Akter et al., 2022)

4.2.1. Case 1: Under normal operation with no load change

In this baseline scenario, the system is simulated under steady-state conditions, with no changes in the load or generation. This case serves as a reference to assess the system's natural behaviour and its stability when there are no disturbances or control interventions. Figure 4-2 shows how the system behaves when there is no disturbance. It can be observed that there is zero frequency deviation, which means the system frequency remains at its nominal value of 50 Hz. With no disturbances over time, the frequency will remain at 50 Hz.

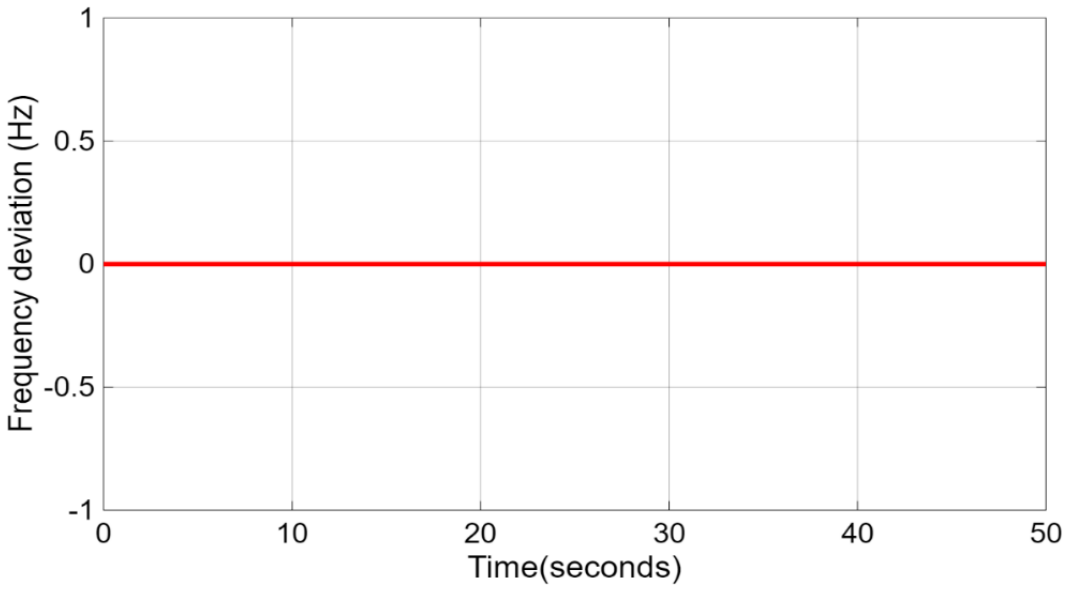

Figure 4-2: Frequency response under normal operations

4.2.2. Case 2: Load changes

In this case, the system is subject to a step change in load demand to evaluate its frequency response without a controller. A sudden change in load represents a typical real-world disturbance, such as a sudden spike in residential or industrial consumption. The simulation is configured with an initial steady state condition, after which a step load increase is applied. Figure 4-3 shows the frequency response when the load change of 5%, 10%, 15%, 20% and 25% is applied as a step change at 10 seconds.

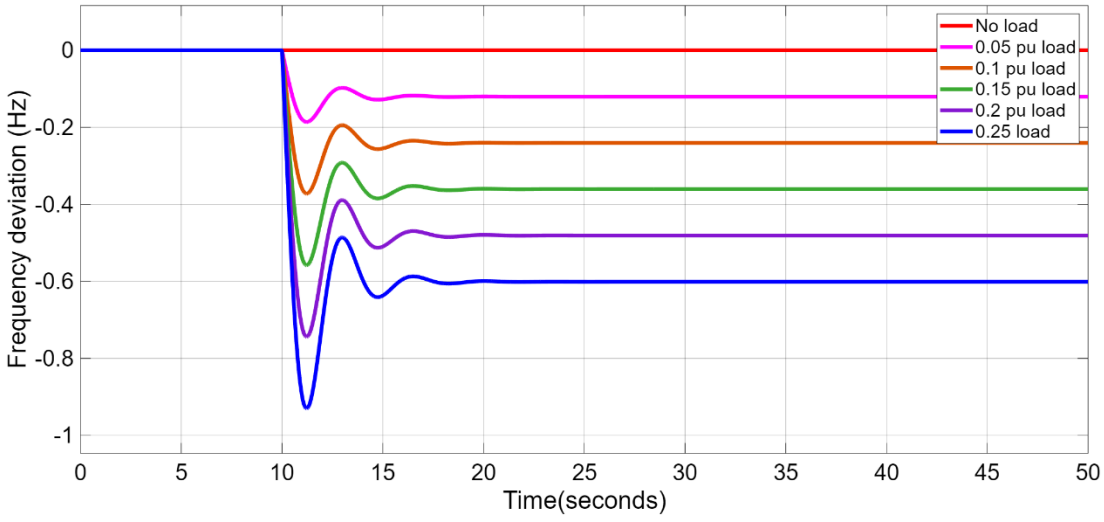

Figure 4-3: Frequency response due to load changes

From the figure, the response demonstrates the impact the load has on the frequency deviation and dynamic performance in an uncontrolled environment. For the smallest disturbance of 5%, the frequency deviation is relatively minor, showing that the system can withstand small fluctuations. When the load changes increase to 10%, the frequency

shows a slightly larger drop, but the deviation remains moderate. As the load continues to increase further by 15%, 20%, and 25%, the system response shows a more pronounced frequency dip, with the deviation growing in proportion to the magnitude of the disturbance. As the load demand continues to change, the generation and demand balance will remain disturbed, which may further cause certain loads to trip or degrade the system's performance.

In all these cases, the frequency eventually stabilizes, but it does so at a new steady-state value, which is below the nominal system frequency. This behaviour highlights the inherent limitation of the system under primary control alone, where the governor action can only partially restore the balance between generation and demand. Without the presence of secondary control, the frequency fails to recover to its nominal value after the disturbances, which leaves the system to operate at an offset steady state. These results underline the role of secondary control mechanisms in eliminating steady state errors, restoring frequency, and maintaining stability in the presence of load changes.

4.2.3. Case 3: With PV system and without BESS

In this scenario, the system is integrated with a PV generation source, while no BESS is included in the system, as shown in Figure 4-4.

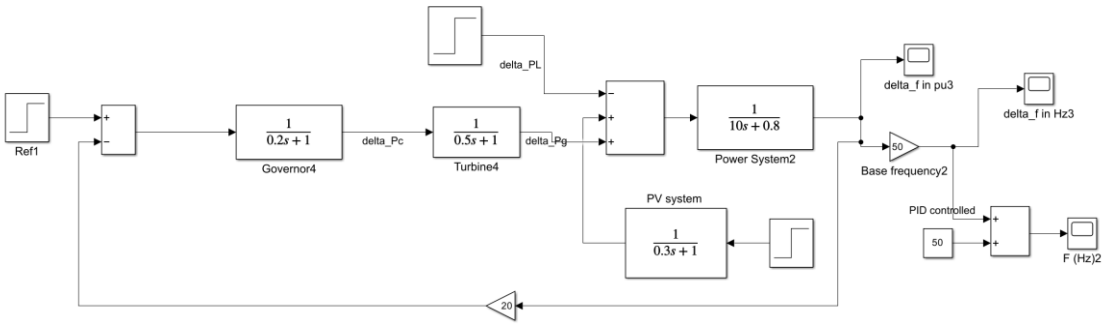

Figure 4-4: Model of a single area system with a PV system

This case evaluates the impact of renewable energy integration on the system's frequency dynamics without storage support. Solar PV generation is intermittent and depends on the weather conditions, which leads to fluctuations in the power output. In these simulations, 10%, 15%, 20%, and 25% solar PV penetration cases are simulated, and the frequency response is shown in Figure 4-5.

In this scenario, the PV input is added from the beginning of the cycle, i.e. at 0s, while maintaining a constant step load change of 10% at 10s throughout the varying solar PV generation. Immediately after the PV integration, the system frequency shows a spike, reflecting the sudden injection of active power into the network.

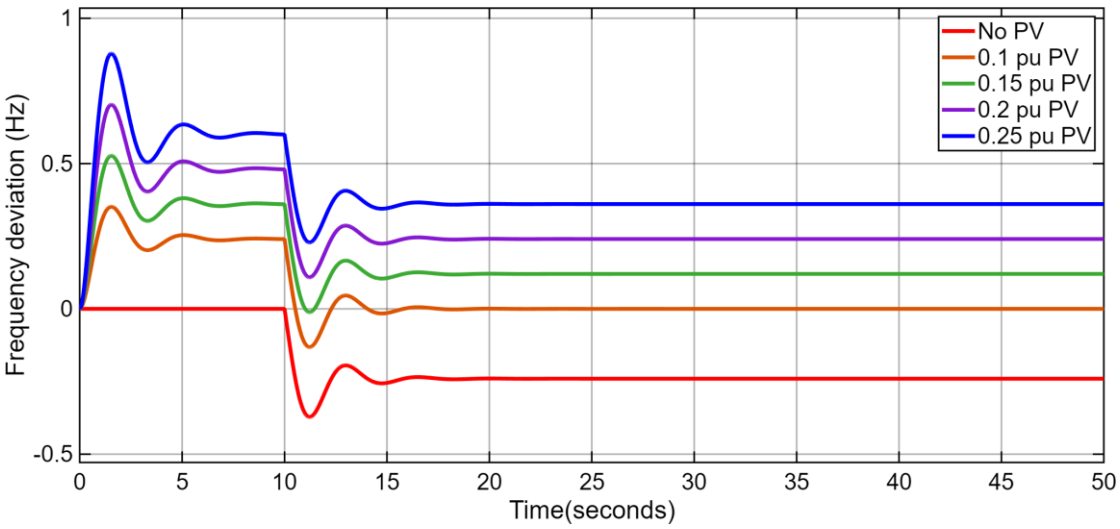

Figure 4-5: Frequency response due to changes in solar PV levels

This transient overshoot is followed by a settling process, where the frequency starts to stabilise at a new steady state value that is slightly higher than the nominal frequency. The rise above the nominal level indicates that, in the absence of coordinated control, the PV contributes excess power that shifts the frequency upwards. When the 10% load change is introduced at 10 s, the system experiences a downward frequency deviation. The added demand exceeds the immediate regulating capability of the system, which causes the frequency to drop. After this disturbance, the system begins to settle again, but now at a lower steady-state value compared to earlier. This shows that while PV integration contributes to the system power balance, it does not provide frequency regulation without support, and the system will remain vulnerable to load fluctuations.

To further investigate the influence of PV penetration level, different integration percentages are applied. At lower PV penetration of 10% and 15%, the frequency deviation following the load disturbance is less. The noticeable difference is when the PV penetration of 10% matches the magnitude of the load disturbance. In this case, the net change in the system power balance is zero as they cancel each other and settle close to zero deviation. At higher PV penetration levels of 20% and 25%, the system experiences a larger frequency spike, also followed by a deeper drop when the load increases. Without a BESS to buffer these variations, the system experiences increased frequency instability. These fluctuations, as observed in the responses, act as a disturbance that the system must absorb, which results in frequency oscillations, a higher peak deviation and a higher steady state error, as the system frequency does not recover to its nominal value. Since the PV system is connected through power electronics and does not contribute rotational inertia, the system's ability to resist the frequency changes is weak.

4.2.4. Case 4: With PV system and BESS

In this case, a BESS is integrated into the system as shown in Figure 4-6. The main aim is to evaluate the impact the BESS has on the frequency response and how it can improve the frequency stability of the system.

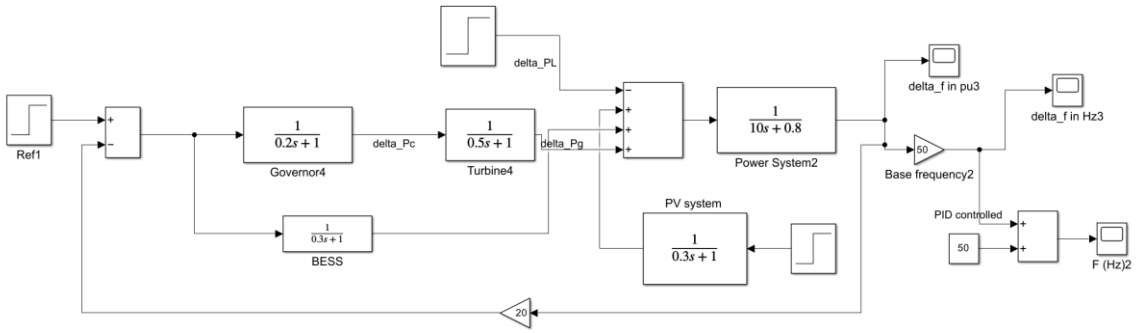

Figure 4-6: Model of the single-area with PV and BESS

Figure 4-7 shows the frequency deviation over time with the penetration of both the PV and BESS at different PV penetration levels from Case 3. With the integration of a BESS, the system's frequency response has improved, showing reduced frequency spike after PV is introduced and has minimized the frequency deviation.

The BESS acts as a fast-responding buffer, absorbing excess energy during high PV output and injecting power during sudden drops or load increases. The simulation indicates an improvement in reducing the frequency nadir and overshoot, has faster settling time, and has dampened the oscillations to improve the overall system, without the controller.

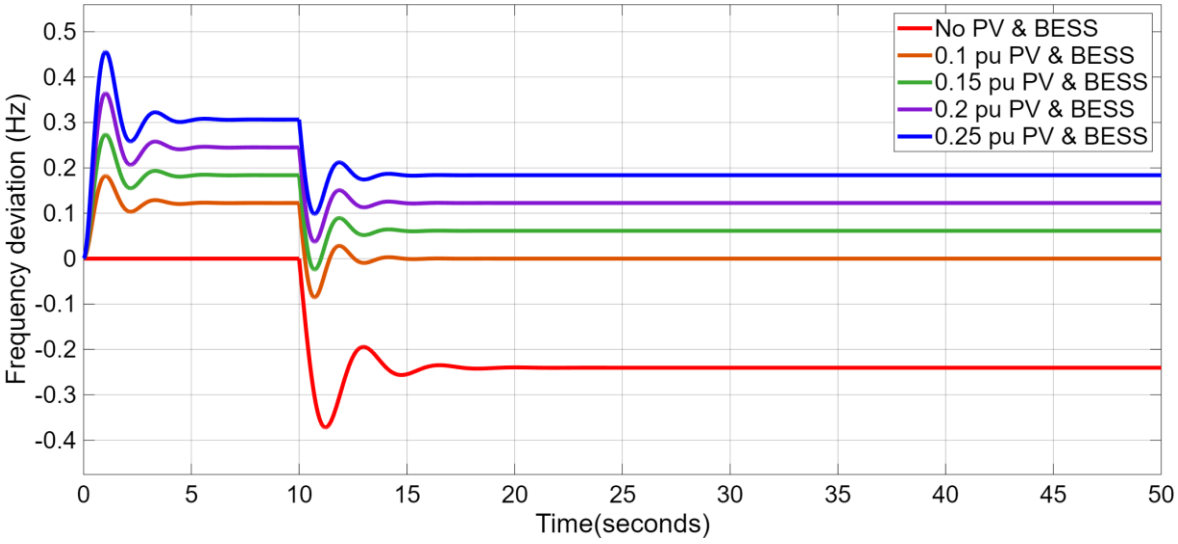

Figure 4-7: Frequency response when PV and BESS are integrated

Unlike the PV system, the BESS can contribute to frequency regulation, mimicking inertial response and improving the system's ability to resist frequency changes, and as a result, settles closer to the nominal value.

4.2.5. Variable load and PV profile

When a variable load profile is introduced into the system, the frequency response becomes more dynamic compared to the step-change cases. The continuous fluctuations act as persistent disturbances, which require the system to constantly adjust its power balance. Figure 4-8 shows the frequency response when a variable load is introduced, in the presence of a PV and BESS.

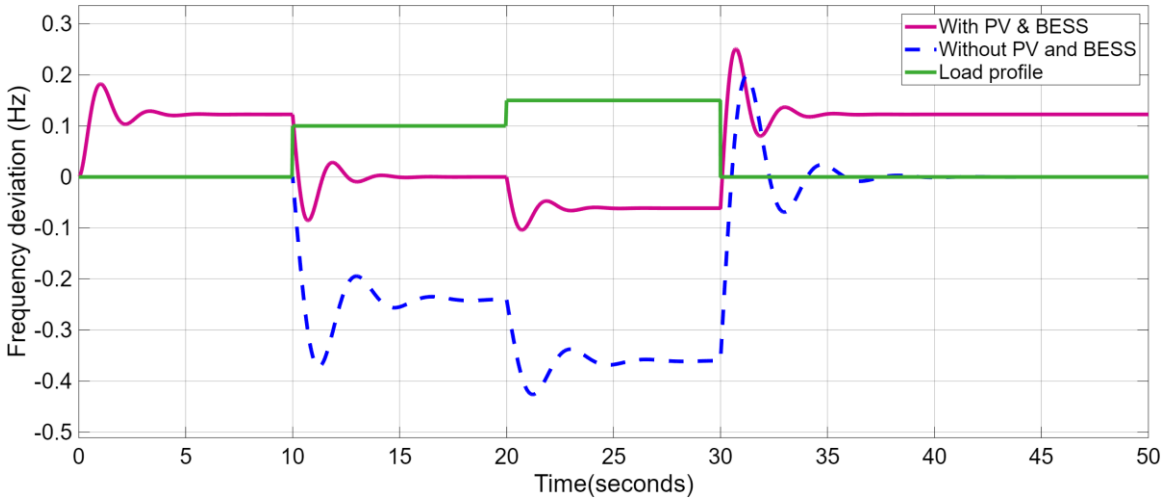

Figure 4-8: Frequency response with a variable load profile

With the BESS in operation, the system shows improved resilience. The BESS injects or absorbs power in response to the short-term load variations. This reduces the frequency deviation and helps maintain the frequency closer to the nominal value. The PV system also contributes by supplying additional active power.

Now, a variable PV generation profile is introduced into the system while the load undergoes a 10% step increase at 10s and remains constant thereafter. Figure 4-9 shows the system's response with a variable PV generation profile. The system's frequency is affected by both the load disturbance and fluctuating PV output. The results show that when the PV generation exceeds the applied load change, the system experiences a higher steady-state error. The PV's contribution overcompensates for the additional demand, which shifts the frequency above its nominal value. Without proper control, this imbalance cannot be corrected, and the system will continue to operate at that steady state value.

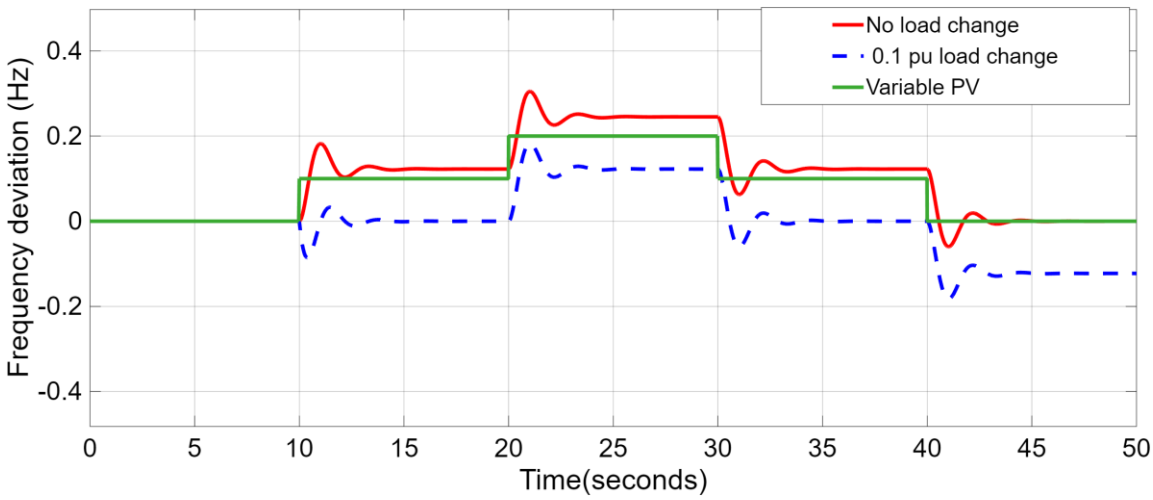

Figure 4-9: Frequency response with variable PV profile

4.2.6. Summary of uncontrolled results

Table 4-3 shows the summary of the results from the frequency responses in cases 1 to 4. This shows the maximum frequency deviation, the settling time, and the steady state error in each case study.

Table 4-3: Summary of results in uncontrolled cases

Case no:	Description	Load step	PV	BESS	Max frequency nadir (Hz)	Settling time (s)	Steady stare error (Hz)
1	Baseline (No changes)	0	No	No	0	0	0
2.1	5% load increase	0.05	No	No	0.192	17.56	-0.175
2.2	10% load increase	0.1	No	No	0.385	17.56	-0.238
2.3	15% load increase	0.15	No	No	0.568	17.56	-0.386
2.4	20% load increase	0.2	No	No	0.764	17.56	-0.487
2.5	25% load increase	0.25	No	No	0.863	17.56	-0.60
3	20% load increase with PV	0.1	Yes	No	0.182	17.56	0.253
4	20% load increase with PV and BESS	0.1	Yes	Yes	0.06	14.74	0.136

4.3. PID-controlled cases

The results obtained in Section 4.2 show that without any controller, the frequency does not settle at its nominal value and continues to deviate as disturbances are introduced in the system. In this section, a PID is introduced into the system with the PV generation

unit and BESS already integrated. This is to assess how a classical control strategy improves the system's frequency performance in the presence of both renewable variability and fast-responding energy storage. The PID controller is tuned using the Ziegler-Nichols method to respond to the frequency deviations by adjusting the control signals to the generation units. It acts as part of the LFC system mechanism, working in coordination with the BESS to regulate the power imbalance caused by both the load disturbance and PV fluctuations. Appendix A shows the process of finding the PID parameters. From those calculations, the obtained gain parameters are as shown in Table 4-4, and the Simulink model with a PID controller is shown in Figure 4-10.

Table 4-4: PID parameters

K_p	K_i	K_d
2.22→2.0	2.262→1.5	0.544

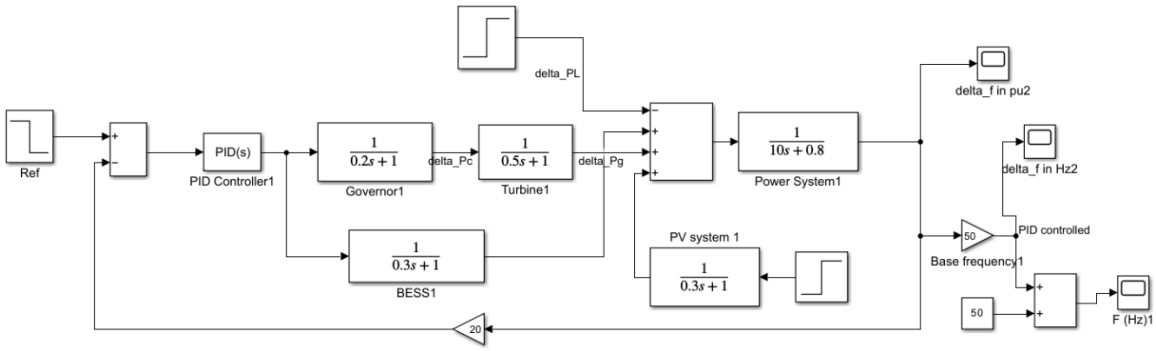

Figure 4-10: Single area system model with PID controller

To evaluate the performance of the PID controller, a series of simulation scenarios is conducted. The first case introduces sudden load changes to assess the ability of the controller to regulate the system frequency under these varying load demands. In the second case, the system is tested to assess how the controller performs due to the PV system and BESS integrated, variable load profile, variable PV, and finally due to generation losses.

4.3.1. Load changes

The first case considers load changes of 15% and 20%. Figure 4-11 and Figure 4-12 shows the frequency deviation and frequency when the system experiences a sudden load change of 15% and 20%, respectively. Without a controller, the change produces a sharp frequency drop followed by oscillations that do not return to nominal. Now, when a PID controller is introduced, the frequency drop is reduced, fewer oscillations occur, and the steady-state error is eliminated. The frequency nadir is less in the controlled case when compared to the uncontrolled case and is restored to nominal faster with the support of a PID controller. This shows the ability of the PID to eliminate errors.

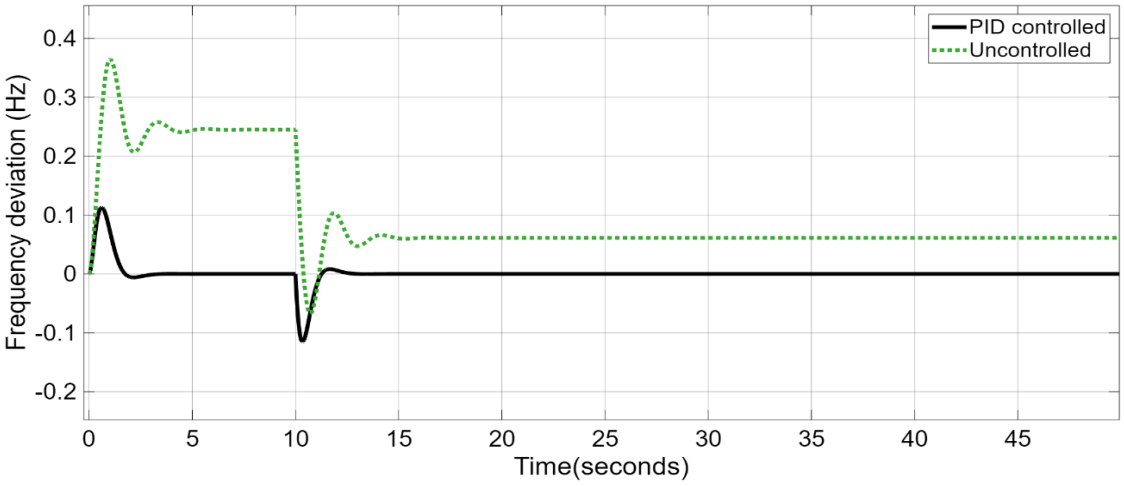

Figure 4-11: Frequency response due to a 15% load change

Figure 4-12 shows the response for a 20% step load increase. The uncontrolled case produced a deeper frequency nadir with more oscillations. The PID-controlled response shows effective damping and restoration towards the nominal with minimal steady state error. The controller is also able to reduce the frequency spike caused by the introduction of PV generation into the system.

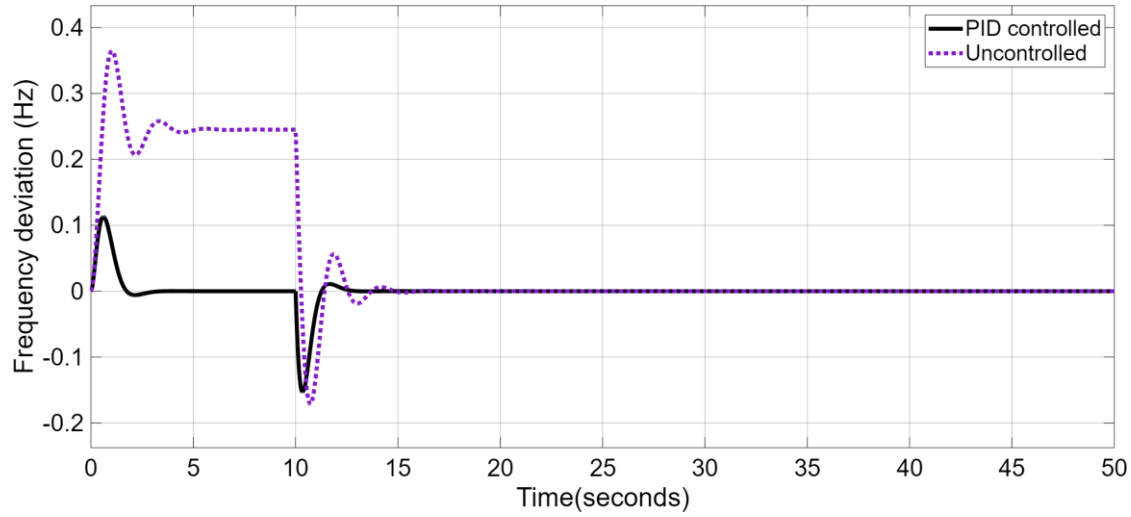

Figure 4-12: Frequency response due to 20% load change

The next scenario considers the system response to a variable load profile. Instead of a single-step disturbance, the load is allowed to change continuously over time. This case provides insight into how well the PID controller can track and stabilise the system when the load does not follow a predictable step. Figure 4-13 shows the response of the

uncontrolled and PID-controlled case for a variable load, while PV is kept at a constant value.

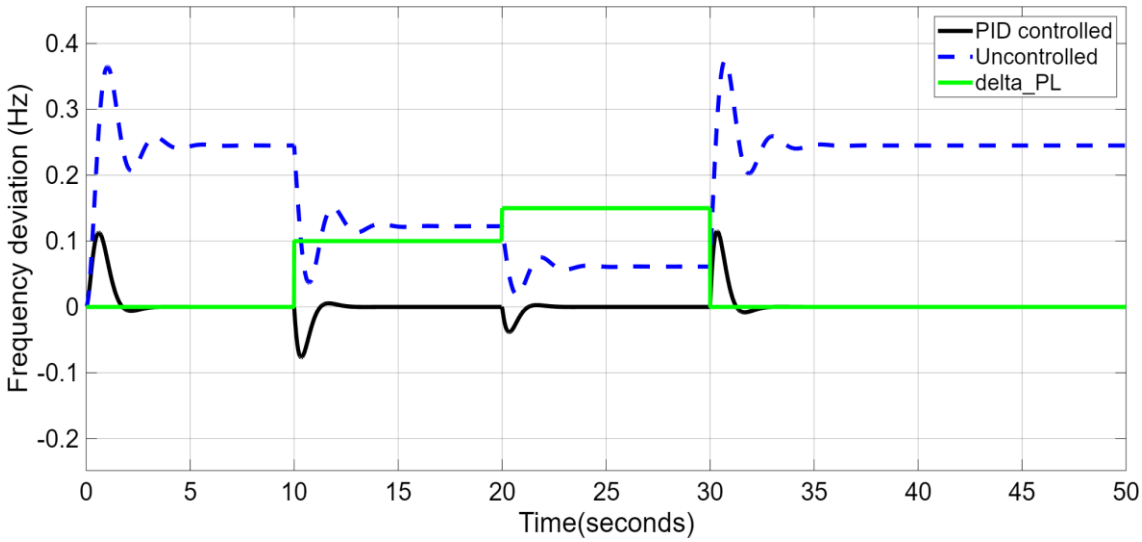

Figure 4-13: Frequency response due to variable load

From Figure 4-13, it is evident that without a controller, the system fails to manage the load fluctuations, resulting in persistent deviation from nominal frequency. The PID-controlled systems maintain frequency and eliminate the steady-state error, while short-term oscillations are still present, the controller corrects errors and restores balance.

4.3.2. Effects of the PV and BESS

When a PID is introduced in a PV and BESS integrated system, after a disturbance, BESS provides fast power support, while the PID helps the system recover steadily. The PID controller reduces oscillations, eliminates the steady state errors and settles faster as shown in Figure 4-14.

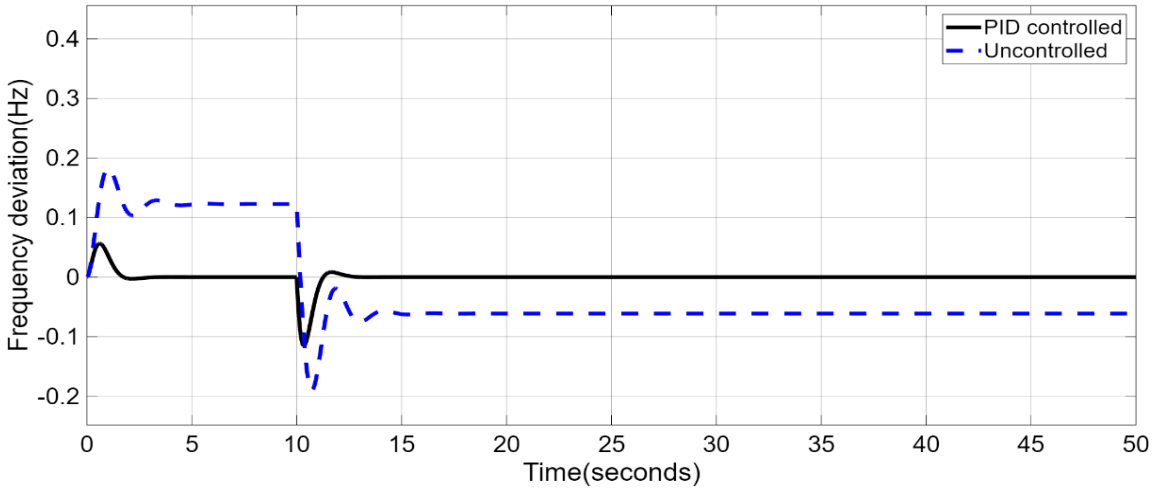

Figure 4-14: Frequency response due to 10% PV penetration

From Figure 4-14, it is evident that BESS, with the help of a controller, is effective for LFC. The ability to absorb or inject power allows them to respond quickly to frequency deviations, which makes them ideal for addressing the fast dynamics introduced by renewable energy variability. In the following scenario, a variable PV profile is added to the system to test the controller's effectiveness further. Figure 4-15 shows the response of this case.

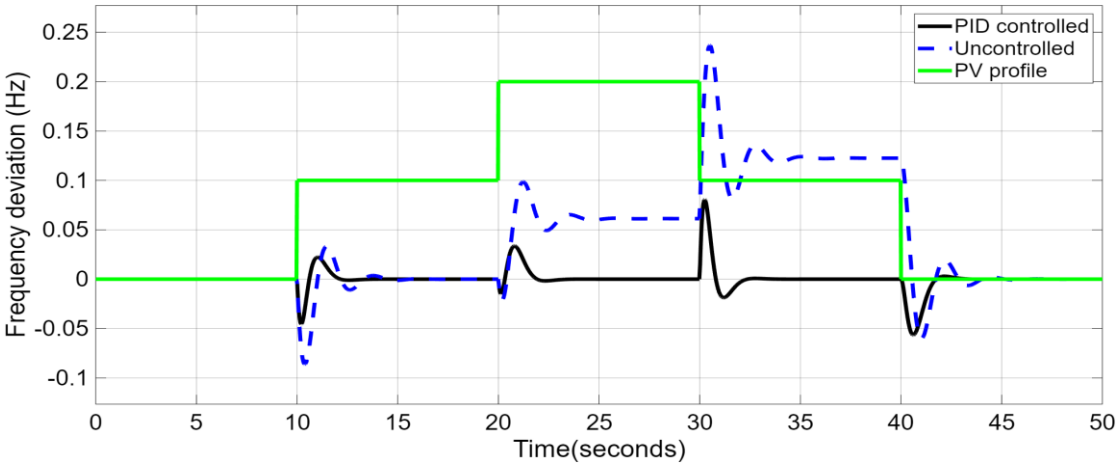

Figure 4-15: Frequency response due to variable PV generation

From Figure 4-15, when compared with the uncontrolled scenario, the PID controller can minimise frequency deviations, even with a changing PV generation profile. The following scenario assumes a loss of BESS while keeping the PV generation variable. Figure 4-16 shows the system's response due to the loss. The results indicate an increase in oscillations, with a gradual settling towards the nominal value.

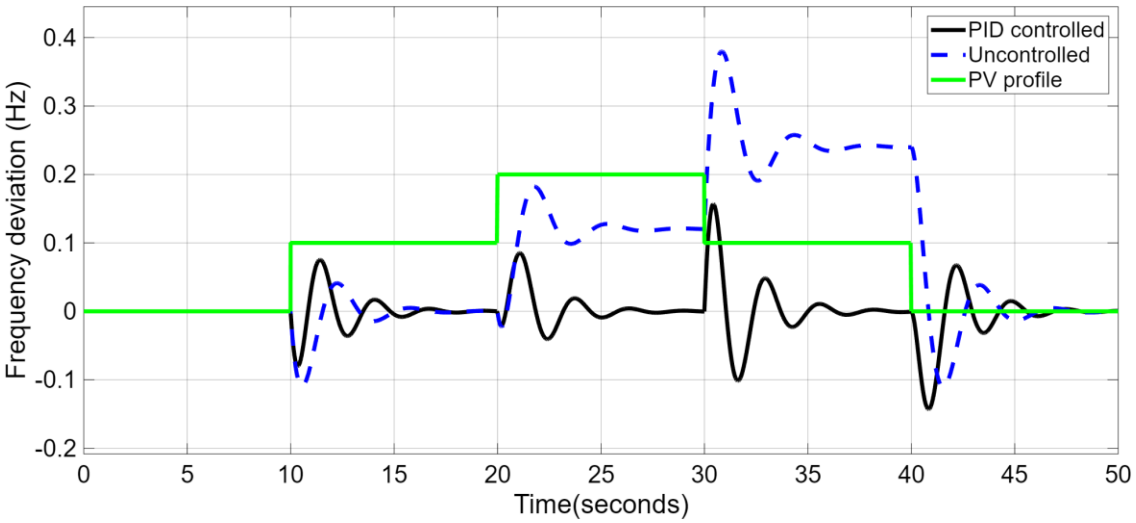

Figure 4-16: Frequency response due to loss of BESS

4.3.3. Generation loss

Following a loss of generation at 20 seconds, shown in Figure 4-17, the system experiences a decline in frequency due to the sudden power imbalance between generation and demand. The primary governor response acted rapidly through the drop

mechanism to inject additional mechanical power, which helped arrest the frequency drop and stabilise the system at a new operating point. This point remains below the nominal frequency, as shown in Figure 4-17. The steady state was not fully eliminated, indicating that the current controller settings are insufficient to fully restore frequency following the disturbance.

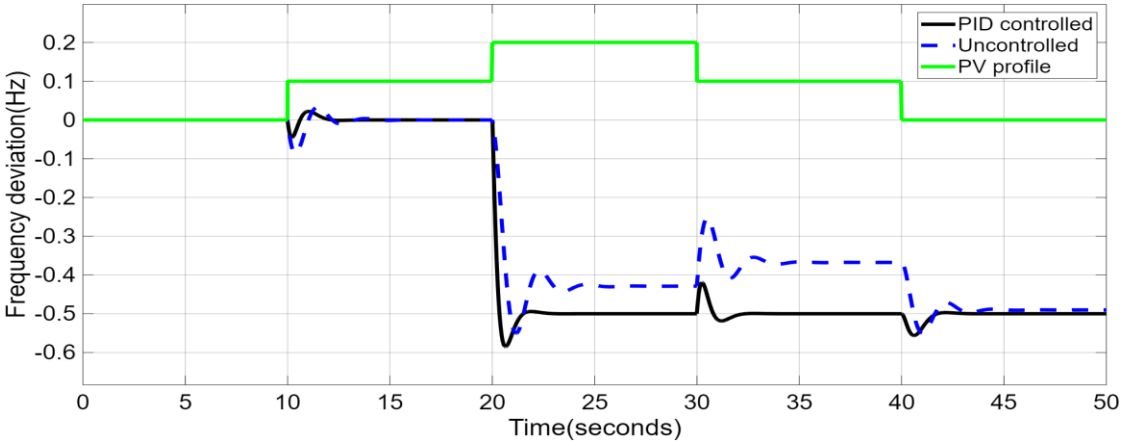

Figure 4-17: Frequency response due to generation loss (PID controlled)

4.4. Conclusion

This chapter discusses the basic analysis of a single-area system without a controller and compares it with the analysis using a classical PID controller. The simulated cases demonstrated the system's natural response to load disturbances and the effect of integrating a PV system and BESS, which shows large frequency deviations and slow recovery times in the absence of a controller. While the PID controller offered noticeable improvements, its fixed-parameter nature limits its adaptability under dynamic and uncertain operating conditions. The next chapter focuses on the application of ZOA to improve the LFC performance by optimising the controller parameters for improved robustness and adaptability.

CHAPTER FIVE

IMPLEMENTATION OF THE OPTIMISATION ALGORITHM

5.1. Introduction

This chapter implements the ZOA to tune the PID gain parameters. The cases simulated to test the performance of the ZOA included changes in the algorithm's parameters, load variations, the effect of PV power and BESS integrated into the system, and generation loss. These results are compared to those obtained when a PID controller was used in Chapter 4. The performance metrics for this algorithm will include the frequency nadir, settling time, and steady-state error. These performance metrics will highlight the strengths and weaknesses of the ZOA in achieving frequency regulation.

5.2. Implementation in MATLAB/Simulink

The ZOA is used to tune the PID controller gains, ensuring minimal frequency deviations and rapid stabilisation under varying load conditions. By leveraging the ZOA's ability to balance exploration and exploitation, the PID parameters are optimised to achieve improved system performance metrics, such as reduced settling time, minimised overshoot, and elimination of steady-state error. The implementation of the objective function is shown in Figure 5-1 and Figure 5-2 shows the modified single-area system used to evaluate the algorithm's performance. The load variation is modelled as a step input, as in the previous chapter, representing changes in demand, while the frequency deviation serves as the output of interest. The ZOA algorithm interacts with the system model to optimise the PID controller gains iteratively, based on defined performance objectives like minimising the ITAE. The results of the simulations are analysed to assess how effective the ZOA is in enhancing the frequency response and stabilising the system under various scenarios, such as load variations and renewable energy integration.

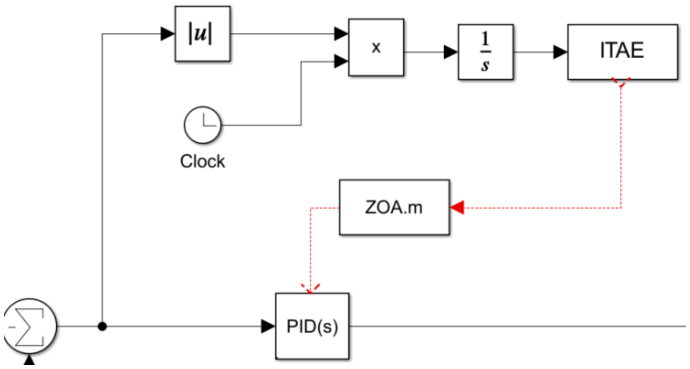

Figure 5-1: Implementation of the objective function

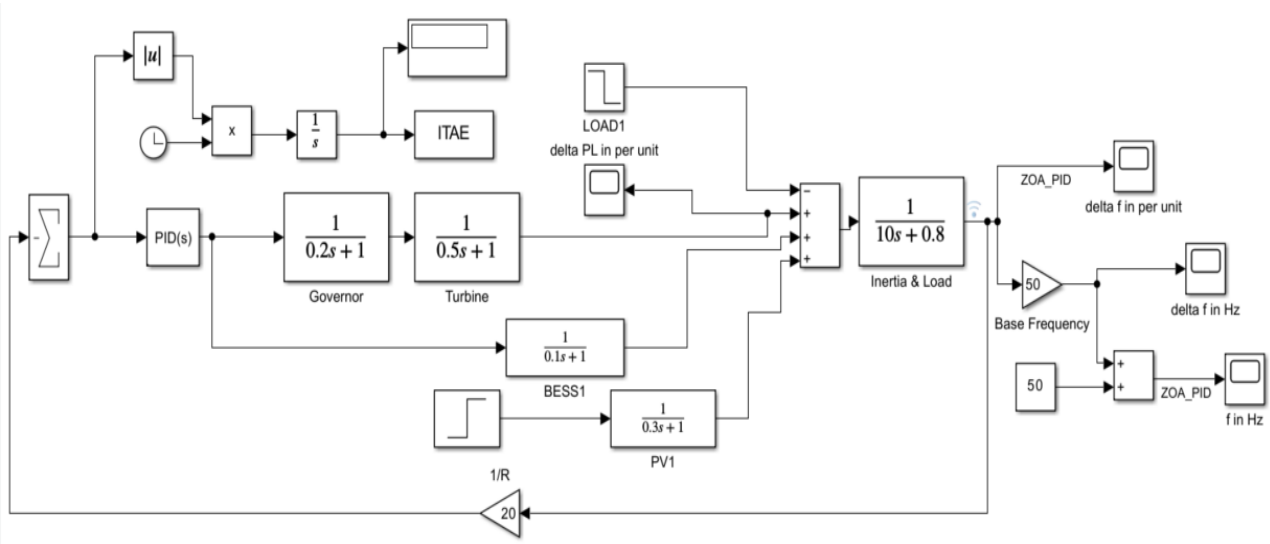

Figure 5-2: Modified single-area system

5.3. Simulation scenarios

This section describes simulation scenarios that test how well the ZOA-based controller performs. These scenarios look at different operating conditions, such as sudden changes in load, input from renewable generation, and the use of BESS. The simulations are based on the earlier cases that used a baseline and PID controller, to compare the ZOA-based controller's performance.

5.3.1. Parameter changes of the algorithm

The changes in the parameters of the ZOA directly influence its convergence behaviour, exploration-exploitation balance, and the quality of the PID controller tuning. The key parameters, such as the population size, maximum iterations, exploitation coefficient, and search space, determine how the algorithm will perform in searching for optimal control gains. A series of simulations is conducted to determine the parameters that would provide the optimal solution. This includes determining the boundaries, which is the search space, the number of search agents, the maximum iteration, and the effects they have on the overall frequency response of the system.

The most important parameter in the optimization process tested is the search space, which defines the boundary values. The boundaries set the limits within which the algorithm can explore potential solutions, which influence both the convergence behaviour and the quality of the results. To test for this effect, the boundary values were varied at 5, 10, 15, and 20, while keeping the maximum iteration at 30 and the search agent at 5. Figure 5-3 illustrates the convergence curve for all four boundary cases plotted together. The results show that the algorithm converged within the specified iterations, though the rate and stage of convergence vary with the boundary size. Smaller boundaries, such as 5 and 10, converged at a higher value than 15 and 20. A lower value

enables the algorithm to find better solutions at a slightly later stage in the iteration process.

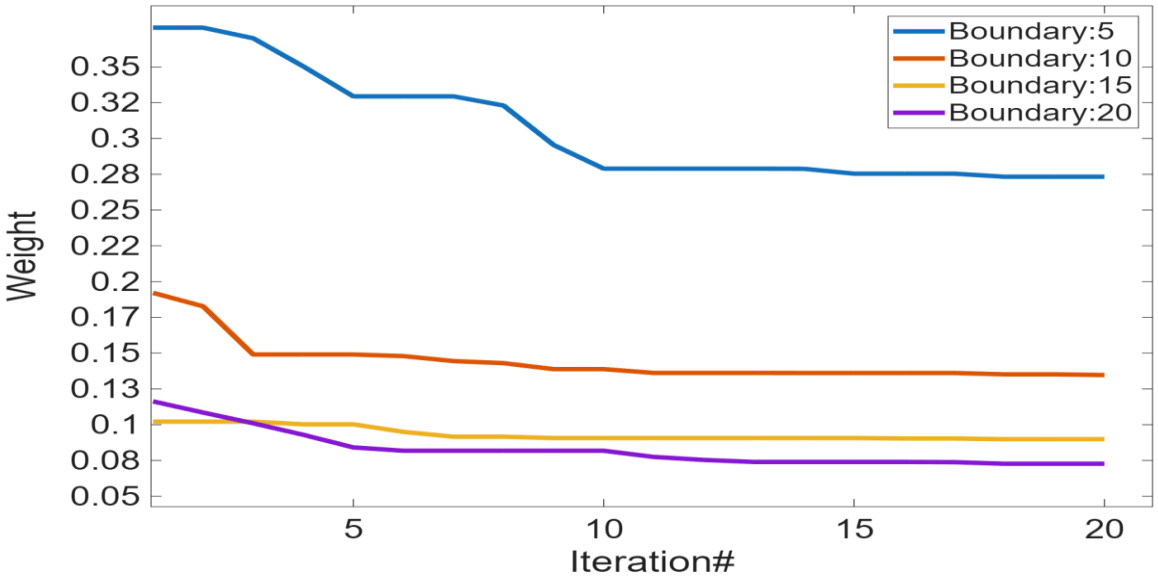

Figure 5-3: Convergence curve at multiple boundaries

Figure 5-4 illustrates the corresponding frequency responses. These indicate that increasing the boundary improves the system's stability by reducing the overshoot and undershoot, with values decreasing to less than 0.008, and at a higher boundary, even less. The settling time is somewhat similar across the different scenarios, but when the boundary is set at 20, the system shows a faster settling time compared to the boundaries at 10 and 15. The latter configurations demonstrate better characteristics for minimizing overshoot, although they settle more slowly. This suggests that the behaviour is primarily influenced by the system's dynamics or control limitations rather than the specific boundary configuration.

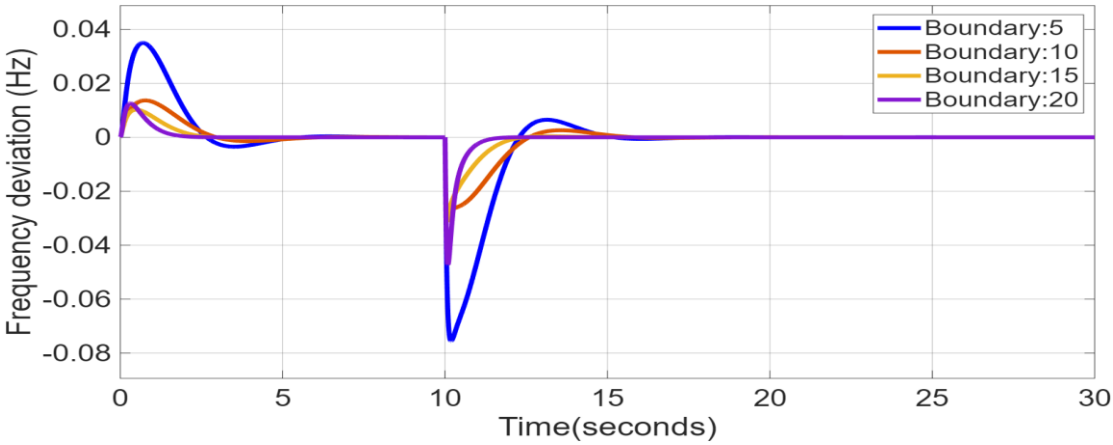

Figure 5-4: Frequency response due to boundary variations

From the boundary tests, it can be concluded that the search space does play a role in the performance of the algorithm. Smaller boundaries allow for earlier convergence but restrict the algorithm's ability to explore, which leads to less accurate solutions and

limited improvements in frequency stability. Larger boundaries allow for a broader search and result in a lower convergence value and improved frequency response. While larger boundaries generally provide better optimization results, the choice of the boundary should balance the solution quality and may vary depending on the characteristics of the system as it changes variables.

For the search agents, a few search agents may result in premature convergence, while having too many agents can slow down the algorithm's convergence due to increased computational costs and prolonged exploration of non-optimal regions without a guarantee that the solutions identified are the global optimum. The search agent in the previous case was initialized to 5 with 20 iterations. Now the search agents are increased to observe how that affects the convergence and the system's response. Figure 5-5 shows the convergence curve when the search agent is 5 and the maximum iterations are 20.

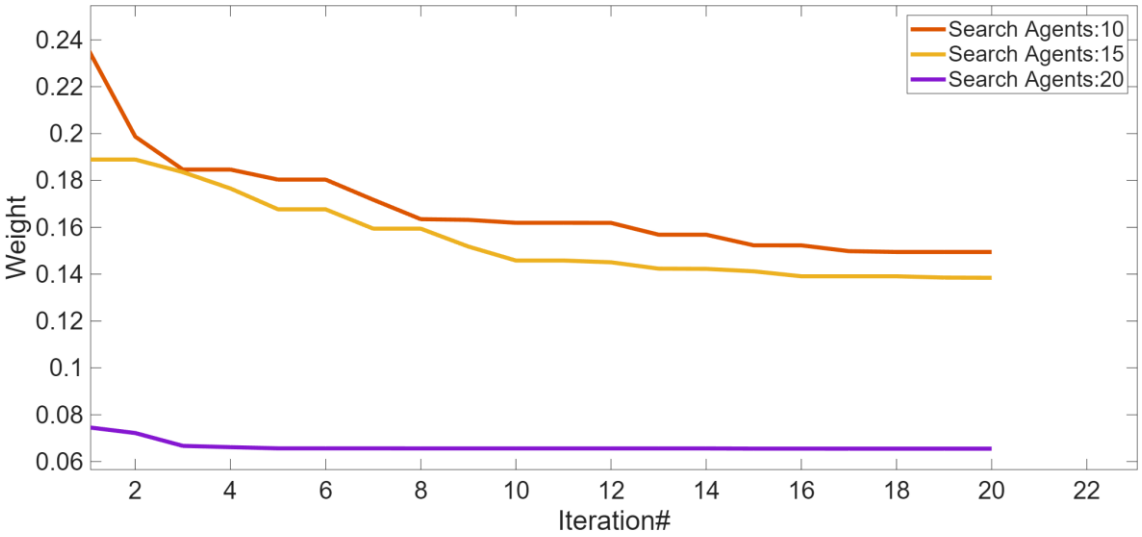

Figure 5-5: Convergence curves due to search agents' variations

With 10 and 15 agents, the convergence was slower and settled at a higher fitness value, which indicates that there are fewer optimal solutions. When the search agents increased to 20, the algorithm converged faster and also achieved a lower final fitness value. These results show that a large population size improves both exploration and exploitation, which allows the algorithm to avoid premature convergence. It does increase the computational time, as such a trade-off between finding the best solution and less computational time is important. Figure 5-6 shows the corresponding frequency response for this case.

The response shows that increasing the population size improved both the convergence behaviour and the frequency response. When 20 agents are used, the system showed a reduced frequency spike following the introduction of the renewable generation, along

with a smaller frequency nadir and shorter settling time compared to 10 and 15-agent cases when a load change was introduced at 10s

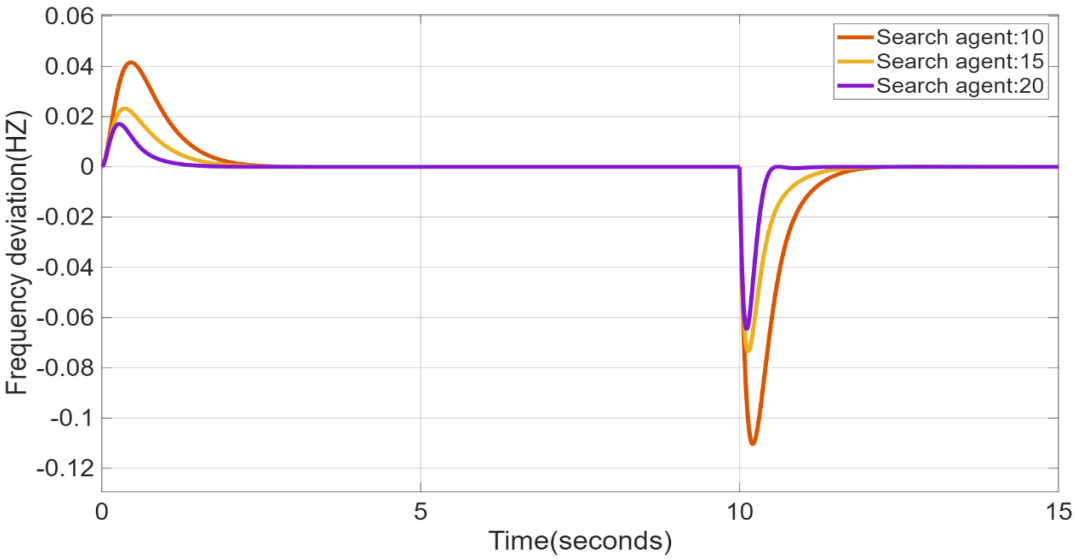

Figure 5-6: Frequency response due to search agents' variations

. The search agent was increased to 10, while the maximum iterations is still 20. The convergence curve shows that the solution was obtained at iteration 19. This solution may be good, but it is not guaranteed to be the best solution, as higher iterations could result in better results. At this stage, it remains an assumption that this could be a good solution; this then proves that the solution is not the best and could be improved by increasing the maximum iterations. Figure 5-7 shows the convergence curve when the maximum iterations are increased to 30, 50 and 100.

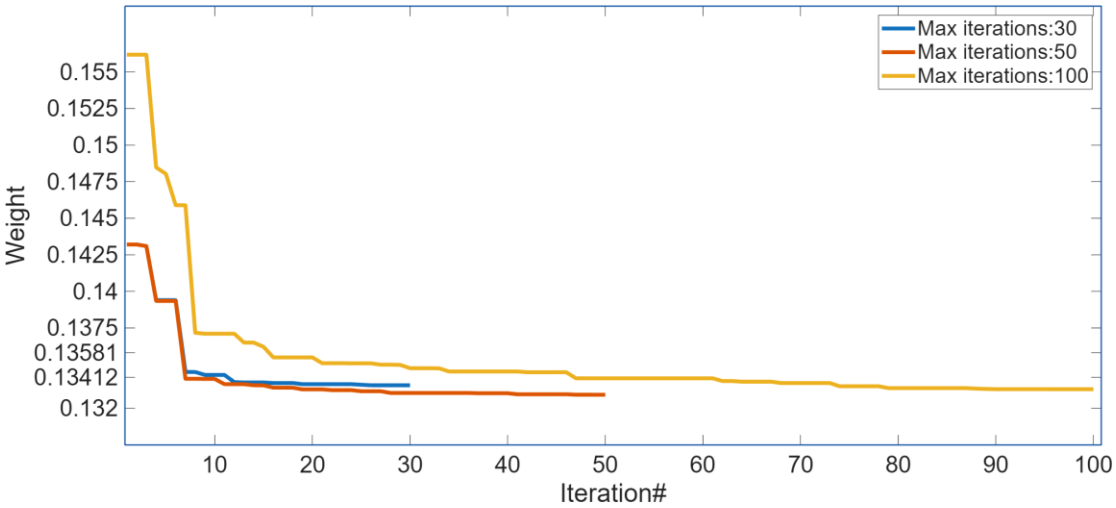

Figure 5-7: Convergence curve due to iterations variation

The maximum iteration count was increased from the baseline of 20 to 30, 50 and 100 to assess the impact on convergence and frequency response. The convergence curve shows that, despite the iteration counts, the algorithm settles to similar fitness values, with the 30- and 50-iteration cases converging earlier than the 100-iteration case. The frequency deviation results are shown in Figure 5-8. At 30 iterations, the system shows

a smaller initial frequency spike after the PV generation is introduced in the system, and a reduced frequency nadir after the load change at 10s, compared to the 50 and 100-iteration cases. Both 50 and 100-iteration cases show very similar responses, with a slightly higher spike than the 30-iteration case, but settle faster to the nominal frequency. This suggests that while fewer iterations can reduce the magnitude of deviations, higher iteration counts allow for a quicker recovery.

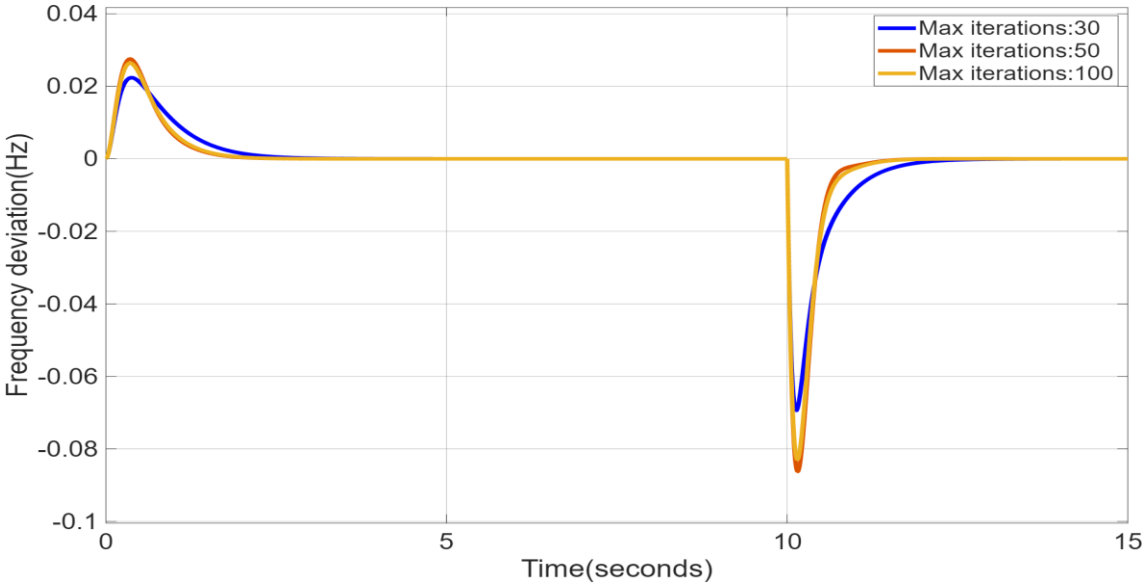

Figure 5-8: Frequency response due to different iterations

This indicates that moderate iterations, which are between 30 and 50, bring balance between reducing disturbances and faster settling times. Increasing the maximum iteration resulted in an increased overshoot and undershoot, and longer computation time. This could be because the optimisation process can sometimes focus too much on refining already suboptimal solutions, leading to over-compensation. The parameter values have to be adjusted to balance the exploration and exploitation, which prevents aggressively fine-tuning the PID gains.

5.3.2. Load variations

In the first scenario, load variations are introduced to evaluate the system's performance under fluctuating demand conditions. This scenario replicates real-world situations in which the load demand changes suddenly, impacting the frequency stability of the power system, particularly in systems with high renewable energy penetration. Such fluctuations can result from residential and industrial load changes, varying weather conditions affecting renewable generation, or sudden disconnection of large loads. The objective of this case is to test how effectively the LFC, with the proposed ZOA-PID controller, can maintain system frequency within acceptable bounds despite these variations. The effectiveness of the controller is assessed based on key performance

indicators, including frequency deviation, settling time, and steady-state error. The system's ability to quickly recover from load disturbances without excessive overshoot or prolonged oscillations is crucial for maintaining grid stability and preventing potential cascading failures. In this case, the integration of PV and BESS further complicates the dynamics, as renewable energy sources introduce additional variability that the controller must accommodate. Figure 5-9 shows the frequency response to a step change representing a 10%, 15%, 20%, and 25% load change decrease in load demand. And the results are shown in Table 5-1.

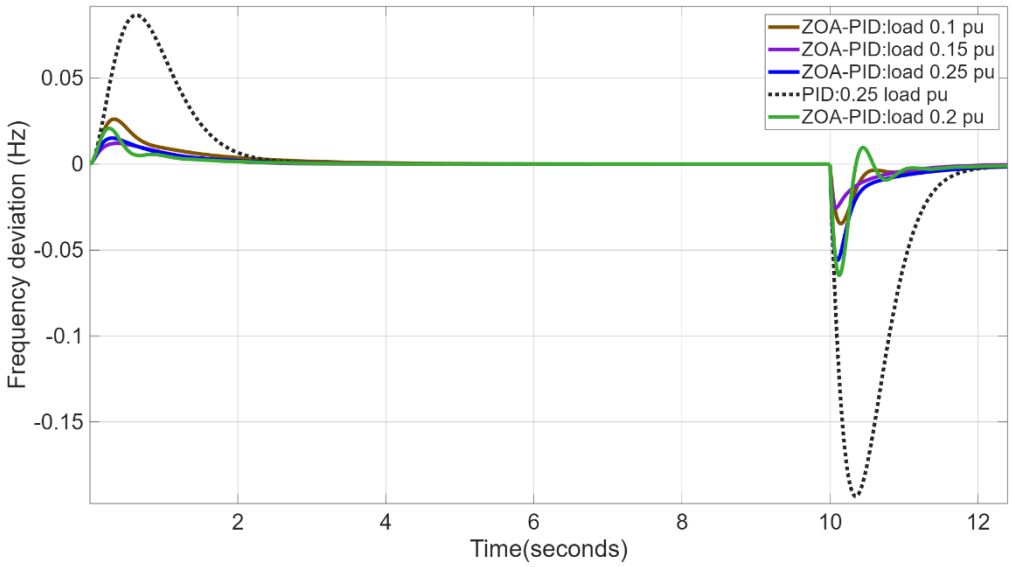

Figure 5-9: Frequency response due to load variation (ZOA-PID)

The results show that the ZOA-PID consistently minimized both the overshoot and undershoot under varying load conditions, and when PV generation was introduced. The ZOA-PID also achieved a faster settling time compared to the PID controller, which shows the superior dynamic response and improved stability.

Table 5-1: Results due to load change

$Load\ (pu)$	K_p	K_i	K_d	$Max\ (Hz)$	$Min(Hz)$	$Settling\ (s)$
0.1	9.625	7.116	1.263	50	49.97	10.48
0.15	8.195	6.2921	1.0941	50	49.67	10.63
0.2	14.848	13.739	3.714	50	49.3	10.87
0.25	14.215	11.89	2.44	50.077	49.93	10.7

5.3.3. Impact of PV power and BESS

In this case, the impact of a variable PV generation profile is evaluated to test the robustness of the ZOA-PID controller. Figure 5-10 shows the frequency deviation when a variable PV profile is introduced into the system. The variable PV generation profile

used in this study is designed to introduce step changes in the renewable power output at different time intervals.

At 10 seconds, the PV generation increases by 10% and remains constant until 20 seconds, where a further 10% increase occurs, bringing the total penetration to 20%. This level is maintained for an additional 20 seconds, where the PV generation decreases by 10%. At 40 seconds, there is another decrease, where the solar power contribution drops to 0% and stays there for the rest of the simulation time. This series of sudden changes tests how well the ZOA-PID controller can manage the variable conditions of solar power generation.

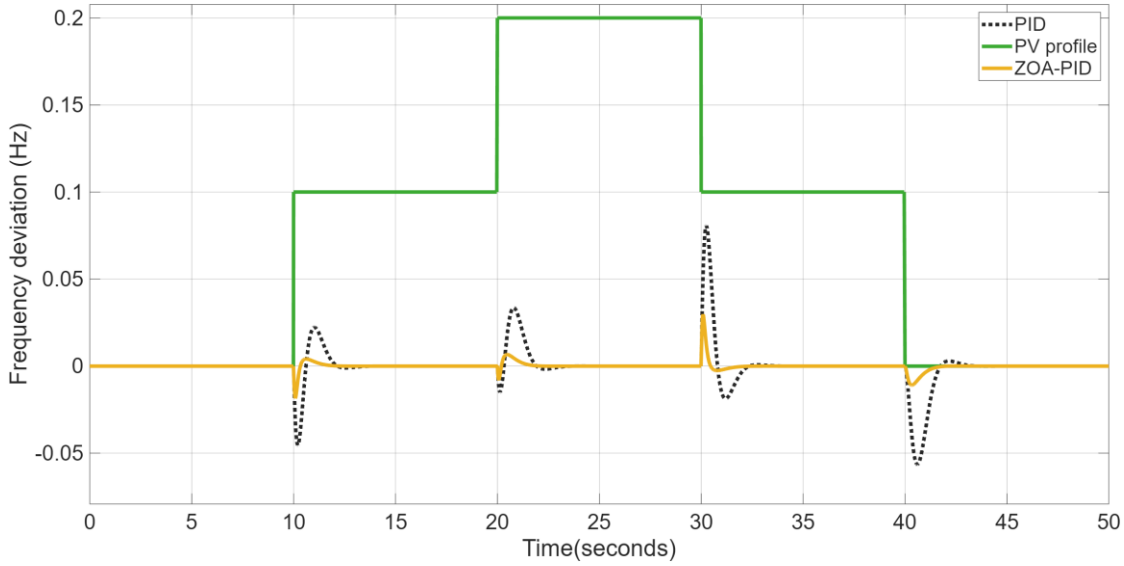

Figure 5-10: Frequency response due to variable PV profile (ZOA-PID)

The results show that the controller has effectively managed the additional PV generation into the system. And the reduced settling also reflects the system's ability to recover after a disturbance. The maximum deviation is much smaller, with a reduced overshoot and undershoot compared to the conventional PID controller. This indicates that the ZOA_PID successfully adapted to the intermittency of the PV output.

To further test the resilience of the system, the effects of a sudden loss of BESS support under the same variable PV conditions are presented in Figure 5-11. The results show an increase in oscillations, indicating that the system’s ability to stabilise the frequency without BESS support is compromised. After the disturbance, the frequency dropped to 49.95 Hz at 10 seconds, and the maximum frequency was 50.075 Hz at 30 seconds, with an increased settling time. The system was still able to recover to some extent; however, it is less stable without BESS, as shown by the increased oscillations. The algorithm played a role in minimising the impact of the disturbance and restored the frequency to its nominal frequency with a small overshoot.

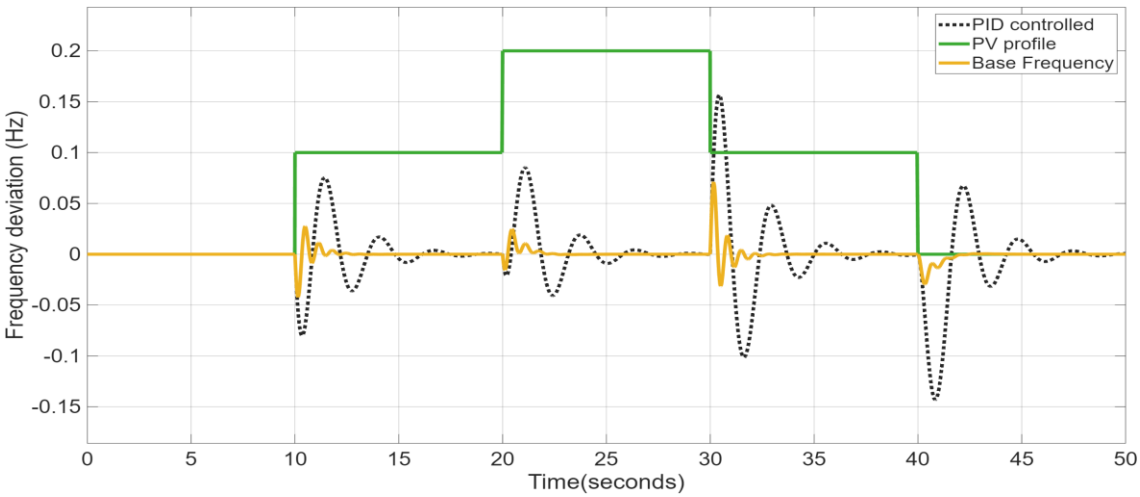

Figure 5-11: Frequency response due to loss of BESS support (ZOA-PID)

5.3.4. Generation loss

The sudden loss of generation represented as a step input caused the system's frequency to surge to 52.5 Hz and settle there, showing inadequate frequency control. The initial frequency spike was due to insufficient generation to match the load. The controller failed to restore the frequency to its nominal level, likely due to being slow or caused by suboptimal tuning of the PID gains. The frequency settling at 52.5 Hz indicates the controller's inability to compensate for the lost power. This response is shown in Figure 5-12.

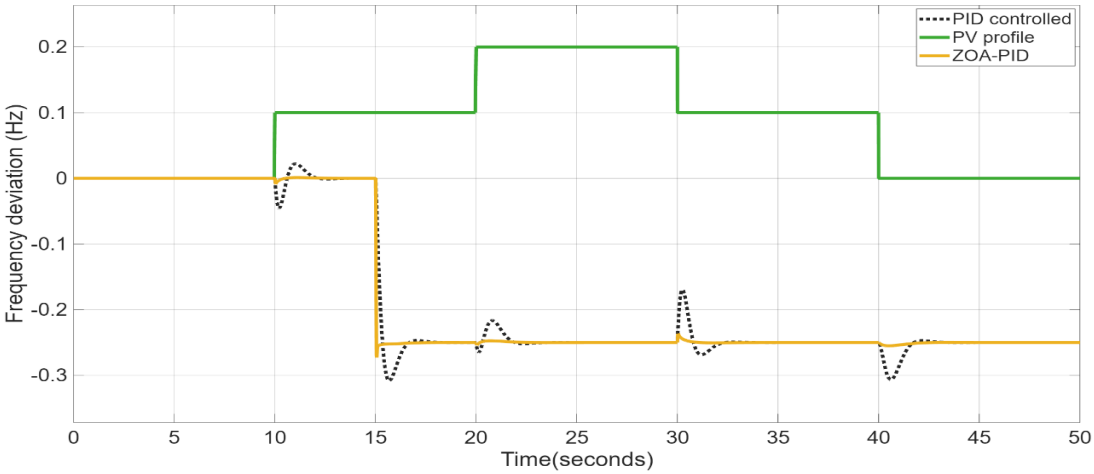

Figure 5-12: Frequency response due to generation loss

5.3.5. Variation in load disturbances

To further test the robustness of the controller, a variable load profile is applied to the system. The results shown in Figure 5-13 confirm that the ZOA-PID maintained its performance advantages, with a reduced overshoot, undershoot and a quicker recovery time compared to a PID controller. These results show that the ZOA-PID remained stable despite the continuous changes in the load demand, which highlights the ZOA-PID's ability to adapt to dynamic disturbances. The results show that the controller can handle

these variations, demonstrating the ability to adapt to changing system conditions. The controller's performance is robust and can handle both the increasing and decreasing loads without a significant deviation in frequency or generation output.

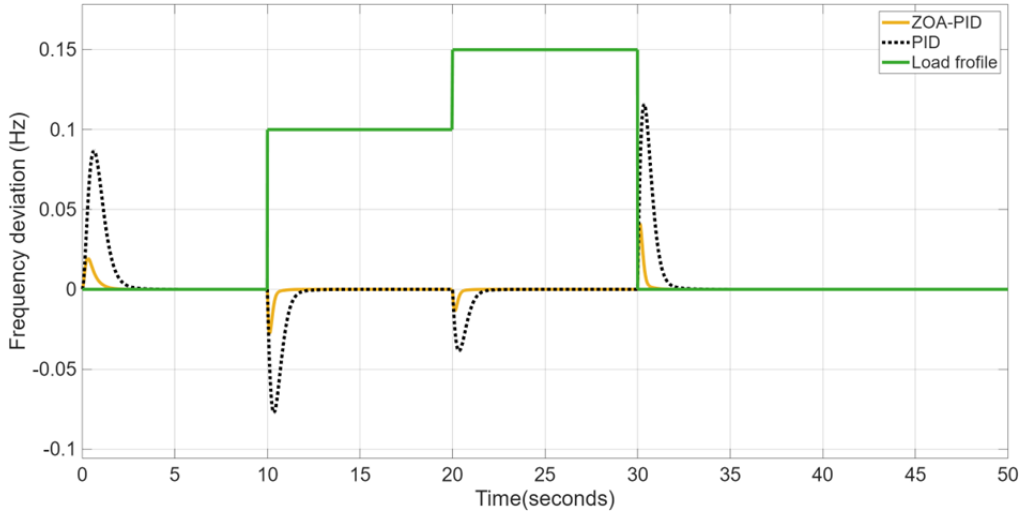

Figure 5-13: Frequency response due to variable load

Table 5-2: PID controller parameters for each case

Scenario	Kp	Ki	Kd
PV penetration	14.986	11.528	2.523
Loss of BESS	12.698	12.754	4.802
Variable load change	15	11.155	1.823

5.4. Comparison with other optimisation algorithms

In this case, the performance of the ZOA is compared to the PSO, which is mostly used for LFC. Figure 5-14 shows the frequency response of the comparison.

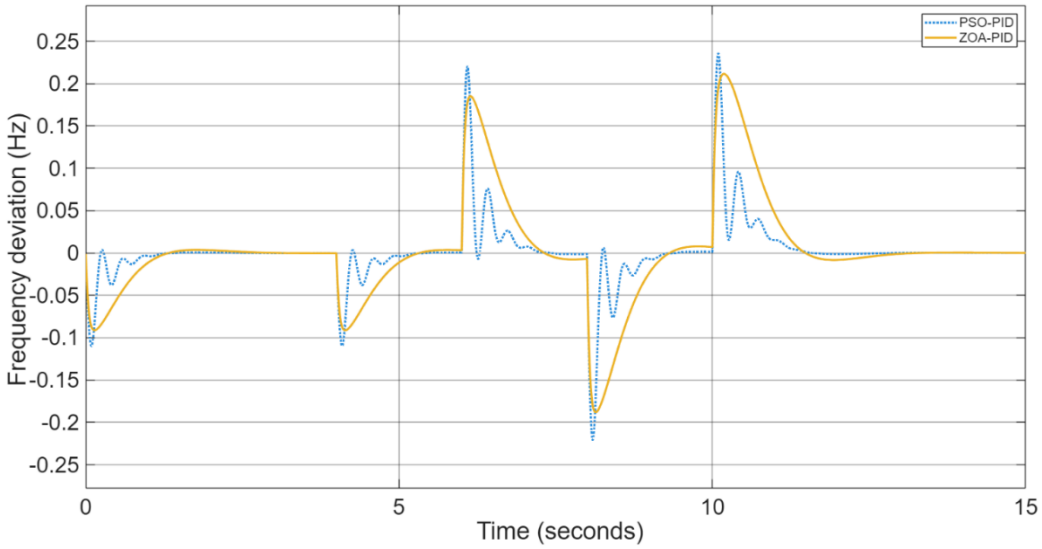

Figure 5-14: Comparison between ZOA and PSO

From the results observed in Figure 5-15, the ZOA shows better performance in reducing the frequency nadir compared to the PSO. The PSO, on the other hand, shows better performance in settling faster than the ZOA after a disturbance was introduced into the system. Though the PSO settles faster, it contains more oscillations than the ZOA, which shows a trade-off between how fast it settles and how much of those oscillations fluctuate. This comparison shows the strength and potential of the ZOA in LFC.

5.5. Conclusion

In this chapter, an analysis of how the ZOA perform for LFC in different cases is presented. The cases included changes in the parameters of the algorithm such as the boundary, search agent and maximum iterations, load variations, the effects PV system and BESS, and generation loss. The results show that the ZOA was able to optimize the PID parameters such that the controller is able to reduce the frequency deviation, eliminate steady state error, reduce the settling time, and maintain the overall stability of the system. A comparison with the PSO was done, which showed the strengths and weaknesses of both methods, and how comparable the new algorithm is with one of the most popular algorithms in power system applications. These results show how valuable the ZOA's potential is for power system control and its adaptability to varying conditions. Next, Chapter 6 applies the ZOA in a two-area system.

CHAPTER SIX

SIMULATION AND ANALYSIS OF A TWO-AREA POWER SYSTEM

6.1. Introduction

In a two-area system, each area operates with its generation units, but they are interconnected through tie lines, allowing power exchange to maintain balance under varying load conditions. Any disturbance in one area not only affects its local frequency but also causes power imbalances in the interconnected area. This chapter investigates the performance of LFC in a two-area system with solar PV generation and BESS in one area. Advanced PID controllers tuned using optimisation algorithms, including PSO and ZOA, are implemented to enhance system stability. The objective is to evaluate the robustness of each control method in minimising frequency deviations, reducing settling time, and ensuring stable power exchange between the interconnected areas. Simulation results under varying load conditions and renewable generation profiles are presented to compare the effectiveness of the optimisation-based controllers. The analysis should show how adaptive tuning strategies, such as the ZOA, outperform conventional approaches by delivering faster and more stable frequency recovery while maintaining tie-line power within acceptable limits.

The test band model studied in this chapter is shown in Figure 6-1 This system has been studied in the literature as a benchmark for evaluating the dynamic performance of various control strategies of LFC applications within power systems. This is due to its well-defined structure parameterisation, which is a reliable platform for testing and comparing conventional and advanced control strategies. In this model, the first area is integrated with both PV and BESS. This inclusion introduces complexity to the frequency control dynamics as studied in Chapter 4. By simulating various operating conditions, including sudden load variations, parameter changes, and disturbances in the tie-line power exchange, the model provides valuable insights into how effective the proposed optimisation algorithm is in mitigating frequency deviations. The detailed parameters of the power system are presented in Table 6-1.

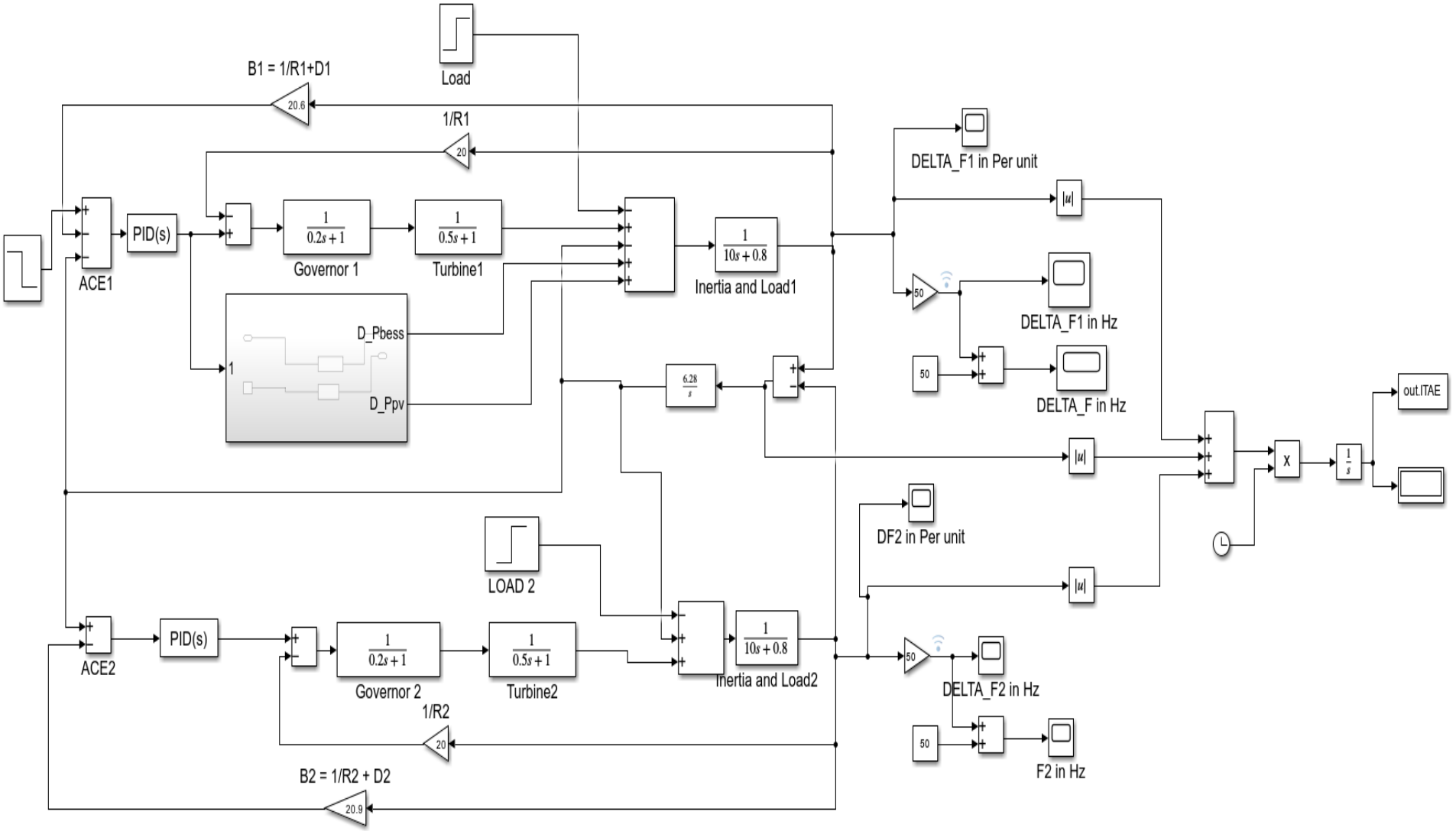

Figure 6-1: Model of the two-area power system

Table 6-1: Parameters of the two-area system (Adapted from **(Ogar, Hussain & Kelum A. A. Gamage, 2023)**)

Parameters	Definition	Area 1 Values	Area 2 values
F	Frequency system	50 Hz	
B	Frequency Bias	20.6 Hz/MW	16.9 Hz/MW
1/R	Regulation constant	0.05 Hz/MW	0.0625 Hz/MW
D	Load-damping coefficient	0.8	0.8
H	System inertia constant	5	5
K_g	Governor gain constant	1	1
K_{PV}	PV gain constant	1	
T_g	Governor time constant	0.2 s	0.2 s
K_t	Turbine gain constant	1	1
T_t	Turbine time constant	0.5 s	0.6 s
T_{PV}	PV time constant	0.3 s	
K_{BESS}	BESS gain constant	1	
T_{BESS}	BESS time constant	0.1 s	

6.2. Simulation scenarios

Different simulation tests are designed to observe how the control algorithm works under various conditions. The tests include load increases in areas 1 and 2 to check if the controller can restore frequency and balance power between the areas. A changing load profile is also applied to test the controller's ability to handle sudden spikes and gradual changes. Other tests include examining the integration of PV systems and BESS in area 1, highlighting the influence of renewable variability and fast-acting storage on frequency stability. The loss of generation in area 2 is also simulated to evaluate how the controller will perform in mitigating the frequency deviations and restoring stability.

For each test, the effects of the algorithm parameter tuning on the system response are investigated, and a comparison is conducted between the ZOA and the PSO-based controller. The comparison will focus on the frequency deviation, settling time, and ACE minimisation. The role of the tie-line power exchange between the inter-area power balancing and overall stability is also examined.

6.2.1. Load disturbance

A step load disturbance was introduced in the simulation to evaluate the dynamic performance of the two-area system under sudden load changes. The cases considered

are load change in area 1 only, load change in area 2, and simultaneous load change in both areas.

In the first case, the disturbance occurred in area 1 at 12 seconds. Figure 6-2 and Figure 6-3 show the frequency response in area 1 and in area 2, respectively. The frequency change was immediate and pronounced in area 1 due to the sudden imbalance between the load demand and generation. This is followed by oscillations as the controller attempts to recover, eventually converging towards zero deviation.

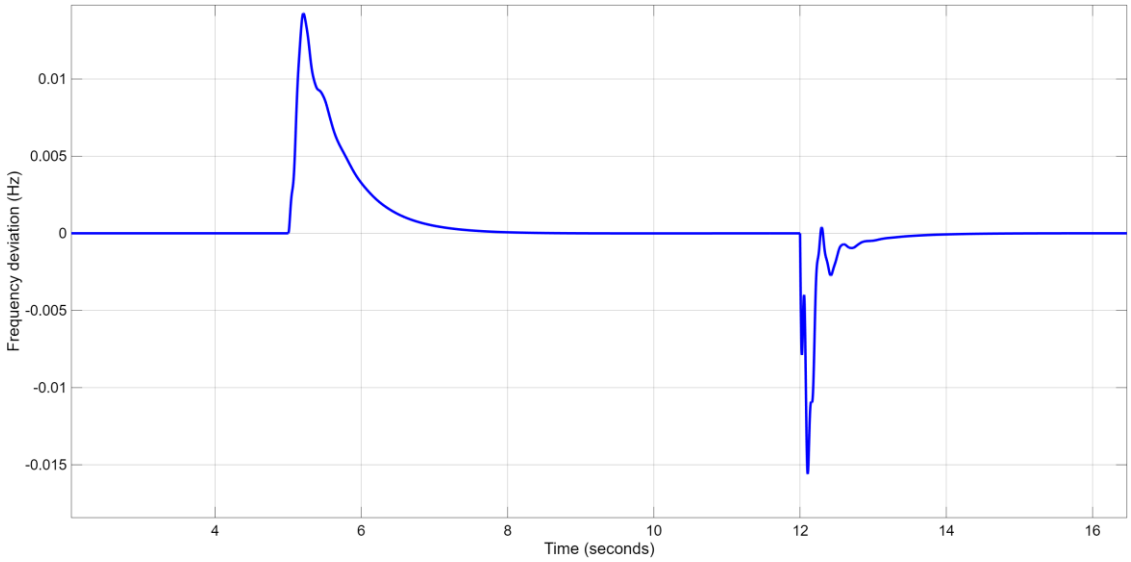

Figure 6-2: Frequency response in area 1

In area 2, the frequency response shows a slight delay before reacting to the disturbance introduced in area 1, as shown in Figure 6-3. This delay is due to the interconnection and the time required for the imbalance to transmit through the tie-line. The frequency nadir in area 2 is also smaller compared to area, which shows that the immediate effect of the disturbance is less severe. However, area 2 takes longer to settle compared to area 1 due to the BESS in area 1. Table 6-2 shows the simulation results.

Table 6-2: The performance metrrics

Parameter	Area 1	Area 2
Initial frequency	50 Hz	50Hz
ACE	2.3693e-08	-3.38714e-0.8
Overshoot	0.00535	0.00365
undershoot	0.0125	0.0062
Settling time	13.57 s	13.88 s
Kp	20	20
Ki	20	1.194
Kd	4.1123	16.349

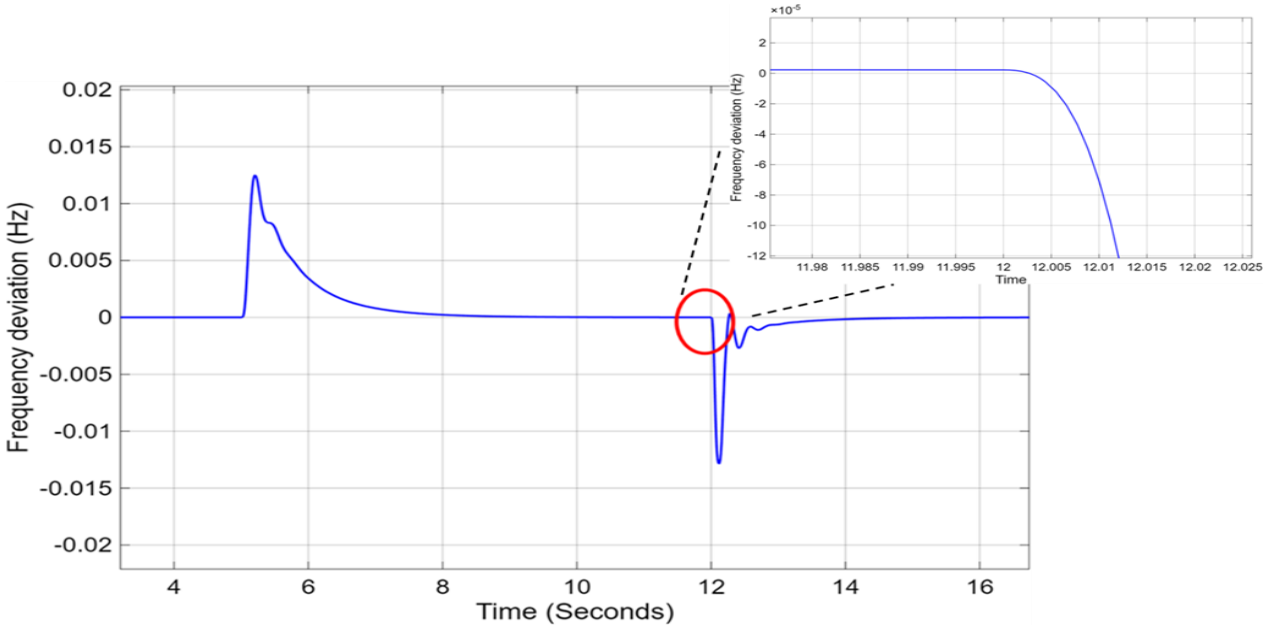

Figure 6-3: Frequency response in area 2

To examine the dynamics of the interconnection, a step load change is applied in both areas at the same time. Each area faces a local mismatch in generation and demand while also exchanging corrective power through the tie-line. Figure 6-5 and Figure 6-6 show the frequency response in area 1 and area 2, respectively, and Table 6-3 shows the simulation results demonstrating the performance of the controller.

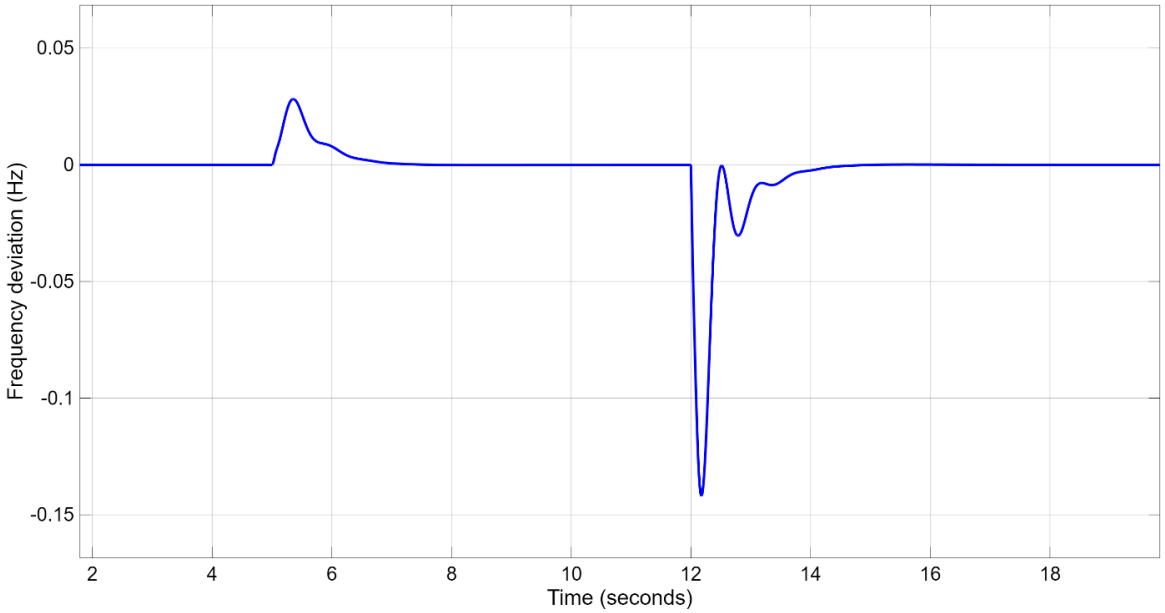

Figure 6-4: Frequency response in area 1 due to changes in areas 1 & 2

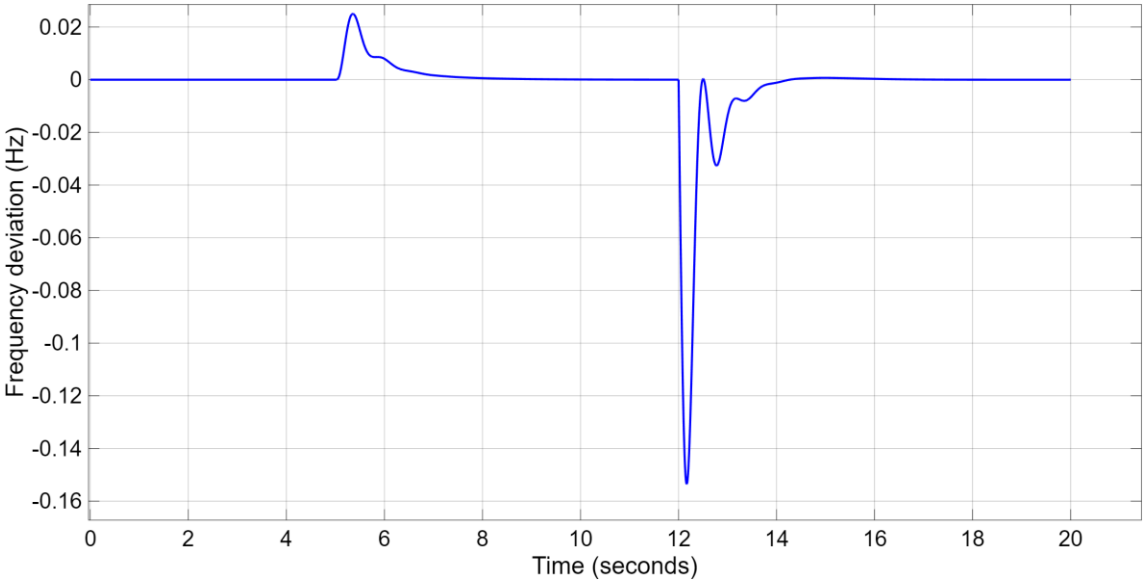

Figure 6-5: Frequency response in area 2 due to changes in areas 1 & 2

Table 6-3: Simulation results due to changes in areas 1 and 2

Parameter	Area 1	Area 2
Initial frequency	50 Hz	50Hz
ITAE	0.03435	
ACE	-1.278e-08	1.480e-0.8
Overshoot		
undershoot	0.0125	-0.1534
Settling time	13.88 s	13.75 s
Kp	9.88	10
Ki	10	10
Kd	2.388	4.067

Lastly, a dynamic load profile was applied to assess the system's capacity to manage continuous fluctuations in demand, as shown in Figure 6-5. Area 1 was subjected to varying loads, while area 2 was equipped with a PV system and BESS to regulate frequency. The load profile simulated real-world demand patterns, featuring gradual increases and decreases in load magnitude over time. As the load shifted, the system experienced persistent frequency deviations. Area 1 demonstrated faster frequency recovery and shorter settling times compared to area 2, despite being the source of the disturbance. This was evident during sharp load changes, where area 1's controller rapidly adapted to the new conditions. In contrast, area 2's frequency response was delayed, even with BESS and PV support, suggesting potential limitations in the control strategy or resource dispatch timing. The frequency nadir was less severe than in step load scenarios, but the ongoing fluctuations pushed the controllers' ability to maintain

stability under dynamic conditions. The time-varying load scenario showcased the control systems' responsiveness and adaptability, particularly in area 1.

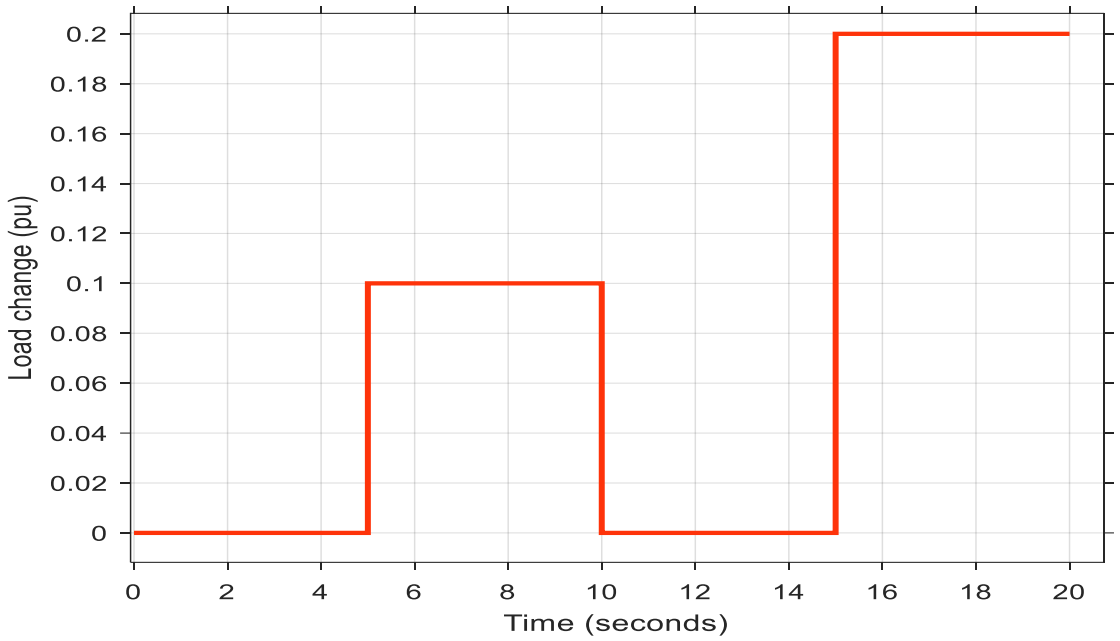

Figure 6-6: Load variation

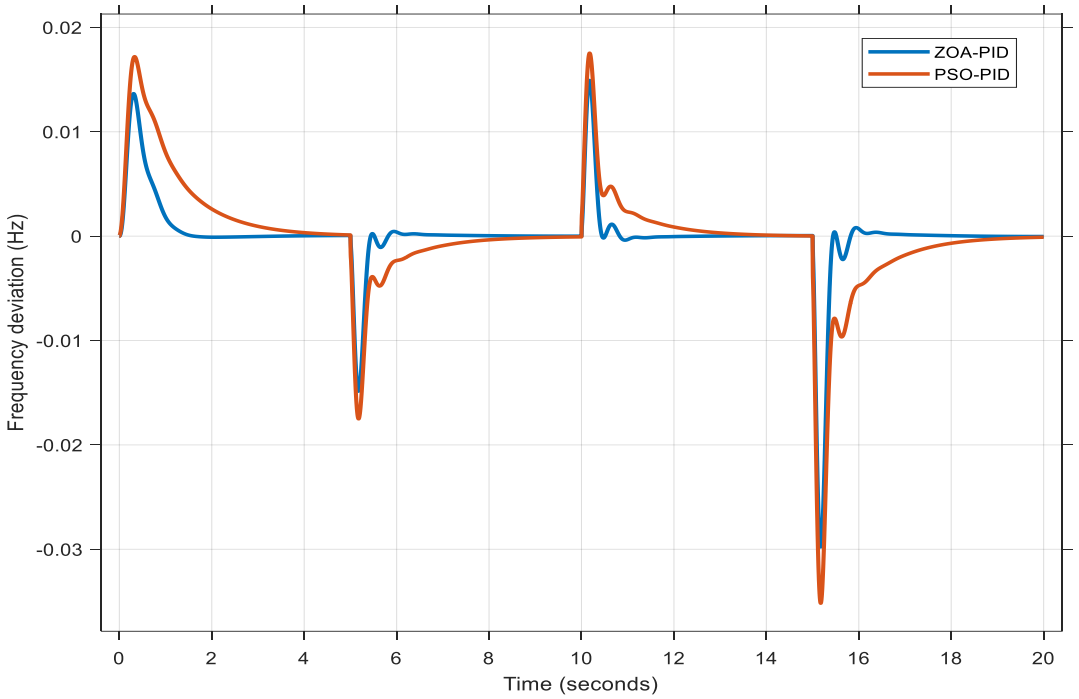

Figure 6-7: Frequency response in area 1

The ZOA algorithm's performance in this scenario highlights its success in maintaining stability under dynamic conditions. Its ability to rapidly adapt to changing load conditions and maintain frequency stability, especially in area 1, demonstrates its potential as a robust control strategy

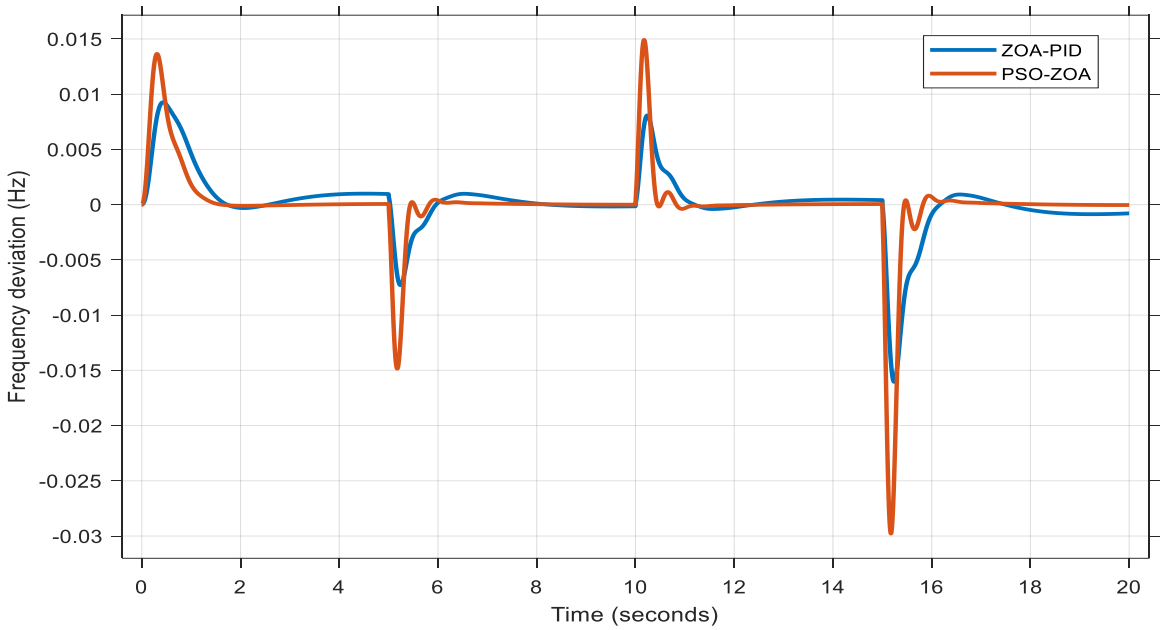

Figure 6-8: Frequency response in area 2

The algorithm reduced the frequency deviations and maintained stability, even in the presence of continuous fluctuations, suggesting that it could be a valuable tool in real-world power system operations. However, the delayed frequency response in area 2, despite the presence of BESS and PV, may indicate areas for further optimisation or refinement of the algorithm to ensure optimal performance across different system configurations. The algorithm shows that in more complex systems, even its performance increases, as shown in Figure 6-7 and Figure 6-8.

6.2.2. Loss of generation

In this case, the system's resilience to a loss of generation is investigated. Unlike a load disturbance, which introduces an increase in demand, a generation loss simulates the sudden outage of a large unit in one of the areas. In this situation, the power outage occurs in area 1, causing the generator output to drop suddenly. This case allows for an investigation into how area 1 with a PV system and BESS responds to the change, and how the controller responds to this change. This is implemented by applying a step change to the mechanical power input block. Figure 6-9 and Figure 6-10 show the frequency response in area 1 and area 2 due to the generation loss in area 1, respectively.

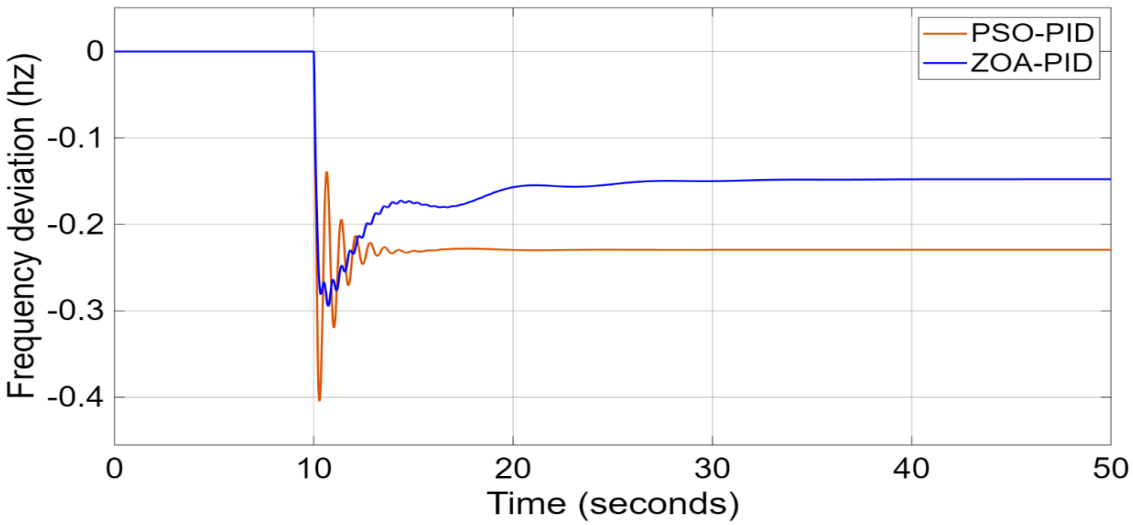

Figure 6-9: Frequency response in area 1 due to generation loss

After the sudden generation outage at 10, there is a sharp frequency drop in both areas, and it slowly recovers but settles at a lower level, which shows there was not enough power. The recovery is assisted by the automatic control and support from area 2. This result is compared to the PSO, which also shows a slow response and settles at a lower level in comparison to the ZOA-PID-based solution. Figure 6-11 also shows the power exchange deviation between the areas.

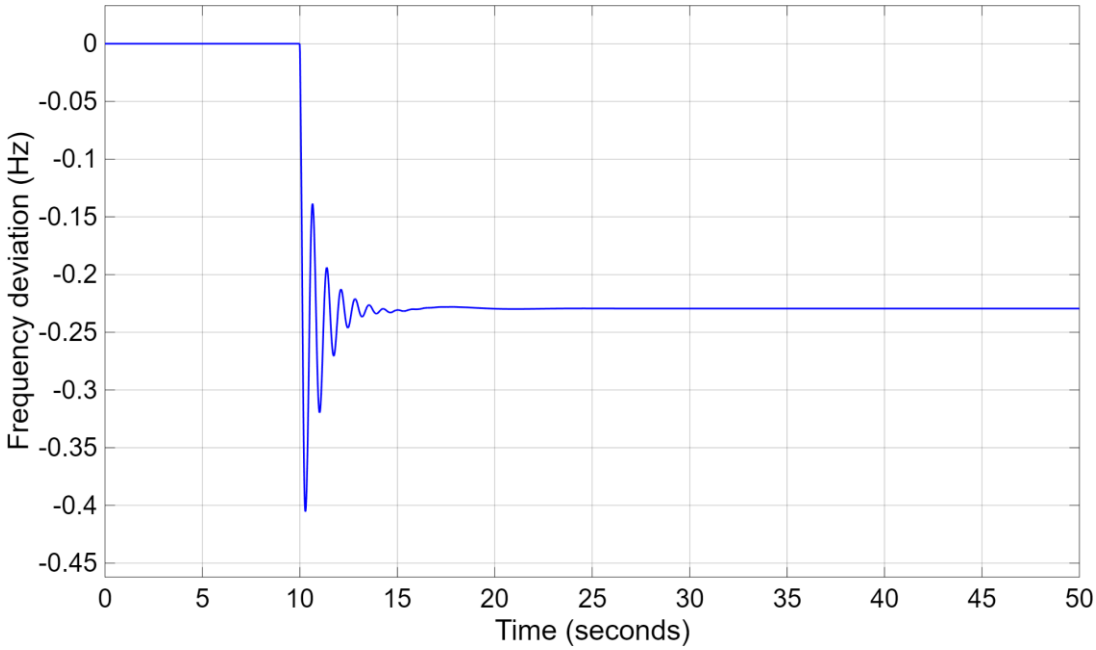

Figure 6-10: Frequency response in area 2 due to generation loss

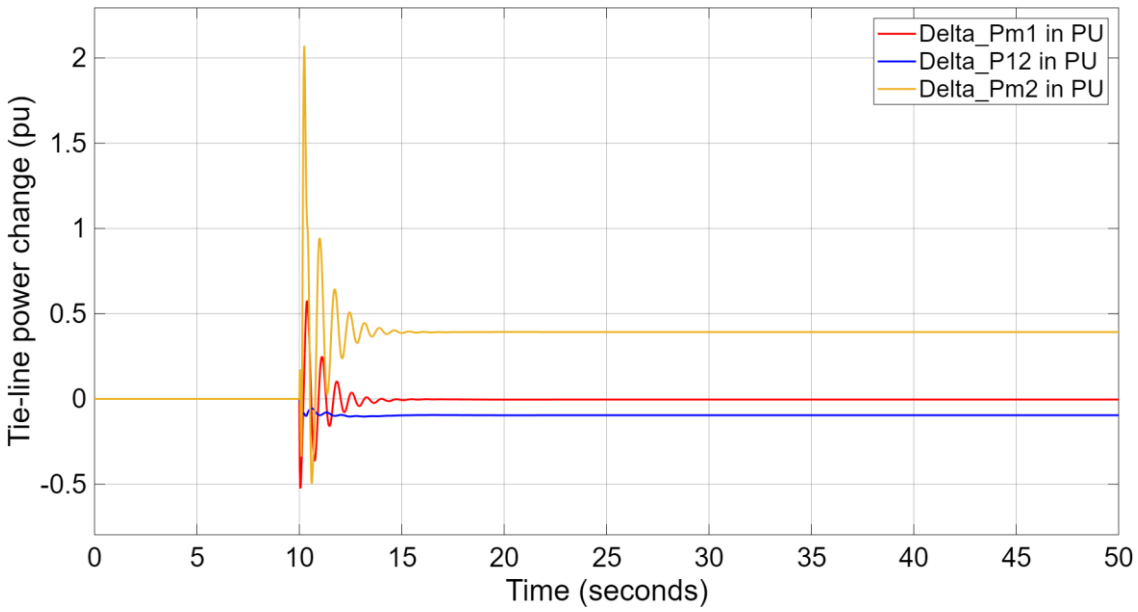

Figure 6-11: Change in tie-line power due to generation loss

Increasing the number of maximum iterations allows the system to converge to optimal gains, which further eliminates the steady-state frequency deviation following the generation loss, as evident in Figure 6-12. While this improves the accuracy and coordination across the tie-line, it also incurs increased computational cost and robustness trade-offs. The overly aggressive PID gains may compromise the stability in the presence of modelling errors. The benefits of the increased iterations must be weighed against the need for a robust control algorithm.

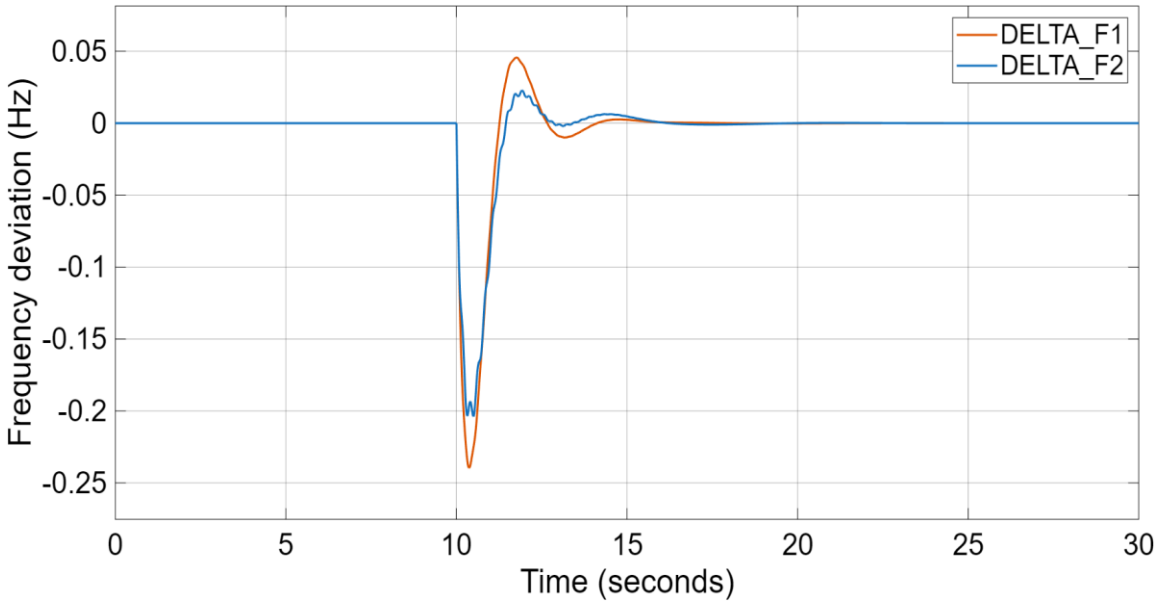

Figure 6-12: Frequency response due to increased iterations

6.3. Conclusion

This chapter presented the implementation and performance analysis of the ZOA applied to a two-area interconnected power system for LFC. The system included a PV system

and BESS in one area to allow for a realistic and dynamic test environment. The ZOA was used to tune the controller parameters in both areas, with a focus on minimising frequency deviation and reducing the frequency nadir and stabilising the tie-line power exchange. Through various simulation scenarios, which involved step and time-varying load disturbances, changes in generation, and varying PV input, the performance of the ZOA was compared with the widely used PSO technique. These results show that ZOA consistently outperformed PSO in the key dynamic performance metric. Areas 1 and 2 showed reduced frequency deviation, shorter settling time, and reduced overshoot under the ZOA-based control. The findings also indicate that the power exchange along the tie-line demonstrated reduced oscillations and exhibited greater stability when ZOA was utilised, enhancing inter-area coordination. The enhanced damping and quicker stabilisation provided by ZOA highlight its efficiency and reliability in optimising LFC systems, especially in multi-area power networks that integrate RES.

CHAPTER SEVEN

CONCLUSION

7.1. Introduction

This research project aims to address the limitations of traditional control design methods. These methods struggle to handle dynamic challenges that arise when RES, such as solar power, is integrated into the system. To mitigate some of the challenges that are introduced by RES, ESS are integrated, which further introduces more challenges that traditional controllers struggle to handle. Since traditional controllers cannot manage this integration, more advanced and adaptive controllers are required to maintain the stability of the system.

The increasing complexity of modern power systems and the need for reliable frequency regulation have led researchers to search for advanced control strategies. This research study presents a ZOA, a new control approach to improve the performance of the system under various conditions. The study developed, tested, and validated the improved controller in both single-area and multi-area LFC systems.

This chapter discusses the results and outputs of the thesis, explaining how each objective was met. Section 7.2 restates the aim and objectives of the research. Section 7.3 highlights the main contributions and outputs, from Section 7.3.1 to 7.3.7, and shows the research methods used and how they were implemented. In Section 7.4, a summary of the main findings and a reflection on how the controller affects frequency regulation. Section 7.5 shows the publications from this research study, and Section 7.6 presents recommendations for future study.

7.2. Research aim and objectives

The research project aims to develop a robust load frequency controller to improve the dynamic performance of power systems integrated with PV and an energy storage system.

The aim of the research project was successfully accomplished by fulfilling the following objectives:

- Investigate the impact of integrating renewable energy sources on load frequency control.
- Review existing control strategies and optimisation techniques.
- Modify a standard power system model and integrate a PV and BESS and analyse its dynamic response under varying load conditions.

- Analyse the dynamic performance of the standard power system with a conventional controller.
- Develop an improved adaptive control system using the ZOA.
- Simulate and analyse the proposed control system in MATLAB/SIMULINK.
- Analyse the performance of the ZOA-based control system in both single-area and two-area power systems**.**

7.3. Thesis deliverables

This section presents the deliverables of the thesis.

7.3.1.Literature review

Chapter 2 examined the principles of LFC and the challenges faced in modern power systems with integrated RES. It further reviewed traditional control strategies, highlighting their limitations in handling the variability introduced by RES. The chapter further investigated different optimisation algorithms and their application in frequency control.

7.3.2. Modelling a single area, two-area system and the optimisation algorithm

In Chapter 3, a detailed single-area power system mathematical model was developed to serve as a basis for testing the proposed control strategy under different operating conditions. The model includes components such as the governor, the turbine, the load, the PV system, and the ESS. The chapter also focused on the steady-state analysis and dynamic analysis of the model to understand the system's behaviour. The modelling of the two-area power system and the ZOA is also included in this chapter.

7.3.3. Base simulation without a controller

The initial simulation of the single-area system was conducted on MATLAB/SIMULINK without any controller to observe the natural response of the system to load disturbances and the introduction of a PV system and BESS. The frequency response was observed. This scenario provided insight into the extent of frequency deviation and the inability of the frequency to return to 50 Hz after a disturbance.

7.3.4. Base simulation with a PID controller

A classical PID controller was implemented in the same model to analyse how conventional control strategies manage frequency deviations. PID gain values were tuned using the Ziegler-Nichols method. This simulation helped in establishing a benchmark in terms of the stability of the system, settling time, undershoot, and peak

overshoot, which were later used for comparison with the optimised-based control strategy.

7.3.5. Mathematical formulation of the ZOA

The ZOA, inspired by the zebra herd behaviour and foraging patterns, was mathematically formulated to solve the LFC optimisation problem. The formulation included the definition of the algorithm, a flowchart detailing the steps taken to reach a solution, population initialisation, position updating and the convergence criteria. The formulation was tailored for tuning the controller parameters in both the single-area and multi-area power systems.

7.3.6. Single area system simulations and analysis using the ZOA

The ZOA was applied to the single-area system to optimise the PID parameters for improved frequency regulation. Various simulation scenarios were tested, which included sudden changes in the load, PV output fluctuations, and variable load changes at different times, to evaluate the algorithms' adaptability and robustness in frequency control. The results demonstrated significant improvements in reducing the frequency nadir and settling time, which in turn improved frequency stability when compared to the PID controller, PSO and GA.

7.3.7. Multi-area system simulation and analysis using the ZOA

To evaluate the algorithm’s scalability in a more complex system, its application was extended to a multi-area LFC model. The system involves power exchange between two areas with different load changes in each area. The ZOA successfully coordinated the frequency between the two areas, which helped maintain frequency stability while managing the disturbances and uncertainties introduced into the system. The results were compared to PSO results.

7.4. Overview of research findings and contribution to academic and industry

This research successfully addressed the challenge of maintaining frequency stability in modern power systems with high renewable energy penetration, in particular from PV sources. By developing a detailed model framework for a single-area and multi-area system that combines PV systems and BESS dynamics, the study demonstrated the limitations of traditional control methods and the potential of optimisation algorithms. The ZOA was developed and implemented for LFC, which resulted in reduced frequency nadir, improved settling time, and increased robustness under the varying load,

generation conditions. Comparative analysis with the PSO and PID controllers validated how effective the ZOA is in frequency regulation.

This research contributes to the advancement of knowledge in power systems and control engineering. The integration of advanced optimisation techniques presents an innovative methodology that can enrich courses in intelligent and adaptive control. The study also deepens the understanding of the behaviour of adaptive and bio-inspired algorithms in managing nonlinear and uncertain power system dynamics. The results could also serve as a benchmark to support future investigations in intelligent control and renewable energy integration. The results indicate potential for deployment in smart grids, microgrids, and energy management systems, enhancing grid stability and coordination in renewable-rich environments for a more resilient industry control solution.

7.5. Publications

The following publications were accepted and presented at the respective conferences as listed below.

N. Tshinavhe, M. Ratshitanga, and N. Tshemese-Mvandaba, 2024, Review of Adaptive Load Frequency Control Strategies for Improving Wind Power Plant Integration, Published on IEEE *32nd Southern African Universities Power Engineering Conference, DOI: 10.1109/SAUPEC60914.2024.1044505*

N. Tshinavhe, M. Ratshitanga, N. Tshemese-Mvandaba and M. Mditshwa, 2025, Optimisation of Load Frequency Control using Zebra Optimisation Algorithm in Renewable Energy Integrated Power System, Published on IEEE 33rd Southern African Universities Power Engineering Conference, DOI: *10.1109/SAUPEC65723.2025.10944384*

7.6. Recommendation for future research

Building on the findings of this study, future research can explore the following areas:

- Implement the proposed control strategy in a real-world testing application using hardware-in-the-loop setups to validate the simulated results.
- Extend the study to include other RES such as wind energy and/or hybrid PV-wind systems to test the controller’s adaptability.
- Consider a larger, more complex multi-area power system with higher renewable penetration.

- Explore combining the ZOA with other intelligent methods, such as fuzzy logic, ANN, or reinforcement learning, especially in the single-area system. This could also be hybridising algorithms such as the ZOA with the PSO or any other optimisation algorithm.

- Investigating the resilience of the control system against cyber threats.

7.7. Conclusion

This chapter reviewed how the research aims and objectives were successfully achieved, highlighting the key deliverables through developing the control strategy. It presented the performance comparison and discussed the contribution to academia and industry, as well as recommendations for future direction.

REFERENCES

Abeynayake, G., Cipcigan, L. & Ding, X. 2022. Black Start Capability from Large Industrial Consumers. *Energies*, 15(19): 7262.

Adetunji, K.E., Hofsajer, I.W., Abu-Mahfouz, A.M. & Cheng, L. 2021. A Review of Metaheuristic Techniques for Optimal Integration of Electrical Units in Distribution Networks. *IEEE Access*, 9: 5046–5068.

Ahmed, E.M., Selim, A., Mohamed, E.A., Aly, M., Alnuman, H. & Ramadan, H.A. 2022. Modified manta ray foraging optimization algorithm based improved load frequency controller for interconnected microgrids. *IET Renewable Power Generation*, 16(16): 3587–3613.

Akinyele, D.O. & Rayudu, R.K. 2014. Review of energy storage technologies for sustainable power networks. *Sustainable Energy Technologies and Assessments*, 8: 74–91. http://dx.doi.org/10.1016/j.seta.2014.07.004.

Akter, K., Nath, L., Tanni, T.A., Surja, A.S. & Iqbal, Md.S. 2022. An Improved Load Frequency Control Strategy for Single & Multi-Area Power System. In *2022 International Conference on Advancement in Electrical and Electronic Engineering (ICAEEE)*. IEEE: 1–6.

Alam, Md., Chowdhury, T., Dhar, A., Al-Ismail, F., Choudhury, M., Shafiullah, M., Hossain, Md., Hossain, Md., Ullah, A. & Rahman, S. 2023. Solar and Wind Energy Integrated System Frequency Control: A Critical Review on Recent Developments. *Energies*, 16(2): 812.

Alam, M.S., Chowdhury, T.A., Dhar, A., Al-Ismail, F.S., Choudhury, M.S.H., Shafiullah, M., Hossain, M.I., Hossain, M.A., Ullah, A. & Rahman, S.M. 2023. Solar and Wind Energy Integrated System Frequency Control: A Critical Review on Recent Developments. *Energies*, 16(2).

Al-Betar, M.A. 2017. $$\beta$$ β -Hill climbing: an exploratory local search. *Neural Computing and Applications*, 28(S1): 153–168.

Alhijawi, B. & Awajan, A. 2024. Genetic algorithms: theory, genetic operators, solutions, and applications. *Evolutionary Intelligence*, 17(3): 1245–1256.

Ali, E. S. & Abd-Elazim, S.M. 2011. Bacteria foraging optimization algorithm based load frequency controller for interconnected power system. *International Journal of Electrical Power and Energy Systems*, 33(3): 633–638.

Ali, E.S. & Abd-Elazim, S.M. 2011. Bacteria foraging optimization algorithm based load frequency controller for interconnected power system. *International Journal of Electrical Power & Energy Systems*, 33(3): 633–638.

Ali, S., Yang, G. & Huang, C. 2018. Performance optimization of linear active disturbance rejection control approach by modified bat inspired algorithm for single area load

frequency control concerning high wind power penetration. *ISA Transactions*, 81: 163–176.

Ali, Z.M., Calasan, M., Aleem, S.H.E.A., Jurado, F. & Gandoman, F.H. 2023. Applications of Energy Storage Systems in Enhancing Energy Management and Access in Microgrids: A Review. *Energies*, 16(16): 5930.

Al-Shetwi, A.Q. & Sujod, M.Z. 2018. Grid-connected photovoltaic power plants: A review of the recent integration requirements in modern grid codes. *International Journal of Energy Research*, 42(5): 1849–1865.

Alzahrani, A., Ramu, S.K., Devarajan, G., Vairavasundaram, I. & Vairavasundaram, S. 2022. A Review on Hydrogen-Based Hybrid Microgrid System: Topologies for Hydrogen Energy Storage, Integration, and Energy Management with Solar and Wind Energy. *Energies*, 15(21).

Amiri, F. & Hatami, A. 2023. Load frequency control for two-area hybrid microgrids using model predictive control optimized by grey wolf-pattern search algorithm. *Soft Computing*, 27(23): 18227–18243.

Amiryar, M.E. & Pullen, K.R. 2017. A review of flywheel energy storage system technologies and their applications. *Applied Sciences*, 7(3).

Arsad, A.Z., Hannan, M.A., Al-Shetwi, A.Q., Mansur, M., Muttaqi, K.M., Dong, Z.Y. & Blaabjerg, F. 2022. Hydrogen energy storage integrated hybrid renewable energy systems: A review analysis for future research directions. *International Journal of Hydrogen Energy*, 47(39): 17285–17312. https://doi.org/10.1016/j.ijhydene.2022.03.208.

Arsalis, A., Papanastasiou, P. & Georghiou, G.E. 2022. A comparative review of lithium-ion battery and regenerative hydrogen fuel cell technologies for integration with photovoltaic applications. *Renewable Energy*, 191: 943–960. https://doi.org/10.1016/j.renene.2022.04.075.

Basa Varajappa, S.R. & Nagaraj, M.S. 2021. Load frequency control of three area interconnected power system using conventional PID, fuzzy logic and ANFIS Controllers. *2021 2nd International Conference for Emerging Technology, INCET 2021*: 1–6.

Bayati, N., Dadkhah, A., Profile, S., Vahidi, B., Hossein, S. & Sadeghi, H. 2015. FOPID DESIGN FOR LOAD-FREQUENCY CONTROL USING GENETIC ALGORITHM Robust placement and sizing of Fault Current Limiter in Distributed Generation networks View project Demand Response Implementation Considering Customers' Behaviour View project 6 PUBLICATIONS 1 CITATION SEE PROFILE 3 PUBLICATIONS 0 CITATIONS FOPID DESIGN FOR LOAD-FREQUENCY CONTROL USING GENETIC ALGORITHM. *Sci.Int.(Lahore)*, 27(4): 3089–3094. https://www.researchgate.net/publication/281243221.

Behera, S., Sahoo, S. & Pati, B.B. 2015. A review on optimization algorithms and application to wind energy integration to grid. *Renewable and Sustainable Energy Reviews*, 48: 214–227. http://dx.doi.org/10.1016/j.rser.2015.03.066.

Benbouhenni, H., Bounadja, E., Gasmi, H., Bizon, N. & Colak, I. 2022. A new PD(1+PI) direct power controller for the variable-speed multi-rotor wind power system driven doubly-fed asynchronous generator. *Energy Reports*, 8: 15584–15594.

Bevrani, H. 2014. Frequency Control and Real Power Compensation. In *Robust Power System Frequency Control. Power Electronics and Power Systems*. Springer: 19–48.

Bevrani, H. 2009. *Robust Power System Frequency Control*. Boston, MA: Springer US.

Bevrani, H., Ghosh, A. & Ledwich, G. 2010. Renewable energy sources and frequency regulation: survey and new perspectives. *IET Renewable Power Generation*, 4(5): 438–457. http://digital-library.theiet.org/doi/10.1049/iet-rpg.2009.0049.

Bevrani, H., Golpîra, H., Messina, A.R., Hatziargyriou, N., Milano, F. & Ise, T. 2021. Power system frequency control: An updated review of current solutions and new challenges. *Electric Power Systems Research*, 194: 107114. https://linkinghub.elsevier.com/retrieve/pii/S037877962100095X.

Bhat Nempu, P., S, J.N., Singh, M. & Shaji, K. 2019. *Fuzzy-PI Controllers for Voltage and Frequency Regulation of a PV-FC Based Autonomous Microgrid; Fuzzy-PI Controllers for Voltage and Frequency Regulation of a PV-FC Based Autonomous Microgrid*.

Biswal, A., Dwivedi, P. & Bose, S. 2023. Frequency Control of Two Region Two-Unit Systems with PDF + (1+PI) Controller. In *2023 International Conference for Advancement in Technology, ICONAT 2023*. Institute of Electrical and Electronics Engineers Inc.

Brivio, C., Mandelli, S. & Merlo, M. 2016. Battery energy storage system for primary control reserve and energy arbitrage. *Sustainable Energy, Grids and Networks*, 6: 152–165. http://dx.doi.org/10.1016/j.segan.2016.03.004.

Bustamante, S., gonzález, J.W., López, G.J. & Cardona, H.A. 2023. UFLS and Smart Load for Frequency Regulation in Electrical Power System: A Review. *IEEE Access*, 11: 110967–110984.

c, S., Yammani, C. & Maheswarapu, S. 2019. Load Frequency Control of Multi-microgrid System considering Renewable Energy Sources Using Grey Wolf Optimization. *Smart Science*, 7(3): 198–217.

Çelik, E., Öztürk, N. & Houssein, E.H. 2023. Improved load frequency control of interconnected power systems using energy storage devices and a new cost function. *Neural Computing and Applications*, 35(1): 681–697.

Chaianong, A. & Pharino, C. 2015. Outlook and challenges for promoting solar photovoltaic rooftops in Thailand. *Renewable and Sustainable Energy Reviews*, 48: 356–372. http://dx.doi.org/10.1016/j.rser.2015.04.042.

Chakrabarti, Abhijit. 2010. *Power system analysis : operation and control*. 3rd ed. Sunita. Halder, ed. New Delhi: PHI Learning Private Limited.

Chang, C.S., Fu, W. & Wen, F. 2007. LOAD FREQUENCY CONTROL USING GENETIC-ALGORITHM BASED FUZZY GAIN SCHEDULING OF PI CONTROLLERS. , (May).

Choudhury, S. 2021. Flywheel energy storage systems: A critical review on technologies, applications, and future prospects. *International Transactions on Electrical Energy Systems*, 31(9): 1–26.

Chua, K.H., Bong, H.L., Lim, Y.S., Wong, J. & Wang, L. 2020. The State-of-The-Arts of Peak Shaving Technologies: A Review. *2020 8th International Conference on Smart Grid and Clean Energy Technologies, ICSGCE 2020*, 2020: 162–166.

Chvatal, V. 1979. A Greedy Heuristic for the Set-Covering Problem. *Mathematics of Operations Research*, 4(3): 233–235.

Coban, H.H., Rehman, A. & Mousa, M. 2022. Load Frequency Control of Microgrid System by Battery and Pumped-Hydro Energy Storage. *Water (Switzerland)*, 14(11).

Cucchiella, F., D'Adamo, I. & Gastaldi, M. 2016. Photovoltaic energy systems with battery storage for residential areas: An economic analysis. *Journal of Cleaner Production*, 131: 460–474. http://dx.doi.org/10.1016/j.jclepro.2016.04.157.

Datta, A., Bhattacharjee, K., Debbarma, S. & Kar, B. 2016. Load frequency control of a renewable energy sources based hybrid system. In *Proceedings - 2015 IEEE Conference on System, Process and Control, ICSPC 2015*. Institute of Electrical and Electronics Engineers Inc.: 34–38.

Datta, U., Shi, J. & Kalam, A. 2019. Primary frequency control of a microgrid with integrated dynamic sectional droop and fuzzy based pitch angle control. *International Journal of Electrical Power and Energy Systems*, 111(December 2018): 248–259. https://doi.org/10.1016/j.ijepes.2019.04.001.

Deng, W., Shang, S., Cai, X., Zhao, H., Song, Y. & Xu, J. 2021. An improved differential evolution algorithm and its application in optimization problem. *Soft Computing*, 25(7): 5277–5298.

Desale, S., Rasool, A., Andhale, S. & Rane, P. 2015. Heuristic and Meta-Heuristic Algorithms and Their Relevance to the Real World: A Survey. *INTERNATIONAL JOURNAL OF COMPUTER ENGINEERING IN RESEARCH TRENDS*, 2: 296–304. http://www.ijcert.org.

Dhanasekaran, B., Siddhan, S. & Kaliannan, J. 2020. Ant colony optimization technique tuned controller for frequency regulation of single area nuclear power generating system. *Microprocessors and Microsystems*, 73.

Dhillon, S.S., Lather, J.S. & Marwaha, S. 2016. Multi objective load frequency control using hybrid bacterial foraging and particle swarm optimized PI controller. *International Journal of Electrical Power and Energy Systems*, 79: 196–209.

Doan, D.-V., Nguyen, K. & Thai, Q.-V. 2022. *Load-Frequency Control of Three-Area Interconnected Power Systems with Renewable …*. www.etasr.com.

Dreidy, M., Mokhlis, H. & Mekhilef, S. 2017. Inertia response and frequency control techniques for renewable energy sources: A review. *Renewable and Sustainable Energy Reviews*, 69(July 2016): 144–155. http://dx.doi.org/10.1016/j.rser.2016.11.170.

Dubitsky, M.A., Rykova, A.A. & Systems Rt&a # 01, -Classification Of Power Reserves Of Electric Power. 2015. *CLASSIFICATION OF POWER RESERVES OF ELECTRIC POWER SYSTEMS*.

Elgerd, O.I. 1987. *Electric Energy Systems Theory: An Introduction*. 2nd ed. McGraw-Hill.

Elgerd, O.Ingemar. 2005. *Electric energy systems theory : an introduction*. Tata McGraw-Hill Publishing Company Ltd.

Eltanaly, A.M. 2018. *Advances in Renewable Energies and Power Technologies: Performance of MPPT Techniques of Photovoltaic Systems Under Normal and Partial Shading Conditions*. I. Yahyaoui, ed. Elsevier.

Fagiolari, L., Sampò, M., Lamberti, A., Amici, J., Francia, C., Bodoardo, S. & Bella, F. 2022. Integrated energy conversion and storage devices: Interfacing solar cells, batteries and supercapacitors. *Energy Storage Materials*, 51(January): 400–434.

Fathy, A., Kassem, A. & Zaki, Z.A. 2022. A Robust Artificial Bee Colony-Based Load Frequency Control for Hydro-Thermal Interconnected Power System. *Sustainability*, 14(20): 13569.

Fu, Y., Zhang, X., Hei, Y. & Wang, H. 2017. Active participation of variable speed wind turbine in inertial and primary frequency regulations. *Electric Power Systems Research*, 147: 174–184. http://dx.doi.org/10.1016/j.epsr.2017.03.001.

Gómez Expósito, Antonio., Conejo, A.J.. & Cañizares, Claudio. 2018. *Electric energy systems : analysis and operation*. CRC Press, Taylor & Francis Group.

Gordon, S., McGarry, C., Tait, J. & Bell, K. 2022. Impact of Low Inertia and High Distributed Generation on the Effectiveness of Under Frequency Load Shedding Schemes. *IEEE Transactions on Power Delivery*, 37(5): 3752–3761.

Gouran-Orimi, S. & Ghasemi-Marzbali, A. 2023. Load Frequency Control of multi-area multi-source system with nonlinear structures using modified Grasshopper Optimization Algorithm. *Applied Soft Computing*, 137.

Gulzar, M.M., Iqbal, M., Shahzad, S., Muqeet, H.A., Shahzad, M. & Hussain, M.M. 2022a. Load Frequency Control (LFC) Strategies in Renewable Energy-Based Hybrid Power Systems: A Review. *Energies*, 15(10): 3488.

Gulzar, M.M., Iqbal, M., Shahzad, S., Muqeet, H.A., Shahzad, M. & Hussain, M.M. 2022b. Load Frequency Control (LFC) Strategies in Renewable Energy-Based Hybrid Power Systems: A Review. *Energies*, 15(10).

Gulzar, M.M., Sibtain, D., Alqahtani, M., Alismail, F. & Khalid, M. 2025. Load frequency control progress: A comprehensive review on recent development and challenges of modern power systems. *Energy Strategy Reviews*, 57: 101604.

Hajiakbari Fini, M. & Hamedani Golshan, M.E. 2018. Determining optimal virtual inertia and frequency control parameters to preserve the frequency stability in islanded microgrids with high penetration of renewables. *Electric Power Systems Research*, 154: 13–22. https://doi.org/10.1016/j.epsr.2017.08.007.

Hote, Y. V. & Jain, S. 2018. PID controller design for load frequency control: Past, Present and future challenges. In *IFAC-PapersOnLine*. Elsevier B.V.: 604–609.

Huang, T. & Lv, X. 2023. Load frequency control of power system based on improved AFSA-PSO event-triggering scheme. *Frontiers in Energy Research*, 11.

IEA, P. 2025. South Africa - Countries & Regions - IEA. https://www.iea.org/countries/south-africa/renewables 10 January 2025.

Inthamoussou, F.A., Pegueroles-Queralt, J. & Bianchi, F.D. 2013. Control of a supercapacitor energy storage system for microgrid applications. *IEEE Transactions on Energy Conversion*, 28(3): 690–697.

Janga Reddy, M. & Nagesh Kumar, D. 2020. Evolutionary algorithms, swarm intelligence methods, and their applications in water resources engineering: a state-of-the-art review. *H2Open Journal*, 3(1): 135–188.

Juang, C.F. & Lu, C.F. 2004. Power system load frequency control by evolutionary fuzzy PI controller. In *IEEE International Conference on Fuzzy Systems*. 715–719.

Kapoor, D., Anand, S., Kulkarni, J. & Abraham, A. *Intelligent Systems Reference Library 187 Optimization Models in Steganography Using Metaheuristics*. http://www.springer.com/series/8578.

Katoch, S., Chauhan, S.S. & Kumar, V. 2021. A review on genetic algorithm: past, present, and future. *Multimedia Tools and Applications*, 80(5): 8091–8126.

Khadanga, R.K., Kumar, A. & Panda, S. 2022. A modified Grey Wolf Optimization with Cuckoo Search Algorithm for load frequency controller design of hybrid power system. *Applied Soft Computing*, 124: 109011.

Khadarvali, S., Madhusudhan, V. & Kiranmayi, R. 2022. Artificial Neural Network Controller in Two-Area and Five-Area System with Security Attack and Game-Theory Based Defender Action. *Energies*, 15(15). https://www.mdpi.com/1996-1073/15/15/5715.

Khalil, A.E., Boghdady, T.A., Alham, M.H. & Ibrahim, D.K. 2023. Enhancing the Conventional Controllers for Load Frequency Control of Isolated Microgrids Using Proposed Multi-Objective Formulation via Artificial Rabbits Optimization Algorithm. *IEEE Access*, 11: 3472–3493.

Kim, J., Gevorgian, V., Luo, Y., Mohanpurkar, M., Koritarov, V., Hovsapian, R. & Muljadi, E. 2019. Supercapacitor to Provide Ancillary Services with Control Coordination. *IEEE Transactions on Industry Applications*, 55(5): 5119–5127.

Kokash, N. 2014. *An introduction to heuristic algorithms*. https://www.researchgate.net/publication/228573156.

Kouba, N.E.Y., Menaa, M., Hasni, M. & Boudour, M. 2017. A new optimal load frequency control based on hybrid genetic algorithm and particle swarm optimization. *International Journal on Electrical Engineering and Informatics*, 9(3): 418–440.

Krpan, M. & Kuzle, I. 2021. on Modelling and Sizing a Supercapacitor Energy Storage for Power System Frequency Control. , (June): 404–409.

Kumar, B., Adhikari, S., Datta, S. & Sinha, N. 2021. Real Time Simulation for Load Frequency Control of Multisource Microgrid System Using Grey Wolf Optimization Based Modified Bias Coefficient Diagram Method (GWO-MBCDM) Controller. *Journal of Electrical Engineering and Technology*, 16(1): 205–221.

Kumar, R. & Sharma, V.K. 2020. Whale Optimization Controller for Load Frequency Control of a Two-Area Multi-source Deregulated Power System. *International Journal of Fuzzy Systems*, 22(1): 122–137.

Kumar Sahu, R., Panda, S., Biswal, A. & Chandra Sekhar, G.T. 2016. Design and analysis of tilt integral derivative controller with filter for load frequency control of multi-area interconnected power systems. *ISA Transactions*, 61: 251–264.

Laiju, N.J.T., Sedaghat, R. & Siddavaatam, P. 2021. Novel Hybrid GWO-WOA and BAT-PSO Algorithms for Solving Design Optimization Problems. In 113–144.

Lalngaihawma, S., Datta, S. & Das, S. 2024. Automatic Generation Control with a Recent ZOA Algorithm Optimized TIDN Controller. In *2024 IEEE 4th International Conference on Sustainable Energy and Future Electric Transportation, SEFET 2024*. Institute of Electrical and Electronics Engineers Inc.

Lalngaihawma, S., Datta, S., Das, S., Alsaif, F. & Ustun, T.S. 2024. Automatic Generation Control of Hybrid Sources Incorporating Renewable Energy Sources and Electric Vehicles in an Interconnected Power System Considering a Deregulated Environment. *IEEE Access*, 12: 124764–124789.

Lambora, A., Gupta, K. & Chopra, K. 2019. Genetic Algorithm- A Literature Review. In *2019 International Conference on Machine Learning, Big Data, Cloud and Parallel Computing (COMITCon)*. IEEE: 380–384.

Lange, C., Rueß, A., Nuß, A., Öchsner, R. & März, M. 2020. Dimensioning battery energy storage systems for peak shaving based on a real-time control algorithm. *Applied Energy*, 280(July): 115993. https://doi.org/10.1016/j.apenergy.2020.115993.

Lerede, D. & Savoldi, L. 2023. Might future electricity generation suffice to meet the global demand? *Energy Strategy Reviews*, 47.

Li, B., Chen, M., Cheng, T., Li, Y., Arshad Shehzad Hassan, M., Xu, R. & Chen, T. 2018. Distributed Control of Energy-Storage Systems for Voltage Regulation in Distribution Network with High PV Penetration. *2018 UKACC 12th International Conference on Control, CONTROL 2018*, 9(4): 169–173.

Li, H.X., Zhang, L., Cai, K.Y. & Chen, G. 2005. An improved robust fuzzy-PID controller with optimal fuzzy reasoning. *IEEE Transactions on Systems, Man, and Cybernetics, Part B: Cybernetics*, 35(6): 1283–1294.

Li, X., Wang, L., Yan, N. & Ma, R. 2021. Cooperative Dispatch of Distributed Energy Storage in Distribution Network with PV Generation Systems. *IEEE Transactions on Applied Superconductivity*, 31(8): 1–4.

Luo, J. 2023a. Designing optimized PID controller using improved bacterial foraging optimization algorithm for robust frequency control of islanded microgrid. *International Journal of Dynamics and Control*, 11(3): 1432–1443.

Luo, J. 2023b. Designing optimized PID controller using improved bacterial foraging optimization algorithm for robust frequency control of islanded microgrid. *International Journal of Dynamics and Control*, 11(3): 1432–1443.

Ma, J. & Xu, T. 2023. Optimal strategy of investing in solar energy for meeting the renewable portfolio standard requirement in America. *Journal of the Operational Research Society*, 74(1): 181–194.

Maeyaert, L., Vandevelde, L. & Döring, T. 2020. Battery Storage for Ancillary Services in Smart Distribution Grids. *Journal of Energy Storage*, 30(May): 101524. https://doi.org/10.1016/j.est.2020.101524.

Maji, S. & Ganguli, S. 2025. Fuzzy Logic Control for Industrial Applications. In *Controller Design for Industrial Applications*. Wiley: 1–20.

Meng, X., Liu, J. & Liu, Z. 2019. A Generalized Droop Control for Grid-Supporting Inverter Based on Comparison Between Traditional Droop Control and Virtual Synchronous Generator Control. *IEEE Transactions on Power Electronics*, 34(6): 5416–5438.

Mohamed, E.A., Aly, M. & Watanabe, M. 2022. New Tilt Fractional-Order Integral Derivative with Fractional Filter (TFOIDFF) Controller with Artificial Hummingbird Optimizer for LFC in Renewable Energy Power Grids. *Mathematics*, 10(16).

Mohammed, T., Momoh, J. & Shukla, A. 2017. Single area load frequency control using fuzzy-tuned PI controller. *2017 North American Power Symposium, NAPS 2017*: 1–6.

Mohammed, T., Momoh, J. & Shukla, A. *Single Area Load Frequency Control using Fuzzy-Tuned PI Controller*.

Mohapatra, S. & Mohapatra, P. 2023. American zebra optimization algorithm for global optimization problems. *Scientific Reports*, 13(1).

Mokhtar, M., Marei, M.I., Sameh, M.A. & Attia, M.A. 2022. An Adaptive Load Frequency Control for Power Systems with Renewable Energy Sources. *Energies*, 15(2).

Moura, F.A.M., Camacho, J.R., Guimaraes, G.C. & Chaves, M.L.R. 2012. Staem Turbines Under Abnormal Frequency Conditions in Distributed Generation Systems. In M. Gokcek, ed. *Mechanical Engineering* . IntechOpen: 381–400.

Naga Sai Kalyan, CH. & Suresh, C. V. 2022. Higher Order Degree of Freedom Controller for Load Frequency Control of Multi Area Interconnected Power System with Time Delays. *Global Transitions Proceedings*, 3(1): 332–337.

Nagaraj, B., Subha, S. & Rampriya, B. 2008. *Tuning Algorithms for PID Controller Using Soft Computing Techniques*.

Nagrath, I.J., Kothari, D.P. & Desai, R.C. 1982. Modern Power System Analysis. *IEEE transactions on systems, man, and cybernetics*, 12(1): 96–96.

Nayak, P.C., Bisoi, S., Prusty, R.C. & Panda, S. 2019a. Performance analysis of PDF+(1+PI) controller for load frequency control of the multi microgrid system using genetic algorithm. In *Proceedings - 2019 International Conference on Information Technology, ICIT 2019*. Institute of Electrical and Electronics Engineers Inc.: 448–453.

Nayak, P.C., Bisoi, S., Prusty, R.C. & Panda, S. 2019b. Performance Analysis of PDF+(1+PI) Controller for Load Frequency Control of the Multi Microgrid System Using Genetic Algorithm. In *2019 International Conference on Information Technology (ICIT)*. 448–453.

Nayak, P.C., Mishra, S., Prusty, R.C. & Panda, S. 2023. Hybrid whale optimization algorithm with simulated annealing for load frequency controller design of hybrid power system. *Soft Computing*.

Neeli, V.S.R.P.K., Chowdary, K.K., Sameera, N. & Chamundeswari, G. 2022. Design of Load frequency controller using Whale Optimization Algorithm (WOA). In *MysuruCon 2022 - 2022 IEEE 2nd Mysore Sub Section International Conference*. Institute of Electrical and Electronics Engineers Inc.

Ogar, V.N., Hussain, S. & Gamage, Kelum A.A. 2023. Load Frequency Control Using the Particle Swarm Optimisation Algorithm and PID Controller for Effective Monitoring of Transmission Line. *Energies*, 16(15).

Ogar, V.N., Hussain, S. & Gamage, Kelum A. A. 2023. Load Frequency Control Using the Particle Swarm Optimisation Algorithm and PID Controller for Effective Monitoring of Transmission Line. *Energies*, 16(15): 5748.

Ojha, S.K. & Obaiah, M.C. 2025. Optimization of a Novel FOPIDN-(1+PIDN) controller for Renewable Integrated Multi-Area Load Frequency Control System with Non-linearities. *IEEE Access*.

Omar, M., Ebrahim, M.A., AbdelGhany, A.M. & Bendary, F. 2016. Tuning of PID controller for load frequency control problem via harmony search algorithm. *Indonesian Journal of Electrical Engineering and Computer Science*, 1(2): 255–263.

Pal, M. & Singh, A. 2024. Load Frequency Control in 2 Area Interconnected Power System Using Ant Colony Optimization. In *2023 4th International Conference on Intelligent Technologies (CONIT)*. IEEE: 1–5.

Palizban, O. & Kauhaniemi, K. 2016. Energy storage systems in modern grids—Matrix of technologies and applications. *Journal of Energy Storage*, 6: 248–259. http://dx.doi.org/10.1016/j.est.2016.02.001.

Pan, C.T. & Liaw, C.M. 1989. An adaptive controller for power system load-frequency control. *IEEE Transactions on Power Systems*, 4(1): 122–128.

Puneet Garg, E. & Singh Brar, G. IJREE-International Journal of Research in Electrical Engineering LOAD FREQUENCY CONTROL OF THREE AREA POWER SYSTEM USING BACTERIAL FORAGING OPTIMIZATION. www.researchscript.com.

Qasim, O., Ali, I.I. & Najeeb, M. 2024. An Optimal Load Frequency Control in a Two-Area Power System Using a Fractional Order Proportional-Integral-Derivative-Based Zebra Optimization Algorithm. *International Journal of Electrical and Electronics Research*, 12(4): 1230–1239.

Rahman, A., Saikia, L.C. & Sinha, N. 2015. Load frequency control of a hydro-thermal system under deregulated environment using biogeography-based optimised three-degree-of-freedom integral-derivative controller. *IET Generation, Transmission & Distribution*, 9(15): 2284–2293.

Rahman, M.J., Tafticht, T. & Doumbia, M.L. 2021. Power Stability and Frequency Control Techniques of DG for a High Penetration Wind-Based Energy Storage System Using Integral–Derivative Controller. *IEEE Canadian Journal of Electrical and Computer Engineering*, 45(3): 232–241.

Rajan, R., Fernandez, F.M. & Yang, Y. 2021. Primary frequency control techniques for large-scale PV-integrated power systems: A review. *Renewable and Sustainable Energy Reviews*, 144.

Ram Babu, N., Bhagat, S.K., Saikia, L.C., Chiranjeevi, T., Devarapalli, R. & García Márquez, F.P. 2023. A Comprehensive Review of Recent Strategies on Automatic Generation Control/Load Frequency Control in Power Systems. *Archives of Computational Methods in Engineering*, 30(1): 543–572.

Rasolomampionona, D.D., Połecki, M., Zagrajek, K., Wróblewski, W. & Januszewski, M. 2024. A Comprehensive Review of Load Frequency Control Technologies. *Energies* , 17(12).

Richter, S.N. & Tauritz, D.R. 2018. The automated design of probabilistic selection methods for evolutionary algorithms. In *Proceedings of the Genetic and Evolutionary Computation Conference Companion*. New York, NY, USA: ACM: 1545–1552.

Rodrigues, Y.R., Abdelaziz, M. & Wang, L. 2020. D-PMU based secondary frequency control for islanded microgrids. *IEEE Transactions on Smart Grid*, 11(1): 857–872.

Saadat, H. 1999. *Power system analysis*. Boston: WCB/McGraw-Hill.

Sabahi, K., Teshnehlab, M. & Aliyari, M. 2009. Recurrent fuzzy neural network by using feedback error learning approaches for LFC in interconnected power system. *Energy Conversion and Management*, 50(4): 938–946. http://dx.doi.org/10.1016/j.enconman.2008.12.028.

Sadeq, D.A.-M., Mohammed Kh, A.-N., Mohammed, A.J., Dakhil, A.M., Abbod, M.F. & Hamed S, A.-R. 2022. Design of a Load Frequency Controller Based on an Optimal Neural Network. *Energies*, 15(17). https://www.mdpi.com/1996-1073/15/17/6223.

Sahu, P.R., Simhadri, K., Mohanty, B., Hota, P.K., Abdelaziz, A.Y., Albalawi, F., Ghoneim, Sherif S. M. & Elsisi, M. 2023. Effective Load Frequency Control of Power System with Two-Degree Freedom Tilt-Integral-Derivative Based on Whale Optimization Algorithm. *Sustainability*, 15(2): 1515.

Sahu, P.R., Simhadri, K., Mohanty, B., Hota, P.K., Abdelaziz, A.Y., Albalawi, F., Ghoneim, Sherif S.M. & Elsisi, M. 2023. Effective Load Frequency Control of Power System with Two-Degree Freedom Tilt-Integral-Derivative Based on Whale Optimization Algorithm. *Sustainability (Switzerland)*, 15(2).

Sahu, R.K., Panda, S. & Rout, U.K. 2013. DE optimized parallel 2-DOF PID controller for load frequency control of power system with governor dead-band nonlinearity. *International Journal of Electrical Power and Energy Systems*, 49(1): 19–33.

Saldarini, A., Longo, M., Brenna, M. & Zaninelli, D. 2023. Battery Electric Storage Systems: Advances, Challenges, and Market Trends. *Energies*, 16(22): 7566.

Sanki, P., Mazumder, S., Basu, M., Pal, P.S. & Das, D. 2021. Moth Flame Optimization Based Fuzzy-PID Controller for Power–Frequency Balance of an Islanded Microgrid. *Journal of The Institution of Engineers (India): Series B*, 102(5): 997–1006.

Sekyere, Y.O.M., Effah, F.B. & Okyere, P.Y. 2024. Optimal Tuning of PID Controllers for LFC in Renewable Energy Source Integrated Power Systems Using an Improved PSO. *Journal of Electronics and Electrical Engineering*.

Seneviratne, C. & Ozansoy, C. 2016. Frequency response due to a large generator loss with the increasing penetration of wind/PV generation - A literature review. *Renewable and Sustainable Energy Reviews*, 57: 659–668. http://dx.doi.org/10.1016/j.rser.2015.12.051.

Shaheen, M.A.M., Hasanien, H.M. & Alkuhayli, A. 2021. A novel hybrid GWO-PSO optimization technique for optimal reactive power dispatch problem solution. *Ain Shams Engineering Journal*, 12(1): 621–630.

Shouran, M., Anayi, F., Packianather, M. & Habil, M. 2021. Load frequency control based on the bees algorithm for the great britain power system. *Designs*, 5(3).

Šimić, Z., Knežević, G., Topić, D. & Pelin, D. 2021. Battery energy storage technologies overview. *International Journal of Electrical and Computer Engineering Systems*, 12(1): 53–65.

Singh, K., Amir, M., Ahmad, F. & Khan, M.A. 2021. An Integral Tilt Derivative Control Strategy for Frequency Control in Multimicrogrid System. *IEEE Systems Journal*, 15(1): 1477–1488.

Singh, K.M. & Gope, S. 2021. Renewable energy integrated multi-microgrid load frequency control using grey wolf optimization algorithm. In *Materials Today: Proceedings*. Elsevier Ltd: 2572–2579.

Subramanian, M. 2010. *Frequency regulation by free governor mode of operation in power stations*. https://www.researchgate.net/publication/280934455.

Suganthi, L., Iniyan, S. & Samuel, A.A. 2015. Applications of fuzzy logic in renewable energy systems - A review. *Renewable and Sustainable Energy Reviews*, 48: 585–607. http://dx.doi.org/10.1016/j.rser.2015.04.037.

Takahashi, R. & Tamura, J. 2008. Frequency control of isolated power system with wind farm by using flywheel energy storage system. *Proceedings of the 2008 International Conference on Electrical Machines, ICEM'08*.

Tan, K.M., Babu, T.S., Ramachandaramurthy, V.K., Kasinathan, P., Solanki, S.G. & Raveendran, S.K. 2021. Empowering smart grid: A comprehensive review of energy storage technology and application with renewable energy integration. *Journal of Energy Storage*, 39(April): 102591. https://doi.org/10.1016/j.est.2021.102591.

Tang, J., Liu, G. & Pan, Q. 2021. A Review on Representative Swarm Intelligence Algorithms for Solving Optimization Problems: Applications and Trends. *IEEE/CAA Journal of Automatica Sinica*, 8(10): 1627–1643.

Tayri, A. & Ma, X. 2025. Grid Impacts of Electric Vehicle Charging: A Review of Challenges and Mitigation Strategies. *Energies*, 18(14): 3807.

Toledo, O.M., Oliveira Filho, D. & Diniz, A.S.A.C. 2010. Distributed photovoltaic generation and energy storage systems: A review. *Renewable and Sustainable Energy Reviews*, 14(1): 506–511.

Topno, P.N. & Chanana, S. 2018. Load frequency control of a two-area multi-source power system using a tilt integral derivative controller. *Journal of Vibration and Control*, 24(1): 110–125.

Trojovska, E., Dehghani, M. & Trojovsky, P. 2022. Zebra Optimization Algorithm: A New Bio-Inspired Optimization Algorithm for Solving Optimization Algorithm. *IEEE Access*, 10: 49445–49473.

Tungadio, D.H. & Sun, Y. 2019a. Load frequency controllers considering renewable energy integration in power system. *Energy Reports*, 5: 436–453.

Tungadio, D.H. & Sun, Y. 2019b. Load frequency controllers considering renewable energy integration in power system. *Energy Reports*, 5: 436–453. https://doi.org/10.1016/j.egyr.2019.04.003.

Ullah, K., Basit, A., Ullah, Z., Aslam, S. & Herodotou, H. 2021. Automatic Generation Control Strategies in Conventional and Modern Power Systems: A Comprehensive Overview. *Energies*, 14(9): 2376.

Umrao, R., Kumar, S., Mohan, M., Chaturvedi, D.K. & Member, S. 2012. Load Frequency Control Methodologies for Power System. , (March 2015).

Vichos, E., Sifakis, N. & Tsoutsos, T. 2022. Challenges of integrating hydrogen energy storage systems into nearly zero-energy ports. *Energy*, 241: 122878. https://doi.org/10.1016/j.energy.2021.122878.

Wang, W., Yuan, B., Sun, Q. & Wennersten, R. 2022. Application of energy storage in integrated energy systems — A solution to fluctuation and uncertainty of renewable energy. *Journal of Energy Storage*, 52(PA): 104812. https://doi.org/10.1016/j.est.2022.104812.

Wang, Z., Wang, Y., Xie, L., Pang, D., Shi, H. & Zheng, H. 2024. Load Frequency Control of Multiarea Power Systems with Virtual Power Plants. *Energies*, 17(15).

Xie, Y., Liu, L., Wu, Q. & Zhou, Q. 2020. Robust model predictive control based voltage regulation method for a distribution system with renewable energy sources and energy storage systems. *International Journal of Electrical Power and Energy Systems*, 118(December 2019).

Xu, W., Li, J., Yang, L. & Yu, Q. 2024. Faults locating of power distribution systems based on successive PSO-GA algorithm. *Scientific Reports*, 14(1): 11259.

Yan, R., Saha, T.K., Modi, N., Masood, N. Al & Mosadeghy, M. 2015. The combined effects of high penetration of wind and PV on power system frequency response. *Applied Energy*, 145: 320–330. http://dx.doi.org/10.1016/j.apenergy.2015.02.044.

Yang, X.-S., Nagar, A.K. & Joshi, A. *Lecture Notes in Networks and Systems 18 Smart Trends in Systems, Security and Sustainability Proceedings of WS4 2017*. http://www.springer.com/series/15179.

Yousef, A.M., Abo-Elyousr, F.K., Elnozohy, A., Mohamed, M. & Abdelwahab, S.A.M. 2020. Fractional order pi control in hybrid renewable power generation system to three phase grid connection. *International Journal on Electrical Engineering and Informatics*, 12(3): 470–493.

Yousef, H.A. 2017. *Power System Load Frequency Control*. Boca Raton : Taylor & Francis, a CRC title, part of the Taylor & Francis imprint, a member of the Taylor & Francis Group, the academic division of T&F Informa, plc, [2017]: CRC Press. https://www.taylorfrancis.com/books/9781351679572.

Zare, P., Davoudkhani, I.F., Zare, R., Ghadimi, H., Mohajeri, R. & Babaei, A. 2023. Maiden Application of Zebra Optimization Algorithm for Design PIDN-TIDF Controller for Frequency Control in Offshore Fixed Platforms Microgrid in the Presence of Tidal Energy. In *2023 8th International Conference on Technology and Energy Management, ICTEM 2023*. Institute of Electrical and Electronics Engineers Inc.

Zeng, M., Zhang, K. & Liu, D. 2013. Overall review of pumped-hydro energy storage in China: Status quo, operation mechanism and policy barriers. *Renewable and Sustainable Energy Reviews*, 17: 35–43. http://dx.doi.org/10.1016/j.rser.2012.05.024.

Zhan, Z.-H., Shi, L., Tan, K.C. & Zhang, J. 2022. A survey on evolutionary computation for complex continuous optimization. *Artificial Intelligence Review*, 55(1): 59–110.

APPENDICES

APPENDIX A: Finding the PID parameters

In this section, the Ziegler-Nichols method is used to tune a PID controller. Below is the step-by-step guide:

1. Set the PID controller to P-mode: Initially, set the PID to operate in P-mode, i.e. set the derivative and integral gains to zero. This is done to determine the ultimate gain K_u of the system.
2. Increase the proportional gain: Increase the proportional gain K_p until the system starts to oscillate, this is the point at which the system becomes marginally stable, as shown in the figure.

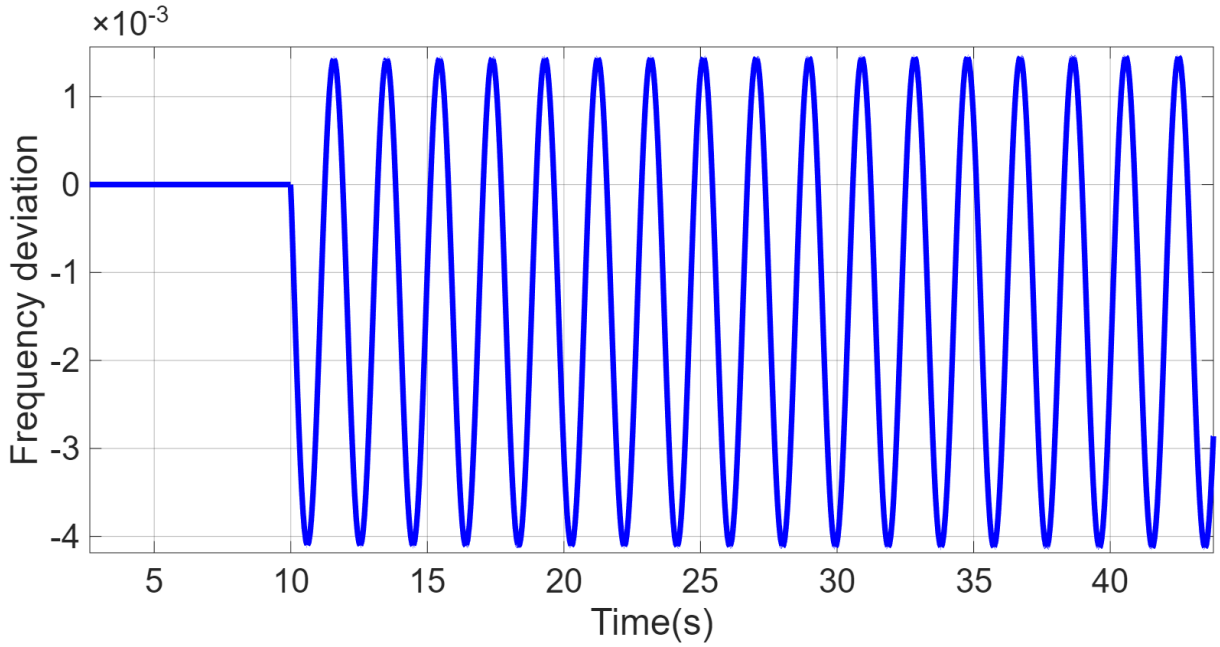

3. Determine K_u and the ultimate period P_u: Note the value of K_p at which the system starts to oscillate, which is K_u. Measure the period of oscillation P_u from the figure.
   The ultimate gain: $K_u = 3.70$
   Ultimate period: $P_u = 1.96s$
4. Calculate the PID gains: use the values of K_u, P_u obtained in 3 to calculate the PID gains using the Ziegler-Nichols tuning rules for the PID.

Controller Type	Kp	Ti	Td
P	0,5 Ku	0	0
PI	0,45 Ku	Pu / 1,2	-
PID	0,6 Ku	Pu / 2	Pu / 8

Therefore for the PID parameters:

$$K_p = 0.6 * 3.70 = 2.22$$

$$T_i = \frac{1.96}{2} = 0.98$$

$$T_d = \frac{1.96}{8} = 0.245$$

The PID equation thus becomes:

$$C(s) = K_P(1 + \frac{1}{T_i(s)} + T_d s)$$

$$C(s) = 2.22(1 + \frac{1}{0.98s} + 0.245s)$$

$$C(s) = 2.22 + \frac{2.265}{s} + 0.54s$$

From these calculations :

$$K_p = 2.22, K_i = 2.265, and\ K_d = 0.54$$

In this case, $K_p < K_i$ which suggests that the proportional action is weaker and the integral is dominant. In this case, the system reacts slowly to immediate errors but responds aggressively to errors, which risks the increase of overshoot and oscillatory behaviour.

5. Implement the PID gains in MATLAB/Simulink: Use the calculated PID gains in MATLAB/Simulink to simulate the system. The response from these parameters is given. This is corrected by increasing Kp to improve the transient response and decreasing the KI to reduce the overshoot. This can be reduced to Kp=2.0 and Ki =1.5

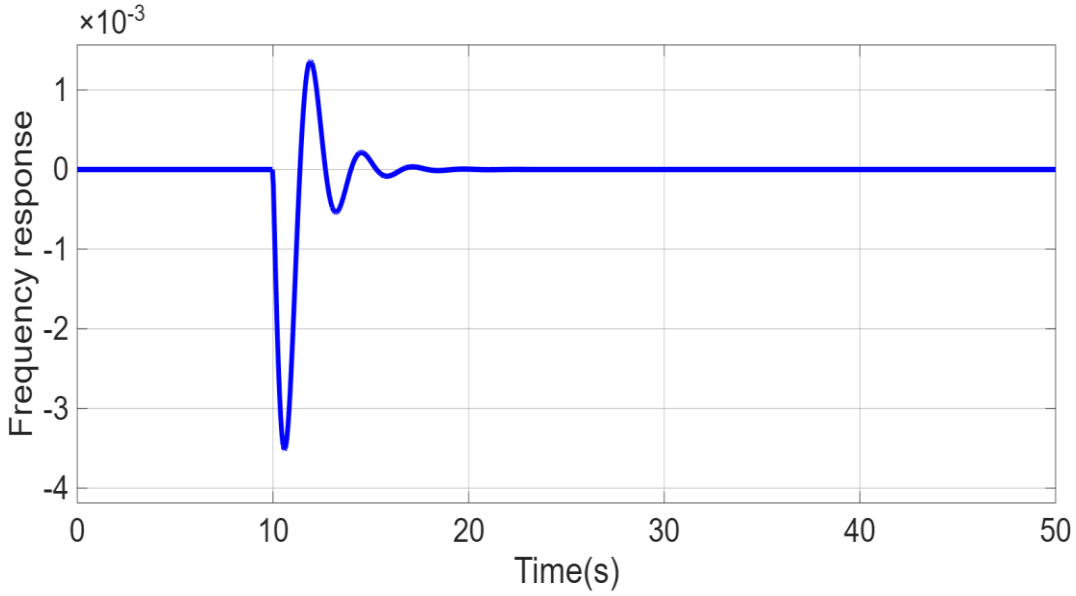

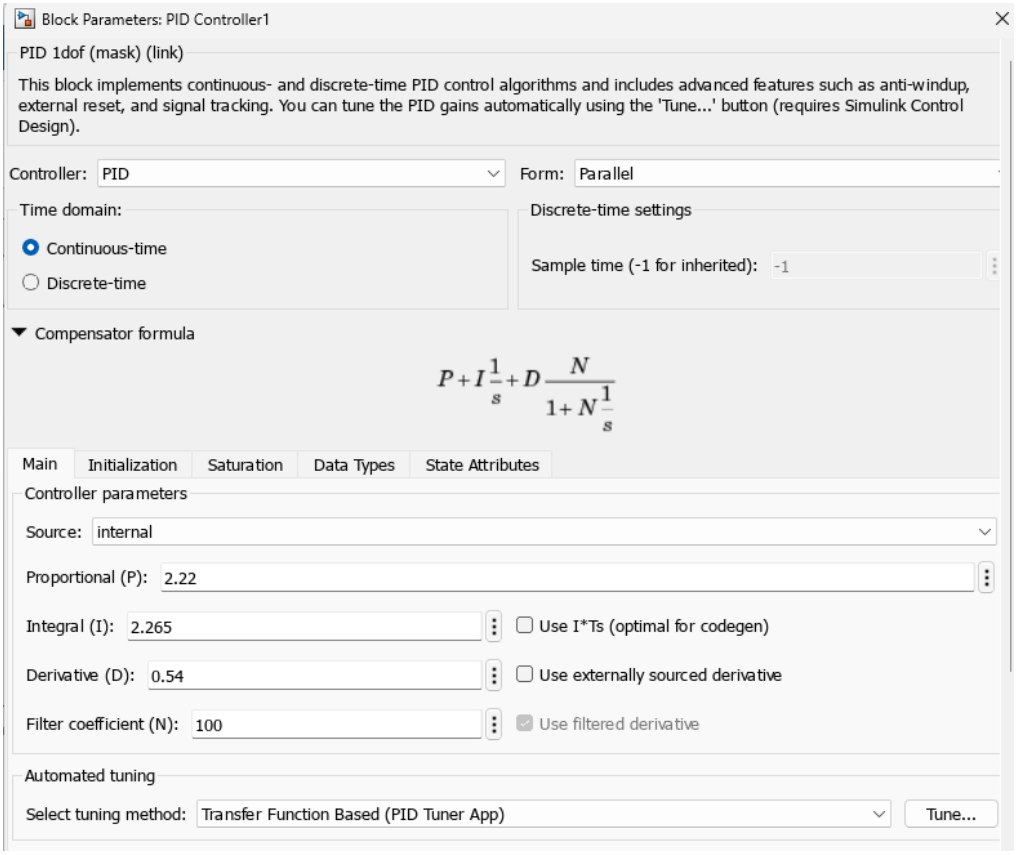
Block Parameters: PID Controller1
PID 1dof (mask) (link)
This block implements continuous- and discrete-time PID control algorithms and includes advanced features such as anti-windup, external reset, and signal tracking. You can tune the PID gains automatically using the 'Tune...' button (requires Simulink Control Design).
Controller: PID
Form: Parallel
Time domain:
Continuous-time
Discrete-time
Discrete-time settings
Sample time (-1 for inherited): -1
Compensator formula
$P+I\frac{1}{s}+D\frac{N}{1+N\frac{1}{s}}$
Main
Initialization
Saturation
Data Types
State Attributes
Controller parameters
Source: internal
Proportional (P): 2.22
Integral (I): 2.265
Use I*Ts (optimal for codegen)
Derivative (D): 0.54
Use externally sourced derivative
Filter coefficient (N): 100
Use filtered derivative
Automated tuning
Select tuning method: Transfer Function Based (PID Tuner App)
Tune...

APPENDIX B: ZOA MATLAB function

```
%%
% Adopted from :
% Zebra Optimization Algorithm: A New Bio-inspired Optimization Algorithm
% for Solving Optimization Algorithm
% IEEE access
% Eva Trojovská1, Mohammad Dehghani1, and Pavel Trojovský1*
% 1Department of Mathematics, Faculty of Science, University of Hradec
% Králové, 50003 Hradec Králové, Czech Republic

% " Optimiser"
%%
clc
clear
close all
%%

%%
Fun_name='LFC'; % Function name
SearchAgents=5; % number of Zebras (population members)
Max_iterations=50;% maximum number of iterations

%% Define bounds and dimension
lowerbound = [0 0 0];
upperbound = [20 20 20];
dimension = 3;

%% Define fitness function
fitness = @tunning;

%% ZOA Function
lowerbound=ones(1,dimension).*(lowerbound);    % Lower limit for variables
upperbound=ones(1,dimension).*(upperbound);    % Upper limit for variables

%% Initialisation
for i=1:dimension
    X(:,i) = lowerbound(i)+rand(SearchAgents,1).*(upperbound(i) - lowerbound(i));
% Initial population
end

for i =1:SearchAgents
    L=X(i,:);
    fit(i)=fitness(L);
end
%%

for t=1:Max_iterations
    %% update the global best (fbest)
    [best , location]=min(fit);
    if t==1
        PZ=X(location,:);  % Optimal location
        fbest=best;    % The optimization objective function
    elseif best<fbest
        fbest=best;
        PZ=X(location,:);
    end

    %% PHASE1: Foraging Behaviour
    for i=1:SearchAgents
```

```
        I=round(1+rand);
        X_newP1=X(i,:)+ rand(1,dimension).*(PZ-I.* X(i,:)); %Eq(3)
        X_newP1= max(X_newP1,lowerbound);X_newP1 = min(X_newP1,upperbound);


        % Updating X_i using (5)
        f_newP1 = fitness(X_newP1);
        if f_newP1 <= fit (i)
            X(i,:) = X_newP1;
            fit (i)=f_newP1;
        end

    end
    %% End Phase 1: Foraging Behaviour

    %% PHASE2: defense strategies against predators
    Ps=rand;
    k=randperm(SearchAgents,1);
    AZ=X(k,:);% attacked zebra

    for i=1:SearchAgents

        if Ps<0.5
            %% S1: the lion attacks the zebra and thus the zebra chooses an escape
strategy
            R=0.1;
            X_newP2= X(i,:)+ R*(2*rand(1,dimension)-1)*(1-
t/Max_iterations).*X(i,:);% Eq.(5) S1
            X_newP2= max(X_newP2,lowerbound);X_newP2 = min(X_newP2,upperbound);

        else
            %% S2: other predators attack the zebra and the zebra will choose the
offensive strategy

            I=round(1+rand(1,1));
            X_newP2=X(i,:)+ rand(1,dimension).*(AZ-I.* X(i,:)); %Eq(5) S2
            X_newP2= max(X_newP2,lowerbound);X_newP2 = min(X_newP2,upperbound);

        end

        f_newP2 = fitness(X_newP2); %Eq (6)
        if f_newP2 <= fit (i)
            X(i,:) = X_newP2;
            fit (i)=f_newP2;
        end

    end %
    %%
    %% Output the cost

    best_so_far(t)=fbest;
    average(t) = mean (fit);
   disp(['Iteration# ',num2str(t),' The best cost = ',num2str(fbest)]);

   cgCurve(t) = fbest;
end

%% Display the optimal value and cost
display(['The best optimal value of the objective function found by ZOA for '
num2str(Fun_name),' is : ', num2str(fbest)]);
display(['The best optimal value of the objective function found by ZOA for '
num2str(Fun_name),' is : ', num2str(PZ)]);
```

```
%% Plot the convergence curve
semilogy(cgCurve);
xlabel('Iteration#')
ylabel('Weight')


function cost = tunning(xx)
assignin('base','xx',xx);
sim('ZOA_LFC.slx');
cost= ITAE(length(ITAE));
end
```

```
Command Window
   Iteration# 1 The best cost = 0.047988
   Iteration# 2 The best cost = 0.047988
   Iteration# 3 The best cost = 0.047988
   Iteration# 4 The best cost = 0.046995
   Iteration# 5 The best cost = 0.046995
   Iteration# 6 The best cost = 0.043058
   Iteration# 7 The best cost = 0.02232
   Iteration# 8 The best cost = 0.02232
   Iteration# 9 The best cost = 0.021239
   Iteration# 10 The best cost = 0.021239
   Iteration# 11 The best cost = 0.020867
   Iteration# 12 The best cost = 0.019882
   Iteration# 13 The best cost = 0.019882
   Iteration# 14 The best cost = 0.01963
   Iteration# 15 The best cost = 0.01963
   Iteration# 16 The best cost = 0.01963
   Iteration# 17 The best cost = 0.01963
   Iteration# 18 The best cost = 0.01963
   Iteration# 19 The best cost = 0.01963
   Iteration# 20 The best cost = 0.019261
   The best optimal value of the objective function found by ZOA for LFC is : 0.019261
   The best optimal value of the objective function found by ZOA for LFC is : 7.5364      6.8413     0.49445
fx >>
```

APPENDIX C: PSO MATLAB function

```
clear all
close all
clc

% Define the details of the table design problem
nVar = 3;                   % number of variables
ub = [20 20 20];            % upper Bound
lb = [0 0 0];               % lower bound
fobj = @tunning;            % Objective function Name

% Define the PSO's paramters
noP = 5;                     % number of particles for initialization
maxIter = 50;                % maximum iterations
wMax = 1;
wMin = 0.1;
c1 = 2;
c2 = 2;
vMax = (ub - lb) .* 0.2;
vMin  = -vMax;


% The PSO algorithm

% Initialize the particles
for k = 1 : noP
    Swarm.Particles(k).X = (ub-lb) .* rand(1,nVar) + lb;
    Swarm.Particles(k).V = zeros(1, nVar);
    Swarm.Particles(k).PBEST.X = zeros(1,nVar);
    Swarm.Particles(k).PBEST.O = inf;

    Swarm.GBEST.X = zeros(1,nVar);
    Swarm.GBEST.O = inf;
end


% Main loop
for t = 1 : maxIter

    % Calcualte the objective value
    for k = 1 : noP
        currentX = Swarm.Particles(k).X;
        Swarm.Particles(k).O = fobj(currentX);

        % Update the PBEST
        if Swarm.Particles(k).O < Swarm.Particles(k).PBEST.O
            Swarm.Particles(k).PBEST.X = currentX;
            Swarm.Particles(k).PBEST.O = Swarm.Particles(k).O;
        end

        % Update the GBEST
        if Swarm.Particles(k).O < Swarm.GBEST.O
            Swarm.GBEST.X = currentX;
            Swarm.GBEST.O = Swarm.Particles(k).O;
        end
    end

    % Update the X and V vectors
    w = wMax - t .* ((wMax - wMin) / maxIter);
```

```
    for k = 1 : noP
        Swarm.Particles(k).V = w .* Swarm.Particles(k).V + c1 .* rand(1,nVar) .*
(Swarm.Particles(k).PBEST.X - Swarm.Particles(k).X) ...

+ c2 .* rand(1,nVar) .* (Swarm.GBEST.X - Swarm.Particles(k).X);


        % Check velocities
        index1 = find(Swarm.Particles(k).V > vMax);
        index2 = find(Swarm.Particles(k).V < vMin);

        Swarm.Particles(k).V(index1) = vMax(index1);
        Swarm.Particles(k).V(index2) = vMin(index2);

        Swarm.Particles(k).X = Swarm.Particles(k).X + Swarm.Particles(k).V;

        % Check positions
        index1 = find(Swarm.Particles(k).X > ub);
        index2 = find(Swarm.Particles(k).X < lb);

        Swarm.Particles(k).X(index1) = ub(index1);
        Swarm.Particles(k).X(index2) = lb(index2);

    end

    outmsg = ['Iteration# ', num2str(t) , ' Swarm.GBEST.O = ' ,
num2str(Swarm.GBEST.O)];
    disp(outmsg);

    cgCurve(t) = Swarm.GBEST.O;
end
writematrix(cgCurve,'psocurve.xls')
semilogy(cgCurve);
xlabel('Iteration#')
ylabel('Weight')
```